2 Periodicity

⋆ 2.1. Repeating Vertices

Origami vertices all by themselves are not terribly interesting. (Although, as we will see in Chapters 7 and 8, there is still quite a lot of a mathematical nature that we can say about isolated vertices.) The infinite variety of origami structures arises when we start bringing vertices together in combinations: a few, tens, hundreds, or even thousands of them in real-world objects. And when we start to contemplate their mathematics, we can even consider structures that contain infinite numbers of vertices and creases—even if we cannot physically fold them.

In a network of vertices, two connected vertices cannot be designed independently; the fold between them must have the same assignment at each vertex. If we choose the folds around one vertex, then we have implicitly made a choice of assignment of one or more folds around its adjacent vertices. In a network that contains loops of folds, assignments must be consistent around a loop; if you make a set of assignments at a vertex, then travel around the loop making assignments to folds at each vertex, when you get back to where you started, the assignment on an incoming edge had better match the assignment you started with. If it doesn't, then somewhere along the way, you've made a choice that resulted in an invalid assignment. We saw this phenomenon in the previous chapter, in the analysis of local flat-foldability (see Section 1.5). We will see many more examples of such loop conditions in upcoming chapters.

There is one sure way to avoid invalidity resulting from inconsistent conditions around loops, and that is to consider crease patterns that contain no loops of vertices. We will start by looking at a few of these.

⋆ 2.2. 1D Periodicity

⋆ 2.2.1. Periodicity and Symmetry

Throughout much of this book we will be looking at periodic structures and, in particular, structures folded from periodic crease patterns. A pattern is *periodic* if it can be shifted through some distance that leaves it unchanged. The distance that it shifts is the *period* of the pattern. Origami in general, and tessellations in particular, are rife with periodic structures. If a pattern is not periodic, then it is said to be *aperiodic*.

Strictly speaking, no finite pattern can be truly periodic. Even if the pattern of folds seems unchanged by a shift, the edges of the paper will not be left unchanged, as illustrated in Figure 2.1: the places where the pattern starts and stops are not left unaltered by the shift. So when we say that a finite crease pattern is periodic, what we really mean is that it is a finite piece of a theoretically infinite pattern that is periodic.

And just to deal with the contrary folk out there who point out that *any* isolated crease pattern could be made part of an infinite periodic pattern, let us say that we are only considering patterns in which the finite piece contains two or more repetitions of the repeating part.

In Figure 2.1, the pattern is periodic in the horizontal direction. If you shift the paper by the distance between the two vertical lines, which is the period, the crease pattern is left unchanged—at least, if we imagine that it continues to the left and right beyond the rectangle of the paper, as indicated by the dotted lines.

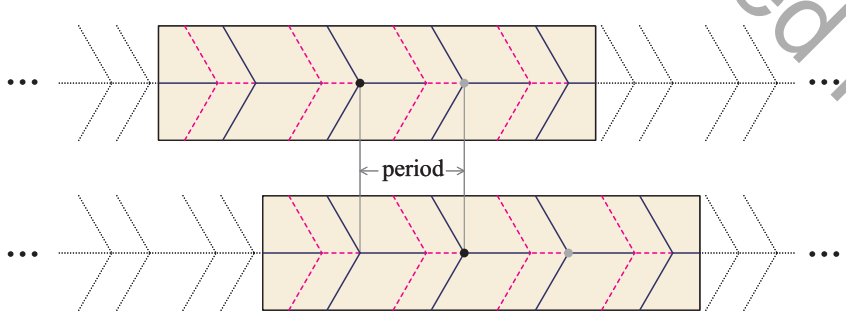

Figure 2.1.
A periodic crease pattern. The period is the distance by which the pattern can be shifted, leaving it unchanged. For finite paper, we assume that the pattern continues beyond the edges of the paper.

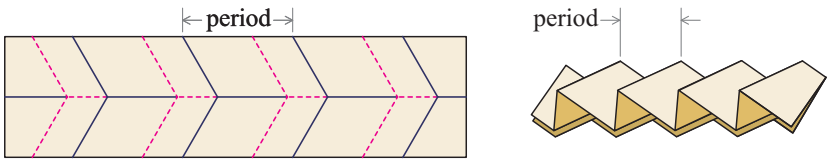

Figure 2.2.
A periodic origami structure.
Left: crease pattern.
Right: folded form.

This pattern is periodic; but is it a valid origami crease pattern? That is, can it fold up flat—or even fold partially, in 3D? As it turns out, this pattern does fold flat with no self-intersection; it creates the zigzag shape shown in Figure 2.2.

In this case, both the crease pattern and the folded form are periodic. Note, though, that the periods of the two are not the same. The period of the folded form is smaller. This will generally be the case when both the crease pattern and folded form are periodic; if a crease pattern gives rise to a periodic folded form, the period of the folded form is strictly less than the period of the crease pattern.

This is a specific example of a broader property of flat origami: in every flat origami fold, the distance between any two points in the crease pattern is the same or larger than the distance between the same two points in the folded form. If a straight line between the two points crosses any folds transverse to the line, the distance is strictly larger.

Back to periodicity. Imagine placing two copies of the same pattern on the table, one on top of the other. When we shift the pattern by the period, we bring each point on the top copy into alignment with another point on the bottom copy, which corresponds to a different point on the top copy. For example, the black dot in Figure 2.1 will come into alignment with the gray dot. We can mark the periodicity on a pattern by drawing an arrow from one feature to its image after the shift, as shown in Figure 2.3.

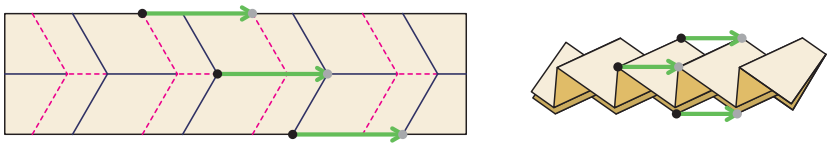

Figure 2.3.
The periodicity can be marked by drawing an arrow from one point to its image after translation in both the crease pattern and folded form.

The position of the arrow isn't unique; we can use any feature of the crease pattern as the point for reference. It's usually convenient to pick a vertex of the pattern, but which vertex is chosen is a matter of personal choice. Whichever vertex you choose as the starting reference, the length and direction of the periodicity arrow are unchanged. The three green arrows in Figure 2.3 are the periodicity arrows for different vertices, but they all have the same length and direction (they are parallel). In the language of Section 1.6, it is a *vector*—a combination of length and associated direction.

If one shift of distance d leaves a pattern unchanged, then two identical shifts will still leave it unchanged. So there is an ambiguity in the definition of the period. If the period is the distance that leaves the pattern unchanged, then d, $2d$, and, in general, nd (for integer n) all qualify as periods under the definition thus far. So we'll modify that definition: the period is the *smallest possible distance* whose shift leaves the pattern unchanged. (As we will see, even that definition permits some ambiguity when we consider multiple periodicities.)

The periodicity of a crease pattern does not necessarily imply periodicity of the folded form. Figure 2.4 shows an example where the crease pattern is periodic but the folded form—at least, this particular folded form—does not need to be; both periodic and aperiodic folded forms are shown. This is because there is information about the folded form that is not fully specified by

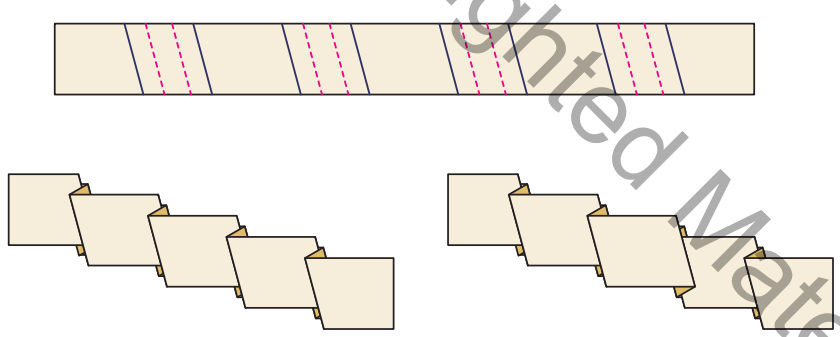

Figure 2.4.
A periodic origami crease pattern that admits both periodic and aperiodic folded forms.
Top: crease pattern.
Bottom left: periodic folded form.
Bottom right: aperiodic folded form.

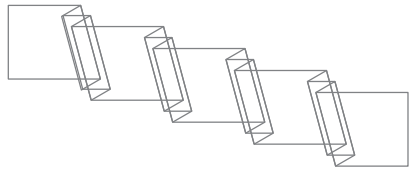

Figure 2.5.
The silhouette of the folded form is periodic if we ignore effects of layer ordering.

the crease pattern, namely, the stacking order of the facets. If the stacking order can be chosen in such a way as to break overall periodicity, that will not be reflected in the crease pattern.

A *pleat* is a side-by-side mountain and valley fold pair. The pattern in Figure 2.4 consists of a series of double pleats; within each pair, one pleat must overlap the other, and we can choose the overlap order independently for each pair. So we can choose to make the folded form periodic (as on the left) or, by changing one or more pleat pairs, to break the periodicity. If, however, we overlook the effects of layer order and look at only the silhouette of the fold lines, then periodicity will be restored, as shown in Figure 2.5. The silhouette is fully determined by the crease pattern, and so here periodicity of the crease pattern does imply periodicity of the folded form.

Still, there are definitely periodic crease patterns that have aperiodic folded forms, whether we consider layer ordering or not. Figure 2.6 shows one such example, both crease pattern and folded form.

You can see the pattern in this figure: the folded form winds up in a circle. As you extend the crease pattern linearly to left and right, the folded form continues to wind around, rotating rather than translating.

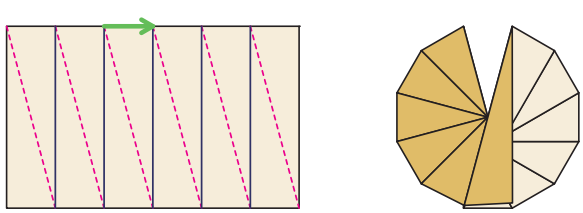

Figure 2.6.
A periodic crease pattern whose folded form is not periodic.
Left: crease pattern, with periodicity vector marked.
Right: folded form.

This deceptively simple pattern displays several very important concepts. First, the obvious: a periodic crease pattern does not necessarily give rise to a periodic folded form. But there's another: as we fold the crease pattern, we must rotate portions of the paper into the folded form, and the longer the pattern runs, the greater the amount of rotation is required. So this pattern can serve a role as a building block, that of a linear-to-rotary motion converter.

Let's come back to the question of periodicity. True, the folded form doesn't display periodicity, as we have defined it above. But it certainly displays *something* repetitive and symmetric. It's clear that if you take this folded form and shift it some way, the pattern of the folded form remains unchanged. But now, that shift is a *rotation*, rather than a translation: a different operation.

If a system is unchanged by the application of some operation, then it is said to exhibit a *symmetry*. Symmetries are deeply embedded in mathematics (and, for that matter, in the physical world). A periodic pattern is symmetric under translation; it is said to have *translational symmetry*. A pattern that is left unchanged by a rotation is said to have *rotational symmetry*. What Figure 2.6 shows is that a *translational* symmetry in the crease pattern can give rise to a *rotational* symmetry in the folded form.

A natural question to ask is, can we go the other direction? That is, can we start with a crease pattern with a rotational symmetry and end up with a folded form that has translational symmetry? The answer is yes, and it is not hard to construct such a crease pattern. Looking back at Figure 2.6, we see that the pattern that is getting repeated by the translational symmetry is the pair of angled folds. When we make both folds, that pair imparts a rotation of what's on one side relative to what's on the other, as illustrated in Figure 2.7. So if the underlying symmetry of the crease pattern was a translation, then the symmetry of the folded form consists of the translation of the crease pattern, combined with the rotation imparted by the folds of the repeating unit.

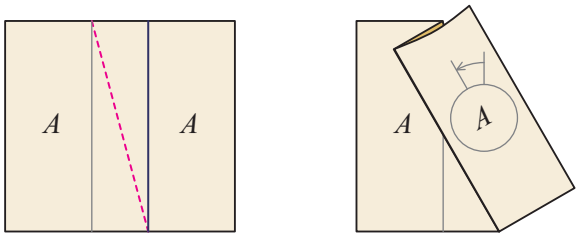

Figure 2.7.
The repeating unit is an angled pair of folds, which imparts a rotation of one side relative to the other.

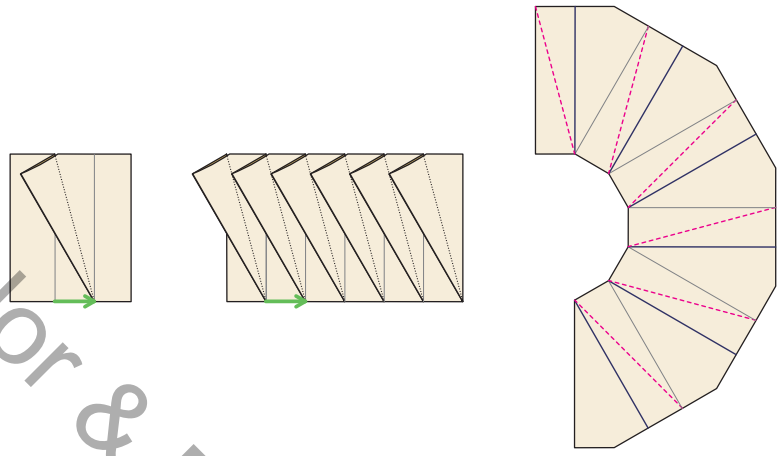

Figure 2.8.
Construction of a rotationally symmetric crease pattern that gives a periodic folded form.
Left: the repeating unit. The repeating part lies between the two vertical creases.
Middle: assembled into a periodic folded form.
Right: the unfolded crease pattern.

The rotation imparted by the underlying unit adds to the translational symmetry of the overall crease pattern. So if we want to start with rotational symmetry in the crease pattern and end with translational symmetry in the folded form, all we need to do is choose an underlying unit that imparts a rotation that cancels the rotation in the symmetry of the crease pattern.

How to ensure perfect cancellation? Well, one way would be to start with the desired folded form and then *unfold it* to get the crease pattern we're after. Take the folded form of our repeating unit in Figure 2.7; splice it into a folded pattern with linear translational symmetry; and then unfold the result, as shown in Figure 2.8.

Figure 2.8 shows that the relationship between translational and rotational symmetry can go both ways within a crease pattern, but it also illustrates a broader principle: in many situations, we can construct an origami pattern by designing the folded form directly, then unfolding it (conceptually, physically, or mathematically) to discover the desired crease pattern.

Translational and rotational symmetry are often linked between the crease pattern and folded form. We will see this phenomenon appear over and over in structures to come—especially when we move into two- and three-dimensional forms.

⋆ 2.2.2. Tiles

Figure 2.8 illustrates a general way of building up periodic and/or rotationally symmetric origami structures (whether crease pattern or folded form). We identify a basic repeating unit, then we join

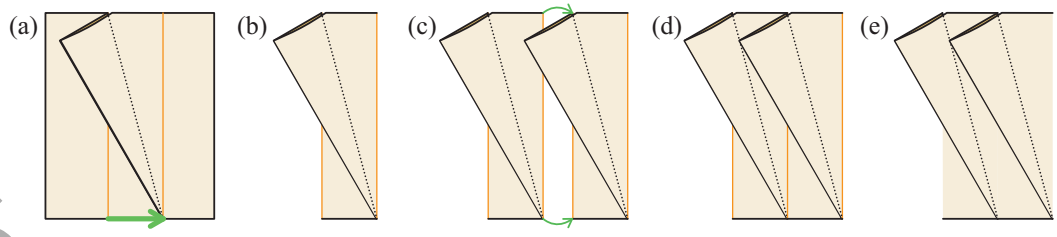

Figure 2.9.
Tiles creating a periodic folded form.
(a) The repeating unit, with tile lines indicated in orange.
(b) The folded form tile, with excess paper cut away.
(c) Join two tiles along their shared tile line.
(d) The joined pair.
(e) Removing the tile lines gives the resulting folded form.

copies of that unit to each other. When we do that, we need to clearly identify the boundaries of the repeating unit that get joined up. These are not necessarily the edge of the paper; in Figure 2.8, I said that the repeating unit was the paper between the pair of vertical (unfolded) crease lines.

To avoid ambiguity, though, we should not be using fold lines to delineate something that is not a fold. In Figure 2.8, the vertical unfolded crease lines are acting as the boundaries of repeating units that get joined to one another to make up a larger crease pattern or folded form, like the tiles of a mosaic. We will call those patches of crease pattern *tiles*, and we call the boundaries along which they join *tile lines*.

Going back to Figure 2.8, we replace those unfolded crease lines with orange tile lines, as shown in Figure 2.9. Once we've defined the boundaries of the tile by the tile lines, we can eliminate the paper extending outside of the tile lines, leaving a pure, stand-alone tile, in this case a tile of the folded form. We can build up arbitrarily large sections of an origami structure by simply joining tiles along their corresponding tile lines.

The power of the tiling approach is that if we begin with a folded form tile, we can unfold it to get a crease pattern tile that we can use to build up a periodic (or in this case, rotationally symmetric) crease pattern in the same way, as Figure 2.10 shows.

There is some freedom in how we choose the tile boundaries; all that's really necessary is that corresponding tile boundaries have the same shape, so that they fit together. Or, put more

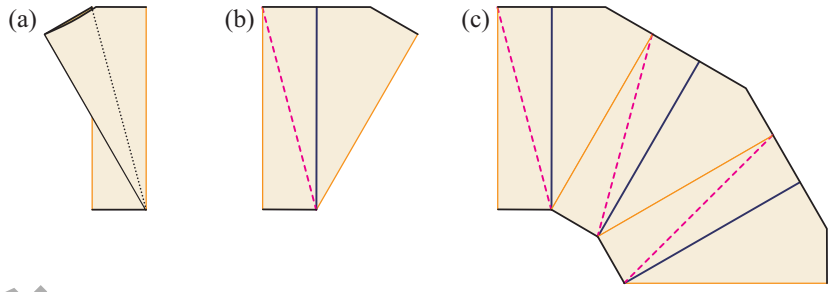

Figure 2.10.
Converting from a folded form tile to a crease pattern tile.
(a) The folded form tile.
(b) Unfolding the folded form tile gives a crease pattern tile.
(c) Three crease pattern tiles joined to create a single crease pattern.

directly, the translation that defines the periodicity (or rotation that defines the rotational symmetry) must transform one tile line into the other within a tile. So, in Figure 2.11, all three crease pattern tiles are perfectly valid, and all can be combined with copies of themselves to give rise to the same crease pattern (aside from what happens at the ends of the strip).

In general, the simpler the tile lines are, the easier the tiles will be to work with. And once one has defined a tile (of either crease pattern or folded form), it is a simple practical matter to create the full pattern by duplicating and pasting copies of the tile side by side, so that the tile lines are aligned. This is especially quick and easy with computer drawing programs, but the technique can even be employed with manual drawing, by making paper copies

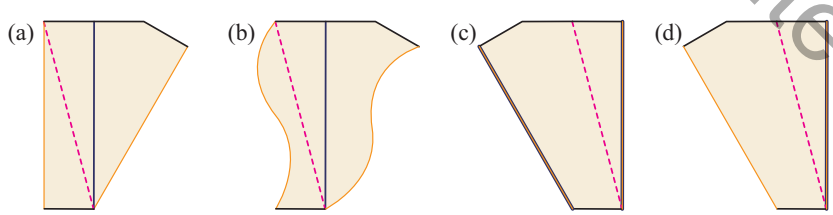

Figure 2.11.
Three equivalent crease pattern tiles.
(a) The crease pattern tile.
(b) Same tile, but with curved tile lines. Note that corresponding tile lines must be rotated copies of one another.
(c) Same tile, but with the tile lines superimposed on the mountain folds.
(d) Same tile, but with one of the mountain folds excluded.

of individual tiles, then using them as a template to build up the full pattern.

A small complication arises if we place the tile lines on the fold lines of the crease pattern, as shown in Figure 2.11(c). It raises the question: does the fold line belong in the tile or not? If we exclude it from the tile, then it will be lost from the overall pattern. If we include it, then we'll have duplicates of that fold when we join two tiles together.

Suppose that the tile lines were slightly displaced to one side or the other. If we do that with the tile of Figure 2.11(c), then one of the mountain folds would be included within the tile and the other excluded; if we then splice two tiles together, all would be well: there would be exactly one mountain fold along each tile line. So, if the tile lines run along folds, we must keep track of corresponding pairs of tile lines and choose one of each pair to include the fold line, as in Figure 2.11(d).

There is also the practical issue when drawing that if a tile line and fold line are coincident, then one is going to cover up the other. (I've dealt with that issue in Figure 2.11 by making the mountain folds fatter where they are overlapped by a tile line.) To avoid this issue and the need to keep track of which tile line gets the fold that it overlaps, I generally try to define my tiles so that no tile lines run along fold lines or vertices, for which similar choices of inclusion/non-inclusion must be made. This is purely a matter of personal taste, though, and in some case, defining tiles along fold lines will be the natural choice.

⋆ 2.2.3. Linear Chains

If a crease pattern consists of a set of crease lines with no vertices in the interior of the pattern, as in Figures 2.4–2.8, then to determine if the crease pattern is valid, we only need to consider the way the layers overlap and the possibility of self-intersection. If, however, the crease pattern contains vertices in its interior, as in Figures 2.1 and 2.2, then we need to ensure that the fold lines between two vertices match in crease assignment and, if the vertices are not fully flat-folded, in measured fold angle.

One way to see this matching requirement is to construct the tile for the repeating pattern. Figure 2.12 shows the crease pattern of Figure 2.1 divided up into tiles and a single tile.

The tile in the figure contains two interior vertices and has creases that cross the tile border. In order to arrange copies of this

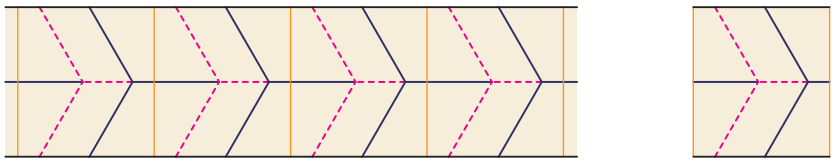

Figure 2.12.
Identifying the tiles in a periodic crease pattern.
Left: the pattern.
Right: the tile.

tile into a periodic chain, the crease crossing the left tile line must do so at the same position and angle as the one crossing the right tile line. In this pattern, this is clearly the case: each horizontal crease hits the left or right tile line exactly halfway up, and the angle is 90°.

With two interior vertices in the tile, this isn't the simplest possible tile of a linear chain, and it is worth asking: what are the possibilities in the simplest case, with only a single degree-4 vertex in each tile and consecutive vertices connected by folds across a tile border?

Without loss of generality, we can choose the vertex to have three valleys and one mountain. Then the two folds that cross the tile line to the left and right must be valleys since we only have one mountain fold to work with.

Next, since the direction of the fold on the left must match the direction of the fold on the right after translation, the two folds must be collinear.

And for the position where each fold hits the tile line to have the same periodicity, the two folds must be oriented along the direction of periodicity.

That, in turn, greatly restricts the other two folds. In order to fold the vertex flat (or even to fold all four creases together by any amount), the two remaining creases must be on opposite sides of the straight-line fold pair, making the same angle with the pair (which we can choose). This gives a family of patterns, characterized by this last angle, one example of which is shown in Figure 2.13, along with its folded form.

That particular family is not too interesting. But now let's consider the possibility that the crease pattern has rotational symmetry, rather than periodicity. In this case, the two valleys can intersect at some angle other than collinearly, and that opens up rather more options.

For one thing, there are two distinct families: we can put both of the two remaining creases on one side of the pair, or one on each side. In the latter case, the mountain fold must go in the $< 180°$

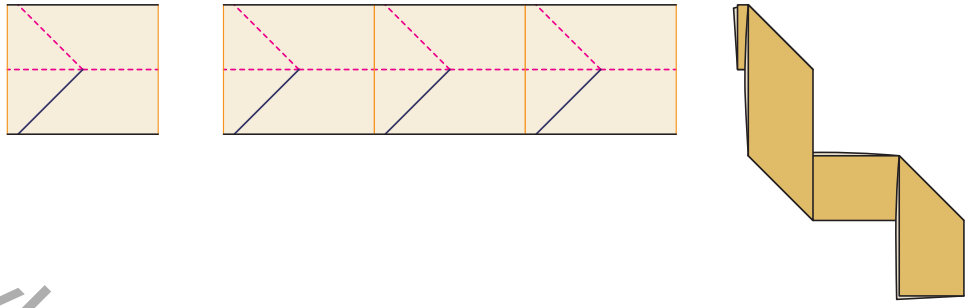

Figure 2.13.
Left: a periodic tile containing a single degree-4 vertex.
Middle: the resulting crease pattern for three tiles.
Right: the folded form.

angle between the pair, with the valley fold going somewhere on the other side. Flat-foldable examples of both cases are shown in Figure 2.14.

In both cases, the crease pattern has rotational symmetry, but the folded forms differ; the upper tile gives a folded form that also has rotational symmetry, while the lower tile gives rise to periodicity (translational symmetry). Both of these patterns are flat-foldable, of course, but the second pattern is interesting in the partially folded state, in which it forms a polygonal helix in three dimensions. I encourage you to fold one and try it out. You might also try out different vertex angles, to see how the choice affects the helicity in the partially folded state.

That's only a single vertex per tile. We can extend the idea in several ways; go to vertices of higher degree, for example, or create a tile with two, three, or more vertices within the tile. There are many interesting periodic structures to discover, and later on, we will examine more of them. But not right now. We've established some important concepts: periodicity, rotational symmetry, and the use of tiles to create periodic structures. Linear chains of tiles display some interesting structure, but the possibilities are far richer when we extend periodicity into two dimensions.

⋆ 2.3. 2D Periodicity

Mathematically, a tiling is a partitioning of the plane into regions—which are the tiles. In the previous section, we partitioned (roughly) linear strips of papers into tiles that are periodic

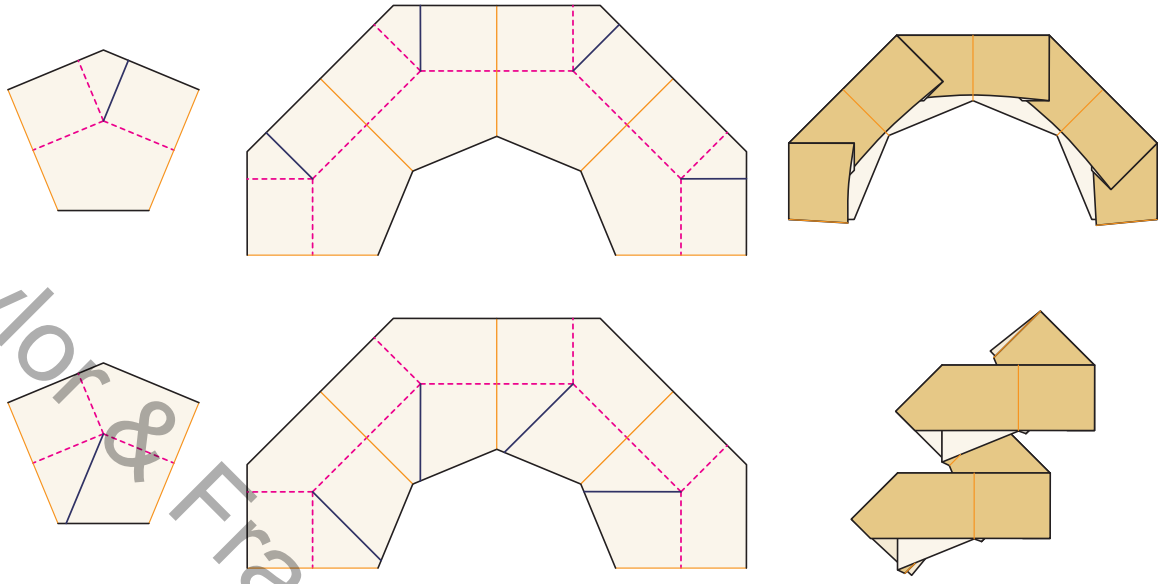

Figure 2.14.
Top row: a tile with rotational symmetry in the crease pattern with folds on the same side of the valley pair.
Bottom row: a tile with rotational symmetry in the crease pattern with folds on opposite sides of the valley pair.
Left: tile.
Middle: crease pattern composed of four tiles.
Right: folded form.

(or in some cases, rotationally symmetric). A periodic pattern can be characterized by its period and the direction of periodicity: two quantities that can be combined in the vector of periodicity, indicated by an arrow in the plane whose length is the period and whose orientation gives the direction of periodicity. If we have a basic building block of a tile, we can create a linear array by placing multiple copies of that tile at multiples of the periodicity.

There are patterns that exhibit periodicity in two different directions, for example, a grid of squares. Such patterns are called *doubly periodic*. In general, a doubly periodic pattern will be characterized by two different (non-collinear) vectors of periodicity. Often, as in a square grid, the two vectors point in orthogonal directions; they don't have to, however. We will refer to the vectors as *basis vectors* for the doubly periodic structure.

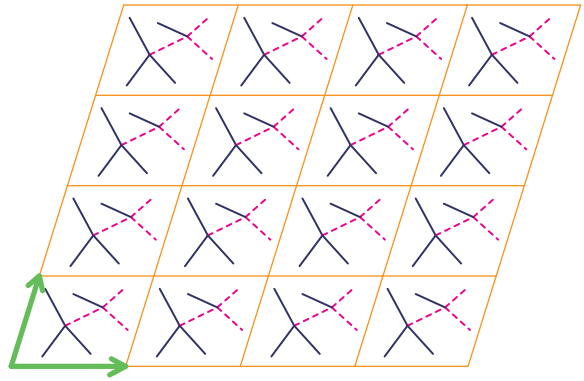

Figure 2.15.
Illustration of a doubly periodic pattern. Tiles are outlined in orange. Basis vectors are shown in green.

Any doubly periodic structure can be partitioned into tiles that are quadrilaterals—in fact, parallelograms—so that the entire pattern can be generated from a single tile by making copies of the tile and translating them by integer multiples of the two basis vectors, as illustrated in Figure 2.15.

Doubly periodic patterns are of interest in origami because with a single tile, one can fill an arbitrarily large region of the plane—thereby creating an arbitrarily large folded structure, which can be of both aesthetic and practical interest. The tiles for a doubly periodic pattern have tile lines on all four sides and must obey two sets of matching conditions. The left and right sides must line up, as with our linearly periodic patterns, but now the top and bottom of the tiles must mate in a similar fashion.

So, now, can we find a doubly periodic pattern that contains a single degree-4 vertex in each tile? We already saw that for a single direction of periodicity, the two folds that hit the two tile lines must be the same parity and collinear. With a doubly periodic pattern, the two folds in the other direction must satisfy the same condition. That amounts to saying that there are either four folds of one type, or two folds each of both types. In either of those two cases, the Maekawa-Justin Theorem requires at least two more folds, so the vertex must be at least degree-6. So the simplest doubly periodic tile cannot consist of a single degree-4 vertex, but that does leave open the possibility that, say, there is a doubly periodic pattern composed of a single type of degree-6 (or higher) vertex—as we will presently see.

But we can still ask the question: is there a doubly periodic pattern that is composed entirely of a single type of vertex? There is, and it is the source of some very interesting folded behavior.

⋆ 2.3.1. Huffman Grid

The simplest possible doubly periodic crease pattern consists of a single vertex, repeated over and over in rows and columns, so that the mountains and valleys emanating from the vertex join up collinearly with those of its neighbors, matching both in direction and in fold angle (crease assignment, in flat-foldable patterns). The simplest nontrivial vertex that could serve as the tile of such a regular array is the degree-4 vertex, so the question naturally arises: which degree-4 vertices can be tiled with copies of themselves to create a crease pattern that folds along all of its creases so that each vertex folds identically?

The somewhat surprising answer is: any of them. The computer scientist David Huffman (with whom we will spend considerable time later on) showed in his landmark paper, "Curvature and Creases: A Primer on Paper" [47], that any degree-4 vertex can be arrayed with copies of itself to produce a doubly periodic crease pattern that folds smoothly with all facets remaining flat during the folding process. Huffman didn't give this structure a name and wasn't the first to describe cylindrical grids of degree-4 vertices, but he seems to have been the first person to analyze it in full generality, and so I will call it a *Huffman grid*. An example of a Huffman grid crease pattern and several stages of the folded form are shown in Figure 2.16.

The Huffman grid is a 2D array of degree-4 vertices, all alike, which are then the vertices of a 2D array of quadrilateral facets, also (necessarily) all alike. The construction is straightforward. One first chooses the degree-4 vertex; this will be called the *generating vertex* of the grid. For the example shown in Figure 2.16, the sector angles around the vertex were chosen to be $(90°, 50°, 100°, 120°)$. We can also choose two lengths, for example, the lengths of the first two creases. For this example, I have chosen lengths of 1 and 2 units, respectively.

Now, we must array copies of this vertex in such a way as to achieve a 2D periodic pattern, keeping in mind that every vertex must have the same sector angles and the same fold angles. It's not enough to have the folds simply match in their mountain or valley assignment; in general, a 3D degree-4 vertex may have all four fold angles differ (in Chapter 8 we will see exactly what the relationships between fold angles are). So that means, for example, as we travel outward from a vertex along any given crease, at the

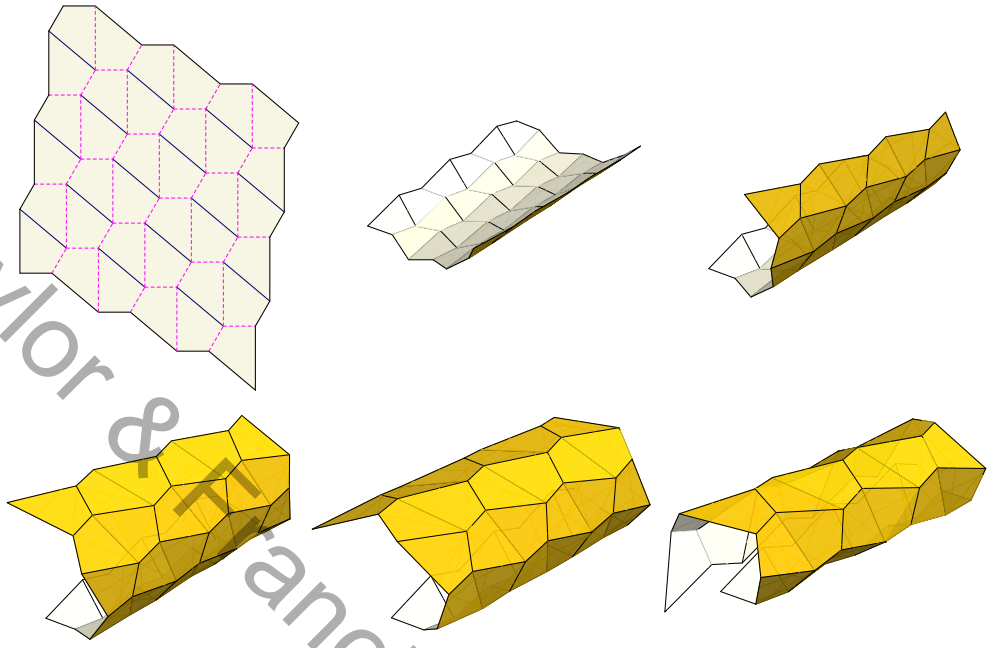

Figure 2.16.
A Huffman grid, parameterized on the angle of the horizontal valley folds.
Top row: left to right, crease pattern and valley folds at 3° and 6°.
Bottom row: left to right, valley folds at 9°, 12°, and 18°.

end of the crease we should encounter a rotated copy of the same vertex.

We can see this requirement more clearly by coloring all four creases uniquely, as in Figure 2.17. We choose the lengths of the green and blue mountain folds, as shown in Figure 2.17(a). Then at the far end of each fold there must be a rotated copy of the vertex, as in (b). The two remaining creases intersect; that intersection defines the lengths of the other two creases. Now that we have all four crease lengths, we can replicate the full pattern by placing copies of the vertex (some merely translated, others translated and rotated) to build out the pattern.

The crease pattern is clearly doubly periodic; we can check this by identifying a feature of the pattern and its translated copies, as shown in Figure 2.18. I have marked all of the vertices that are translated copies of one another with black dots. Although all of the vertices are alike, half of them are rotated (by the same amount) relative to the black-dot vertices; these constitute a second set and are marked with gray dots. Thus, each tile contains two vertices: one black, one gray.

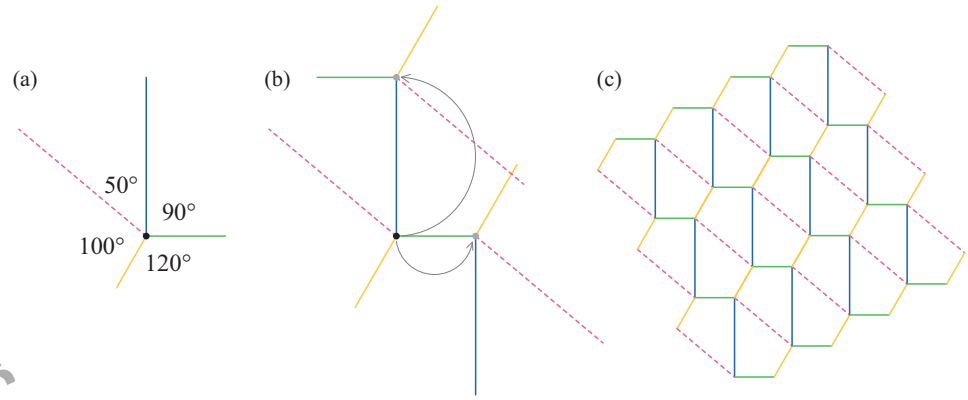

Figure 2.17.
Construction of a Huffman grid.
(a) The generating vertex. We can choose two crease lengths, the blue and green.
(b) At each end of the two creases, we place two rotated copies of the vertex. The intersections of the magenta and amber crease lines define the other two crease lengths.
(c) Replicating the grid (at 50% of the size in (a) and (b)).

The tile for this Huffman grid is a rectangle (in this case; more generally, a parallelogram) whose edges have the length and orientation of the periodicity vectors. The position of the tile can be taken anywhere within the crease pattern; it doesn't have to have its corners coincide with vertices of the crease pattern, but it is elegant and convenient in this case to do so. To ensure that when we replicate the tile, we get no duplicate vertices, each tile contains a single black vertex and a single gray vertex. Then using

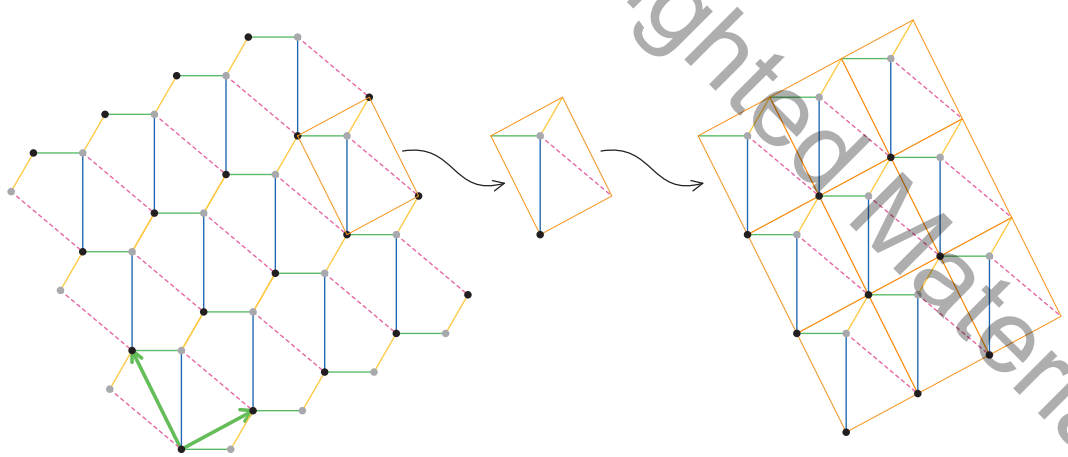

Figure 2.18.
Identification of the periodicity vectors (green, lower left) and tile (orange) for the Huffman grid.
Right: building up the pattern by replicating and translating the tile.

this tile, an arbitrarily large region of the crease pattern may be built up by replicating and translating copies of the tile.

Now that we know how to construct the pattern, let's look at how it behaves under folding, looking back at Figure 2.16. It is rather surprising: as one starts to fold the pattern, it curls up quite quickly to form a polygonal cylinder. And the curling happens quickly; as can be seen from the figure, by the time the valley folds have reached the quite shallow fold angle of 18°, the paper has curled in almost a complete loop and is about to collide with itself.

This pattern is never going to fold flat—in fact, it won't even get close, at least not without self-intersecting.

It's just a little bit surprising that a doubly periodic crease pattern would give rise to a cylindrical folded form, rather than a doubly periodic folded form—but only a little surprising. After all, we saw with linear periodic patterns that periodicity in the crease pattern could give rise to rotational symmetry in the folded form, and vice versa. In the Huffman grid, there are two directions of periodicity. One gives rise to a translational symmetry along the axis of the cylinder; the other gives rise to rotational symmetry, about the cylinder.

In fact, neither symmetry is exact; if you look closely at Figure 2.16, you'll see that the pattern of polygons along the cylinder is not pure translation but instead has a slight helicity. The same goes for the rotational symmetry; vertices are not strictly rotated about the axis of the cylinder, but instead they are slightly offset as one goes around. There are two directions of symmetry in the folded form, but both are a mixture of translation along the axis and rotation about the axis. Both are helical, but one is closer to translation, the other to rotation.

It might seem that this behavior could be peculiar to the particular Huffman grid that I chose here, but no: in fact, every Huffman grid exhibits this cylindrical curling behavior. As one flexes the crease pattern from flat to folded, it curls up with the cylindrical radius getting tighter and tighter. And, in general, the orientation of the axis of the cylinder relative to the crease pattern is not obvious. (It will not be until Chapter 8 that we will discover what this relationship is.)

Any Huffman grid composed of a single vertex type is guaranteed to work if the generating vertex itself is a degree-4 vertex that satisfies a few simple conditions. It doesn't have to be flat-foldable,

so it doesn't necessarily have to satisfy the Kawasaki-Justin Theorem. It does, however, have to have three mountain folds and one valley fold (or vice versa); all four sector angles cannot be 90°; and the three folds of the same type cannot all lie in the same half-plane. If the vertex satisfies those conditions, the Huffman grid constructed from it will work, and by "work" I mean that the entire structure can flex with all facets remaining flat—a property known as *rigid foldability*.[1] In fact, the structure has a *single degree of freedom*, meaning that if it flexes at all, all of the folds must flex together with the fold angles taking on a prescribed one-to-one relationship with each other. We will learn more about rigid foldability and degrees of freedom in Chapter 7.

If you fold a Huffman grid from paper, this single-degree-of-freedom property may not be obvious, because the facets in paper are not constrained to flatness; the quadrilaterals can usually flex easily along their diagonals, and so the entire structure will be somewhat "squishy" (depending on the stiffness of the paper). It is fairly easy to distort the cylinder away from cylindrical symmetry, for example, twisting one end more tightly than the other, to make it somewhat conical. But this is a distortion that relies upon bending of the facets. If you make the structure from truly rigid material (say, sheet metal with actual hinges for the folds), the constraint to cylindrical folded form will be more clearly evident in the behavior of the physical model.

And I do encourage you to fold and experiment with physical models: not just the crease pattern of Figure 2.16, which you can easily replicate on a larger scale, but also with changing the angles of the generating vertices and the lengths of the edges of the quadrilaterals.

In general, the symmetry of a Huffman grid will be helical, neither pure translation nor pure rotation. By varying the angles of the generating vertex, you can vary the direction of the symmetry. There is one version, however, that gives rise to pure translation and rotational symmetry: the grid that comes from using the mirror-symmetric bird's-foot vertex as the generating vertex. An example of one of these patterns is shown in Figure 2.19, which is based on a generating vertex with sector angles (120°, 60°, 60°, 120°) and crease lengths (1, 2, 3, 2). I will call this

[1] Although the name sounds oxymoronic (how can something be rigid and foldable?), the term means that the *facets* remain flat and rigid and all flexing happens along the folds.

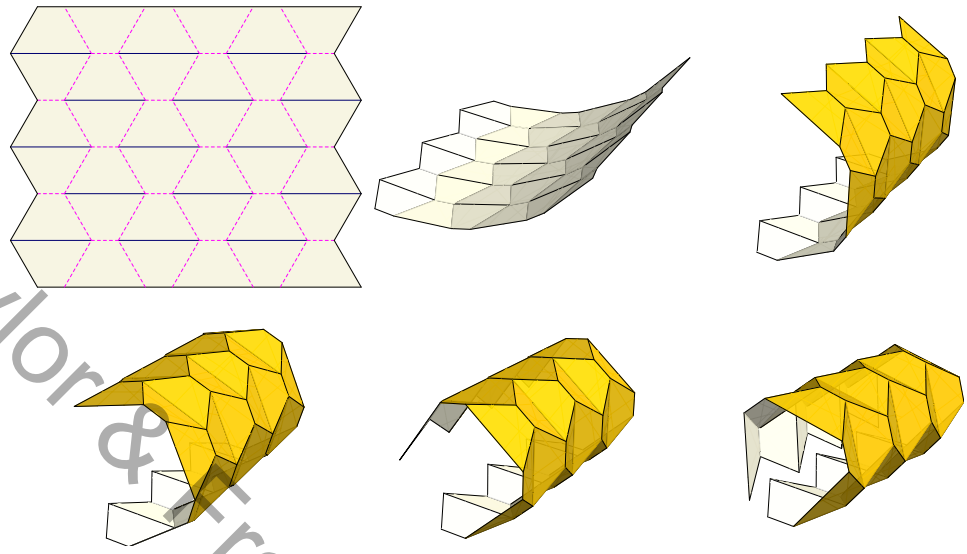

Figure 2.19.
The chicken wire pattern, a Huffman grid constructed from a mirror-symmetric vertex, again parameterized on the angle of the horizontal valley folds.
Top row: left to right, crease pattern and valley folds at 6° and 18°.
Bottom row: left to right, valley folds at 24°, 30°, and 36°.

the *chicken wire* pattern, and versions of it have been around for a long time. (It is closely related to the Yoshimura pattern, which we will shortly meet.) Martin Gardner described a method of achieving the hexagonal pattern of mountain folds (though not the valleys) by coiling paper into a tube and pinching it, and he noted that one of his correspondents reported seeing the method in the 1930s [35, pp. 83, 92].

The chicken wire pattern has pure translational symmetry along the axis of the cylinder and pure rotational symmetry about the axis. Furthermore, as can be seen in the last subfigure, as the pattern curls up, the jagged edge of one side appears to approach mating with the corresponding edge of the other. This is more than appearance; there is going to be a "magic" fold angle at which the teeth meet, and because of the rotational symmetry, if the vertices at the tip of the teeth line up with their corresponding notches, the edges all along the teeth will line up exactly. The value of the magic fold angle will depend on various parameters of the geometry: the angles and distances of the generating vertex, of course, and also upon the number of repetitions in the pattern.

If you examined the crease patterns of Figure 2.16 and 2.19 side by side, you might not even think of them as the same structure. They are, however, the same fundamental concept; it is only the symmetry of the generating vertex in Figure 2.19 that makes it special. This symmetric form, in fact, predates Huffman's work; it was identified in 1970 by Japanese engineer Koryo Miura [86], of whom we will see more shortly.

The general case of this pattern uses a non-symmetric generating vertex that, in general, gives helical symmetry to the grids of quadrilaterals. The general case can also exhibit this behavior that as the valley fold angle is increased, the two serrated edges are brought together, but having the teeth of one side fit into the notches of the other is not guaranteed for all vertices. Rather, there are going to be magic combinations of vertex angles, fold lengths, and numbers of repetitions that give precisely the right helicity for one side to line up with the other.

How many different things can we vary when designing a Huffman grid? We can choose the angles of the generating vertex and the various fold lengths, but as we have already seen, we cannot choose all of them independently. For the general degree-4 vertex, since there is no requirement for flat-foldability, we can choose the first three sector angles ($\alpha_1, \alpha_2, \alpha_3$) nearly arbitrarily, but then the fourth sector angle α_4 is determined. It is given by $\alpha_4 = 2\pi - (\alpha_1 + \alpha_2 + \alpha_3)$, so the first three sector angles must sum to less than 2π. And, of course, the crease assignment must be valid. So that gives three degrees of freedom for angles, plus the number of possible assignments, which, as we saw in the previous chapter, can range from four to eight, depending on what the sector angles are.

For distances, we can pick lengths of two folds of the vertex, but then, as we have seen, the lengths of the other two folds are determined by the intersection of their rotated copies. And, as with the sector angles, we don't have complete freedom to choose fold lengths. Just as the sector angles must all be greater than or equal to zero, in order to create a Huffman grid composed of degree-4 vertices around quadrilateral facets, all four fold lengths must be greater than zero. Figure 2.20 shows what happens as we decrease the length of one of the two folds of the generating vertex. The intersection of the other two folds determines the other two fold lengths, and there comes a point where one of the fold lengths goes to zero—or worse, goes negative.

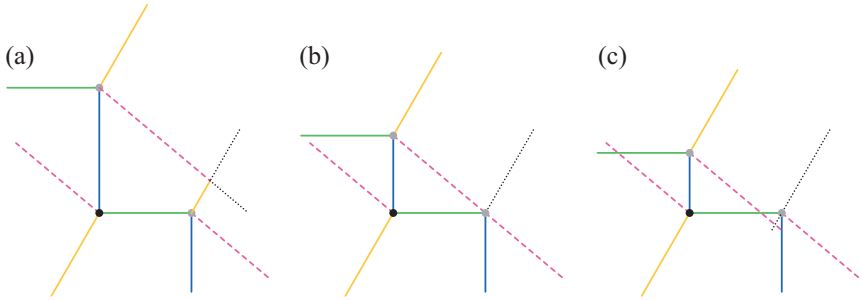

Figure 2.20.
Varying the fold lengths.
(a) All four fold lengths are positive.
(b) The amber mountain fold length has gone to zero.
(c) The amber mountain fold has a negative length, which results in a crossing embedding.

Negative fold lengths are not allowed. In fact, the concept of a "negative fold length" may seem nonsensical, if we are thinking of fold lengths as absolute distance between two vertices. But if we think of a fold length as a *signed distance*, that is, a distance measured in a particular direction, then a negative fold length just means that you're moving in the opposite direction from what you intended, and a negative distance between two vertices simply means the vertices have the wrong order along the line connecting them. That would mean, in general, that the other creases around the vertices intersect with each other in unplanned ways—they cross—and since we have already stipulated that creases must meet only at (predefined) vertices, a solution that gives rise to a negative fold length between two vertices is inconsistent with our definition of what a crease pattern is. Using the language of graph theory, the crease pattern graph has a *crossing embedding*.

So negative fold lengths will be banished from our crease patterns. But something else interesting can happen: the fold length can go to zero, in which case the fold between the two vertices vanishes and the two vertices merge into a single vertex. This is something that can give rise to a valid (and indeed, foldable) crease pattern. If we merge two degree-4 vertices, then we will be left with a degree-6 vertex. We can apply this process to the Huffman grid, and in doing so, we achieve a new pattern composed of degree-6 vertices and triangular facets that also has a rich history in the world of periodic origami: the Yoshimura pattern.

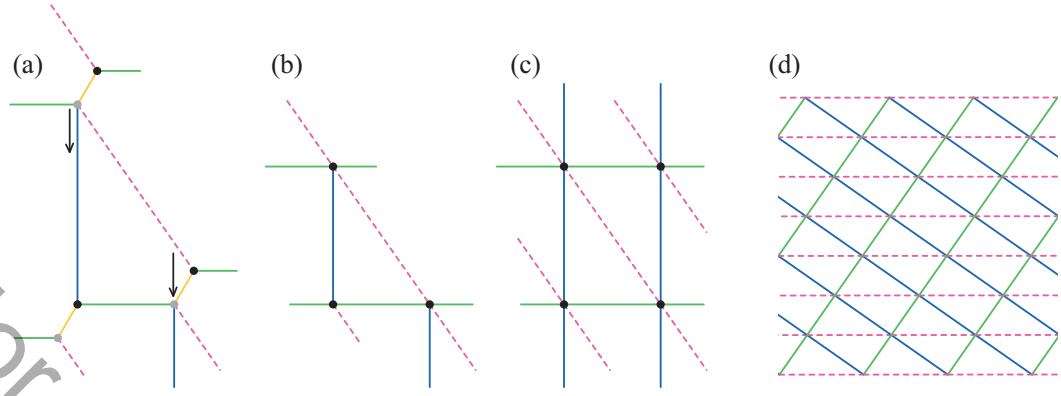

Figure 2.21.
Evolution of the Yoshimura pattern from a Huffman grid.
(a) A quadrilateral of the Huffman grid. We shorten the blue fold until the yellow fold length goes to zero.
(b) The quadrilateral collapses to a triangle.
(c) Extending the pattern.
(d) A larger patch of the pattern, at 50% scale and rotated to make the valley folds horizontal.

⋆ 2.3.2. Yoshimura Pattern

Let's take a generating vertex similar to that of Figure 2.20 and choose fold lengths that take the orange mountain fold length down to zero. In this case, the Huffman grid will collapse to the pattern shown in Figure 2.21, which I have rotated so that the valley folds now run horizontally.

This pattern is called the *Yoshimura pattern* after the Japanese researcher Yoshimaru Yoshimura, who observed it in the buckling pattern of longitudinally stressed cylinders back in the 1950s [129]. Yoshimura wasn't exploring this pattern as a development of the quadrilateral grid; rather, it was a naturally occurring pattern. If you take a cylinder and compress it along its axis, it will eventually buckle. Depending on the material properties and stresses, one of the failure modes is the formation of a diamond-like pattern of folds: the Yoshimura pattern.

To be absolutely precise, though, the original Yoshimura pattern was not the one shown in Figure 2.21; it was one that was rather more symmetric, shown in Figure 2.22. And the original Yoshimura pattern was observed in a closed cylinder, not a flat sheet.

The pattern is undoubtedly much older; it forms naturally in the draping of fabric and can be seen in the left sleeve of the *Mona*

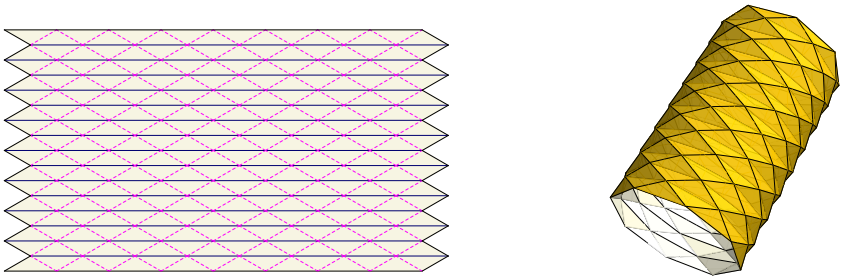

Figure 2.22.
The original Yoshimura pattern.
Left: crease pattern.
Right: folded form.

Lisa, among other places, as shown in Figure 2.23. In fact, the right sleeve looks suspiciously like the chicken wire pattern shown in Figure 2.19.

Figures 2.21 and 2.22 are the same basic crease pattern, the difference being that one is more symmetric than the other. Both display the same behavior, one reminiscent of the Huffman grid; as the valley fold is flexed, the pattern curls cylindrically or helically, as shown in Figure 2.24, which shows the folded form for both patterns.

In general, the Yoshimura pattern is going to show some form of helical symmetry (a mixture of translation along the axis and rotation about the axis) like the Huffman grid. And also like the Huffman grid, a symmetric vertex will give rise to symmetry that is pure rotational in one direction and pure translational in the other.

Unlike the Huffman grid, though, which has a single degree of freedom, the Yoshimura pattern has multiple degrees of freedom

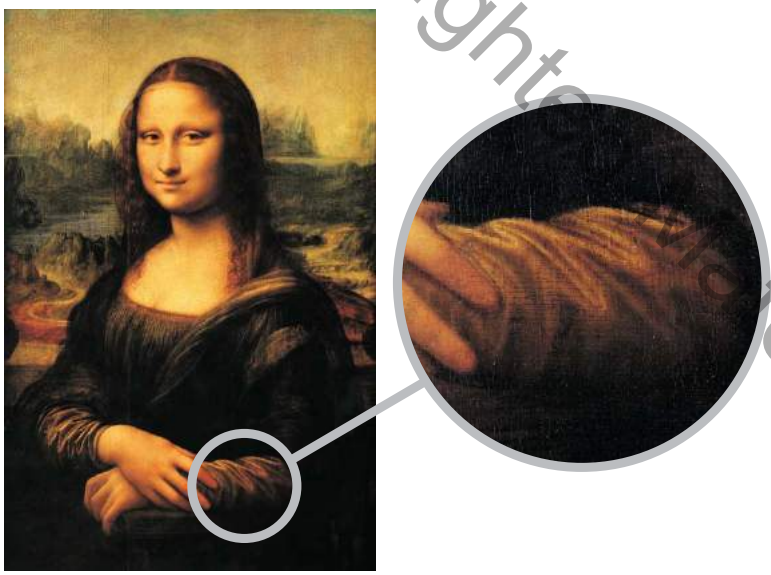

Figure 2.23.
The *Mona Lisa*, by Leonardo da Vinci. A close-up of the sleeve reveals the cylindrical buckling pattern that we now call the Yoshimura pattern, mixed, a bit, with the chicken wire pattern.

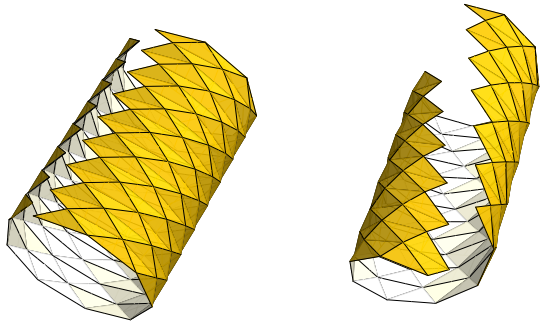

Figure 2.24.
Left: the symmetric Yoshimura pattern, slightly opened from Figure 2.22.
Right: the asymmetric pattern, showing its helical symmetry.

if its edges are unconstrained, i.e., if it is folded from a sheet, rather than a closed cylinder. When the edges are joined to make a cylinder, it becomes rigid, but when the edges are unconstrained, the pattern is quite bendy, even if all of the triangular faces are individually rigid.

This additional flexibility comes about because each of the vertices has multiple degrees of freedom. The number of degrees of freedom in a vertex of degree n is $n - 3$. A degree-4 vertex, such as that of the Huffman grid, has a single degree of freedom. In the Yoshimura pattern, the vertices are degree-6, which would suggest that each vertex has a total of three degrees of freedom.

But wait: suppose we are seeking symmetric solutions—those with translational, rotational, or helical symmetry. Then all the vertices need to work together, connected to one another by folds whose angles must be consistent. If we assume a single vertex that is replicated everywhere, then we must make sure that fold angles and the sector angles between them are consistent from vertex to vertex.

Let's look at the question of just how general the Yoshimura pattern can get. Figure 2.25 shows a patch of the Yoshimura pattern composed of identical vertices but with all four mountain folds colored distinctly (and with different sector angles around the vertex).

This pattern can be built up from a building block that is a quadrilateral of four mountain folds whose diagonal is crossed by a single valley fold. The mountain folds can all be different lengths and have different fold angles. But there is only one valley fold in the building block, which shows up twice in each vertex.

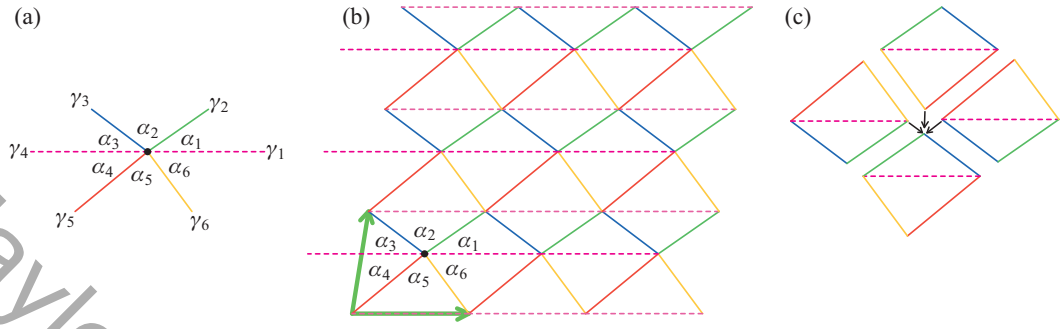

Figure 2.25.
(a) A general Yoshimura-pattern vertex, with sector angles $\alpha_1, \ldots, \alpha_6$ and fold angles $\gamma_1, \ldots, \gamma_6$.
(b) A patch of a general Yoshimura pattern. Sector angles are labeled; periodicity vectors are shown in green.
(c) Four quadrilaterals come together at each vertex.

We don't have three degrees of freedom at each vertex if the structure is periodic, because the two valley folds γ_1 and γ_4 must have the same fold angle. That takes away a degree. In general, for a given pattern, we can choose *two* fold angles (say, γ_2 and γ_6); then every other angle is determined. (In Chapter 8 we will see how to calculate those other fold angles.)

In Figure 2.25, those two valley folds are collinear. Is this coincidence, or must it always be so? Looking at Figure 2.25(c), we see that if each vertex is built up from copies of the same quadrilateral, then the geometry of the construction dictates that the valley folds are all parallel to one another. And that means that folds γ_1 and γ_4 must indeed be parallel.

This, in turn, places constraints on the sector angles. We cannot choose them arbitrarily; rather, we must have that

$$\alpha_1 + \alpha_2 + \alpha_3 = 180^\circ \quad \text{and} \quad \alpha_4 + \alpha_5 + \alpha_6 = 180^\circ. \tag{2.1}$$

So, in the design of the pattern, we can choose any two of the first three angles and any two of the second three, and at that point, all six sector angles will be determined.

What about the fold lengths? Now, in the Huffman grid, we could choose the lengths of two folds, but the other two were determined by fold intersections. Here, we have six folds around each vertex, so potentially six lengths to choose. But we also have many requirements on the intersections between folds.

In fact, if we choose the length of the valley fold and choose all of the sector angles, all four mountain fold lengths are deter-

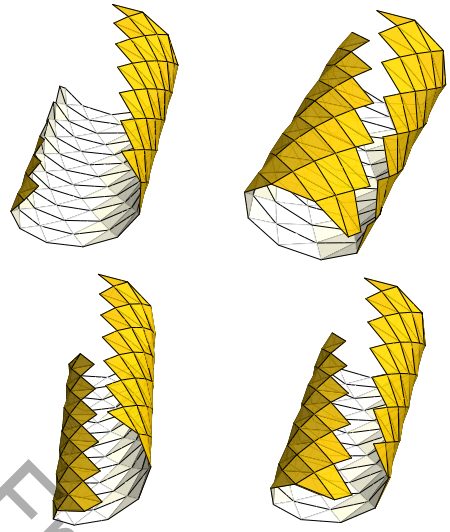

Figure 2.26.
The asymmetric Yoshimura pattern for different values of the two mountain folds γ_2 and γ_6.
Top left:
$(\gamma_2, \gamma_6) = (25°, 25°)$.
Top right:
$(\gamma_2, \gamma_6) = (25°, 35°)$.
Bottom left:
$(\gamma_2, \gamma_6) = (35°, 25°)$.
Bottom right:
$(\gamma_2, \gamma_6) = (30°, 30°)$.

mined. Take a look at one of the quadrilaterals in Figure 2.25(c). Extending upward from the endpoints of the valley fold are folds γ_2 (from the left) and γ_3 (from the right); their intersection defines the lengths of both mountain folds. The same goes for the two folds extending downward, γ_6 and γ_5. So a single length, that of the valley fold, and four of the six sector angles entirely define the crease pattern.

Now, in the folded form, even if we demand periodicity, we still have two degrees of freedom; we can choose, for example, γ_2 and γ_6 independently. Varying these two angles affects the amount of curl in the pattern, but also the helicity. Figure 2.26 shows the pattern of Figure 2.21 with four different values of the two angles.

Comparing the figures in the upper right and lower left in particular, you can see that the primary difference is a helical shift. The teeth coming from each edge of the paper are about the same distance apart, but they are shifted laterally with respect to each other. That means that for any Yoshimura pattern, there is going to be *some* set of fold angles that brings the edges together, thereby creating a tube (and if the edges are joined, a rigid tube).

If we join the ends of the sheet, it becomes quite rigid—there are no degrees of freedom at all. In fact, it becomes considerably stronger than a smooth cylinder of the same diameter from the same material. This property means that this pattern has practical applications. It was used for a soft drink can for a Japanese brand, shown in Figure 2.27.

Figure 2.27.
A Japanese soft drink can based on the Yoshimura pattern.

The pattern in the soft drink can has several beneficial effects. First, there is the purely decorative one; it's a lovely pattern. Not clear from this picture is the fact that with carbonated beverages, the can is under pressure and the pattern is smoothed out; when the can is opened, the pattern pops into high relief. More practically, the strengthening provided by the truss-like structure of folds means that a thinner gauge of metal may be used, allowing for savings of both weight and cost—vital in the consumer goods industry.

Yoshimura identified this pattern in buckling cylinders, but its application to soft drink technology came from someone else: Koryo Miura, who, as already noted, studied and analyzed this pattern and its relatives (like the chicken wire pattern). He did a lot more, discovering, describing, and lending his name to an entire family of structures used for deployable origami. It's about time that we meet him, and them.

⋆ 2.3.3. Miura-ori

In Miura's study of the Yoshimura pattern, he noted that all of the varieties of the pattern exhibited cylindrical curvature as the fold pattern was flexed. If the vertices were mountain-like, as in Figure 2.25, then the curvature would be convex toward the viewer; if the fold parities were flipped, then the curvature would be concave toward the viewer. He further observed that one could splice together a convex and a concave portion of the crease pattern, giving rise to a pattern that curled both ways, as illustrated in Figures 2.28 and 2.29.

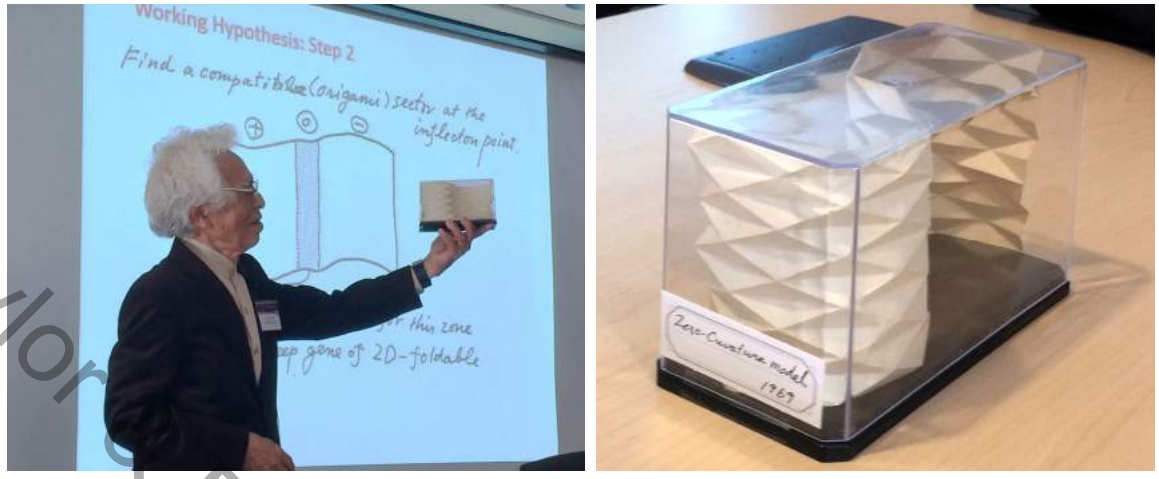

Figure 2.28.
Left: Koryo Miura demonstrating his original model of the Yoshimura pattern including a change of curvature.
Right: close-up of the model.

There is an interesting detail in the way the two halves of the pattern are spliced together. It is not as simple as reversing the crease parity on one side of the Yoshimura pattern. Rather, the pattern is split; half of it is crease-reversed; and then the two halves are offset relative to one another by half of the vertical periodicity before being rejoined, as illustrated in Figure 2.30.

The reversal/offsetting/splice operation creates a new set of shapes within the pattern, a vertical row of parallelograms, which you can see in the very middle of Figure 2.30(d). It also alters the vertices in the middle, changing their degree from 6 to 4.

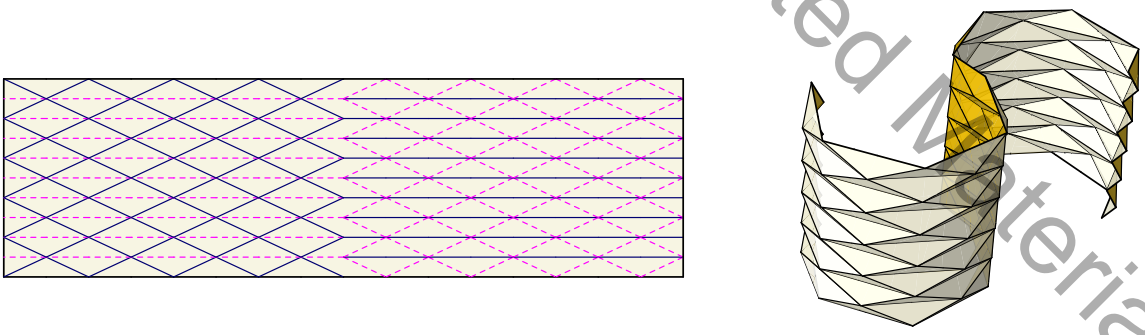

Figure 2.29.
Left: crease pattern for the reversing Yoshimura pattern.
Right: folded form.

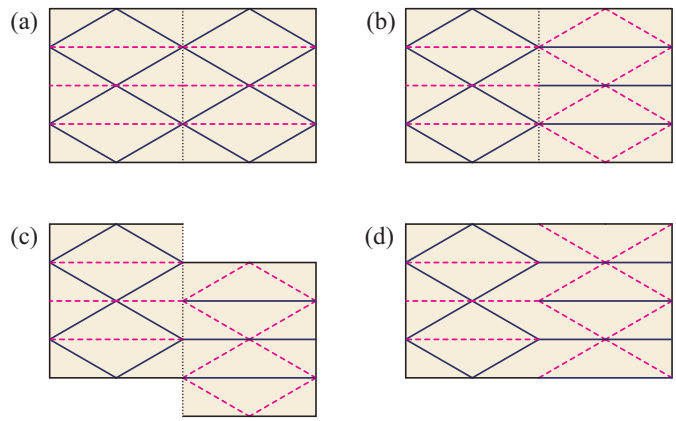

Figure 2.30.
Sequence for reversing half of a Yoshimura pattern.
(a) Divide the pattern in half.
(b) Invert the crease parity in one half.
(c) Offset one half of the pattern.
(d) Rejoin the two halves, extending and removing the pattern to keep the paper rectangular.

This construction allows one to reverse the curvature of the Yoshimura pattern. We focus our attention on the diagonal creases. On the left side, each zigzag diagonal mountain fold imparts some large-scale convex cylindrical curvature to the pattern. On the right side, each zigzag diagonal valley fold imparts large-scale concave curvature. Where the two zigzags occur side by side in the middle, the two curvatures cancel each other out, and so the middle of the paper appears to have no net curvature.

Miura realized that if one built a pattern consisting of alternating mountain and valley zigzags, i.e., reproducing just the pattern in the middle of Figure 2.30, it would produce a pattern with no net curvature, resulting in a pattern that opens and closes while maintaining a roughly planar configuration. And indeed, that is precisely the case, as Figure 2.31 shows.

This pattern, the *Miura-ori*, has become famous within the world of applied origami and has become a regular workhorse of deployable structures. Indeed, Miura himself proposed it for use in a solar array, in a mission for JAXA, the Japanese space agency, that flew in 1995 [87].

A key feature of the Miura-ori is that it folds rigidly with a single degree of freedom, meaning that if the facets of the pattern were perfectly stiff, then the entire pattern could fold and unfold

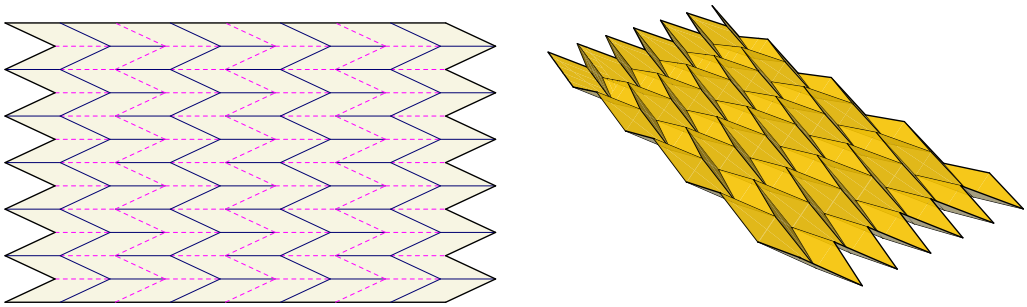

Figure 2.31.
Left: crease pattern for a Miura-ori pattern.
Right: partially folded form (turned over).

in a single motion. Flexing any one panel would be sufficient to actuate every crease in the pattern. In practice, small deviations from ideality—stiffness of the folds, bending of the facets, and so forth—prevents the perfect coupling of all of the folds, but the tendency of them to all move together greatly facilitates the deployment of mechanisms based on the Miura-ori. Why this is the case—that the pattern is rigidly foldable, and that it has a single degree of freedom—will have to wait until Chapters 7 and 8—but we can explore many of the properties of Miura-oris by analyzing their static unfolded and folded forms.

The Miura-ori is more than this specific pattern; it is a family of patterns, because we may vary several parameters while preserving the basic properties of in-plane deployment motion and flat-foldability. The crease pattern is composed of parallelograms, arranged in rows and columns, with the creases forming a set of zigzag lines that run one way and collinear lines that run the other. The zigzag folds are all the same parity along a single zigzag line, with the lines alternating mountain and valley from one to the next. The horizontal folds, by contrast, while collinear, alternate mountain/valley along each segment of each horizontal line.

By convention, we will call the same-parity-along-the-fold zigzag folds of a Miura-ori the *major* folds of the pattern, and the alternating-parity straight folds the *minor* folds. (We will meet the justification for these names in Chapter 7.) It turns out that the fold angles along the major folds are the same all along the fold, and the mountain and valley major fold angles are equal and opposite. This is also the case for the minor fold angles (mountain and valley fold angles are equal and opposite), but in general, the

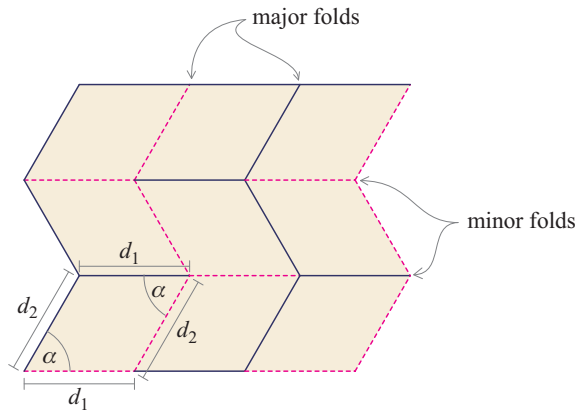

Figure 2.32. Characteristic dimensions and terminology of a symmetric Miura-ori crease pattern.

major and minor fold angles are different from each other for any non-flat state of foldedness.

With these constraints on folds and the assumption that the pattern is doubly periodic, there are only three additional parameters that, when chosen, fully define the crease pattern:

- the length d_1 of a minor fold,
- the length d_2 of a major fold,
- the angle α between horizontal and zigzag folds,

as shown in Figure 2.32. By convention, we can choose the angle α to be the acute angle, so that the four angles of each parallelogram are α (two each) and $180° - \alpha$ (also two each).

Any of these parameters can be varied, and they will affect the dimensions of the crease pattern and folded form (of course); less obviously, they affect the way that the mechanism deploys. A detailed analysis of the latter must await further analytical development, but it is useful to construct different examples from stiff paper (scoring the creases) and play with them to get a feel for the differences.

The particular parameters ($d_1 = 1, d_2 = 1, \alpha = 60°$) give rise to a very symmetric version of the Miura-ori that we may adopt as a "baseline" form. A 6×6 version of this pattern is illustrated in Figure 2.33 as a crease pattern, partially folded form with a minor fold angle of 90°, and nearly completely folded form with a minor fold angle of 170°.

Figure 2.34 shows another 6×6 array with $\alpha = 80°$. As the characteristic angle α gets larger, several things happen, all visible

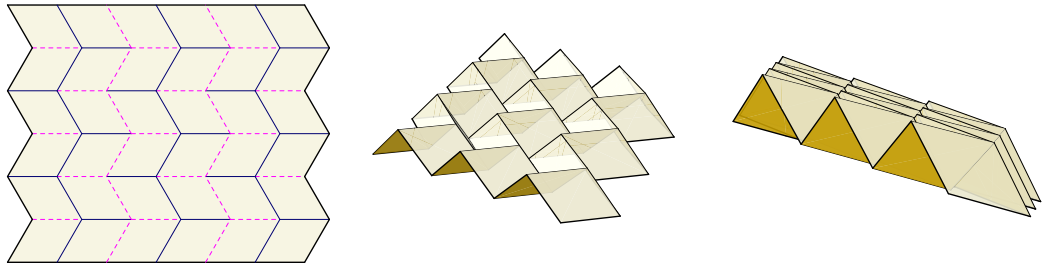

Figure 2.33.
Left: crease pattern for a Miura-ori pattern with ($d_1 = 1, d_2 = 1, \alpha = 60°$).
Middle: partially folded form.
Right: nearly fully folded form.

in the figure: the individual parallelograms approach rectangles, and the fully folded form becomes shorter along its length. Conversely, at any given point in the fully folded form, there are more layers as more of the facets mutually overlap. So, as a deployable structure, larger α gives a more efficient stowed form. There is, however, a tradeoff, which can be seen in the middle subfigure of Figure 2.34. While the minor creases are partially folded (with a fold angle of 90°), the major creases are nearly fully folded. As the characteristic angle increases, the folding motion takes on two distinct forms. As you start to fold the crease pattern, most of the action happens on the major folds. Then, as they are nearly folded, the minor folds undergo most of their motion. This two-stage motion decreases the coupling between the major and minor folds, and it can give rise to undesired compliance in a folding structure with very large values of α.

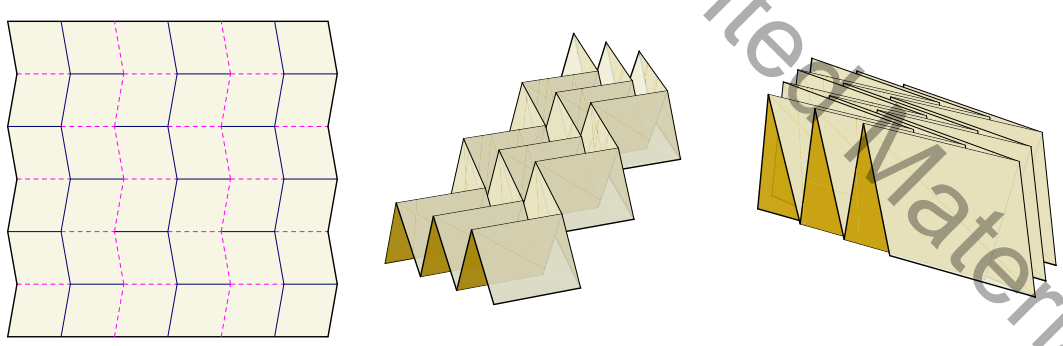

Figure 2.34.
Left: crease pattern for a Miura-ori pattern with ($d_1 = 1, d_2 = 1, \alpha = 80°$).
Middle: partially folded form.
Right: nearly fully folded form.

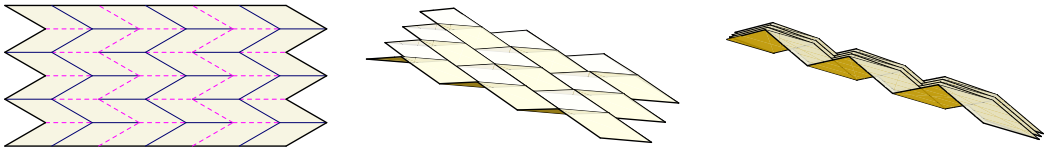

Figure 2.35.
Left: crease pattern for a Miura-ori pattern with ($d_1 = 1, d_2 = 1, \alpha = 30°$).
Middle: partially folded form.
Right: nearly fully folded form.

In fact, the limiting value of α is $\alpha = 90°$, at which point the facets become purely rectangular and the major and minor folds become entirely uncoupled. An $\alpha = 90°$ Miura-ori can be created by pleating the paper in one direction, like a fan (making the major folds), then pleating the fan in the opposite direction (making the minor folds). This process gives the smallest possible package—every facet overlaps every other facet precisely—but at the cost of completely decoupling the major and minor folds and losing the desirable single-degree-of-freedom motion offered by the Miura-ori.

We could also go the other direction, making α smaller. An example with $\alpha = 30°$ is shown in Figure 2.35. Not surprisingly, the pattern is stretched out, rather than compressed, and the major and minor folds vary at closer to the same rate.

The other variable parameters are the two distances d_1 and d_2. These can be independently varied, although what matters is their ratio. Figure 2.36 shows the effect of varying their ratio; compare these to Figure 2.33.

It is a very common occurrence in the world of origami that one may discover a structure or mechanism, only to find that someone else came up with the exact same thing by an entirely different route. As already noted, the Yoshimura pattern forms naturally via compressive deformation of a cylindrical surface. It should not be too surprising that the Miura-ori concept has also been found before. Figure 2.37 shows a figure from a 1959 patent by Henry Hochfeld for "Process and Machine for Pleating Pliable Materials" [46]. Not only does it show what is clearly a Miura-ori pattern, but it even describes a machine for creating the same.

In fact, similar folded patterns may be seen in much older forms, going back to 16th-century decorative napkin-folding [106]. Mattia Giegher's 1639 work *Li Tre Trattati* (Three Trea-

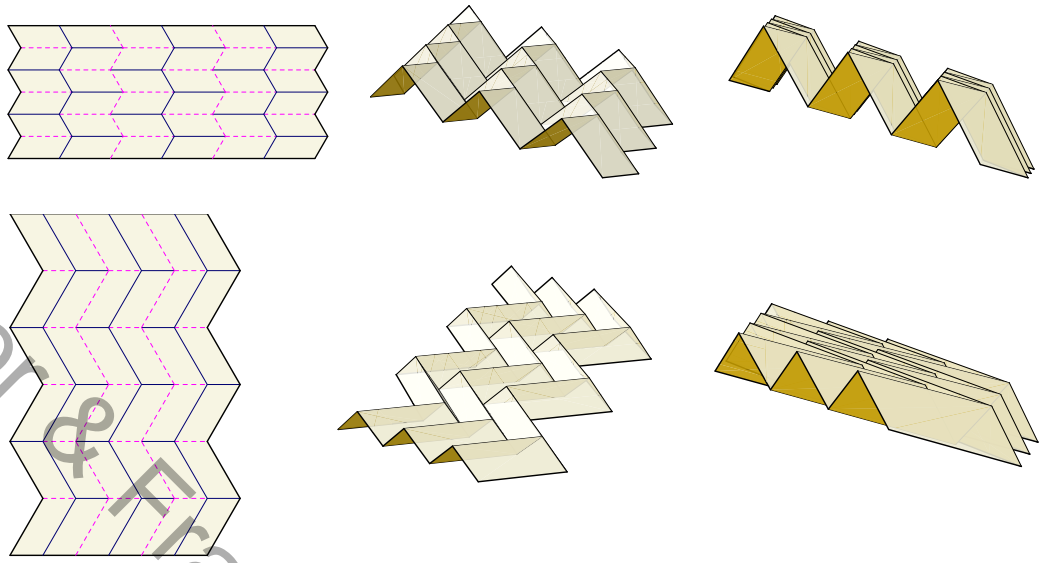

Figure 2.36.
Top row: a Miura-ori pattern with ($d_1 = 2, d_2 = 1, \alpha = 60°$).
Bottom row: a Miura-ori pattern with ($d_1 = 2, d_2 = 2, \alpha = 60°$).
Left: crease pattern.
Middle: partially folded form.
Right: nearly fully folded form.

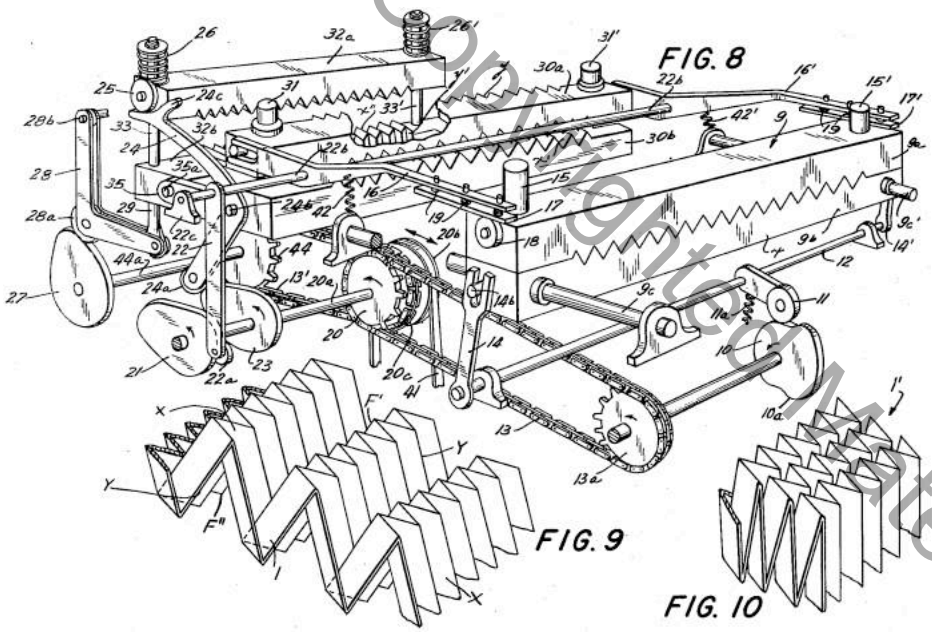

Figure 2.37.
A figure from Henry Hochfeld's 1959 patent on folding pleated materials, showing a version of the Miura-ori.

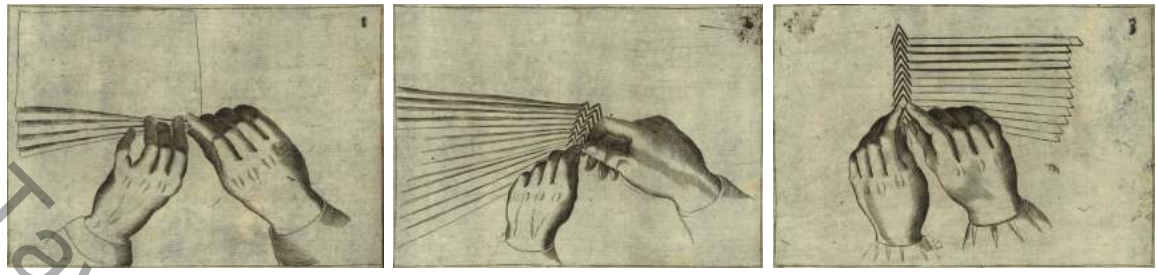

Figure 2.38.
How to fold a pleated sheet into a Miura-ori, from *Li Tre Trattati*, 1639.

tises) on table decoration using napkin-folding shows how one folds a pleated napkin into what is unmistakably a Miuri-ori, as seen in Figure 2.38.

(One might cry foul, that the folding of starched napkins isn't the same as paper-folding. However, Giegher taught these techniques at the University of Padua, and he almost certainly taught his pupils using paper as a practice material. So, not only was this an example of early European "origami," Giegher's course might have been the original university origami curriculum![2])

The Miura-ori pattern shows up again and again over time, whenever people have been exploring the folding of paper. Examples of Miura-ori appear in the work of Josef Albers's students of the Bauhaus school of the 1920s [128, p. 435] and in quite a few patents from 1958 to the present [121, 46, 36, 16, 64]. It was Miura, however, who recognized the generalization and application of the pattern, and it is still perhaps appropriate that his name is the one permanently attached to the concept.

⋆ 2.3.4. Miura-ori Variations

I started the previous subsection by pointing out the relationship between the Miura-ori and the Yoshimura pattern; if we join two Yoshimura patterns with the same angle α but opposite parity, the building block of the Miura-ori provides the "glue" to create the joint. The relationship goes deeper than that, though, because there is a fortuitous seeming coincidence involved in such a splice: when we cut and reassemble the two half-patterns with offsets, we create a new set of vertices along the join line—and there is no *a priori* reason to expect that vertices assembled in such a way

[2] I am indebted to origami historian Joan Sallas for background on Giegher.

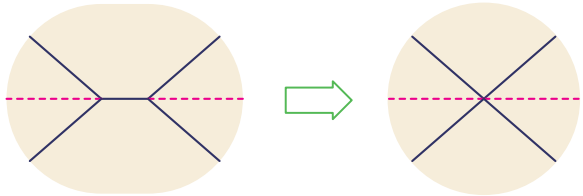

Figure 2.39.
Two back-to-back degree-4 Miura-ori vertices, when merged, give rise to a degree-6 Yoshimura pattern vertex.

would be flat-foldable, let alone possessing of compatible fold angles at all stages of partial folding.

But the vertices of the Miura-ori and those of the Yoshimura pattern are compatible; if we chop a Yoshimura pattern in half, the sector angles and fold angles around the newly created vertices are such that after reassembly, the former add up to 360° and the latter match along the joints.

We can see this by approaching such a joint from another direction: by placing two degree-4 vertices of a Miura-ori at opposite ends of a line and collapsing the line segment between them, similarly to how we went from the Huffman grid (of quadrilaterals) to the Yoshimura pattern (of triangles) as was shown in Figure 2.20. This process of collapse is illustrated in Figure 2.39.

We take two Miura-ori vertices of the same type (here, mountain-like) so that a common minor fold connects them back to back. If their common fold has the same position within each vertex relative to the other folds at the vertex, then we can be assured that the fold angles of the two vertices match at all positions from unfolded to folded. If we now shorten the length of the fold between the two vertices, we will arrive at a degree-6 vertex, in which the upper and lower triangles (that touch at only a vertex) have the same angular relationship to each other as the two corresponding connected facets of the Miura-ori.

The other three folds of each Miura-ori vertex then become the six folds of the Yoshimura vertex, and since the fold angles were mutually compatible before the merge, they must be similarly compatible after the merge. Thus, the fold angles of a Miura-ori with characteristic angle α form a set of compatible fold angles of a Yoshimura vertex based on the same sector angle.

(It is important to note, though, that we can't necessarily go the other way. A degree-6 vertex has two degrees of freedom in

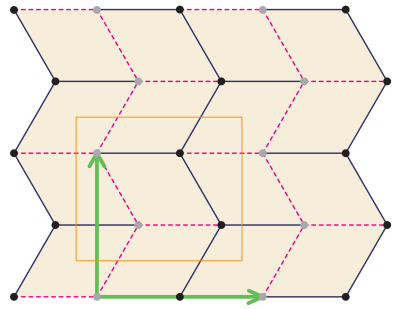

Figure 2.40.
The periodicity vectors (green) and tile (orange) for the Miura-ori.

its partially folded state, and every possible configuration cannot necessarily be split into two degree-4 vertices.)

The Miura-ori, like the Yoshimura pattern and the Huffman grid, is 2D periodic, and it is instructive to identify both the periodicity vectors and a single tile of the pattern. Figure 2.40 shows both for the ($d_1 = 1, d_2 = 1, \alpha = 60°$) Miura-ori.

A single tile of the Miura-ori contains two each of mountain-like and valley-like vertices. That allows for still more variation while preserving 2D periodicity. For example, we can choose all four lengths around each vertex to have different values if we are careful to construct the mountain and valley vertices in pairs with the same relative lengths, as in Figure 2.41.

This pattern has a significant qualitative difference from the previous Miura-oris. First, in all of the previous examples, all of the major folds lay in one of two common planes along the top and bottom in all stages of partial folding. In this example, though, the

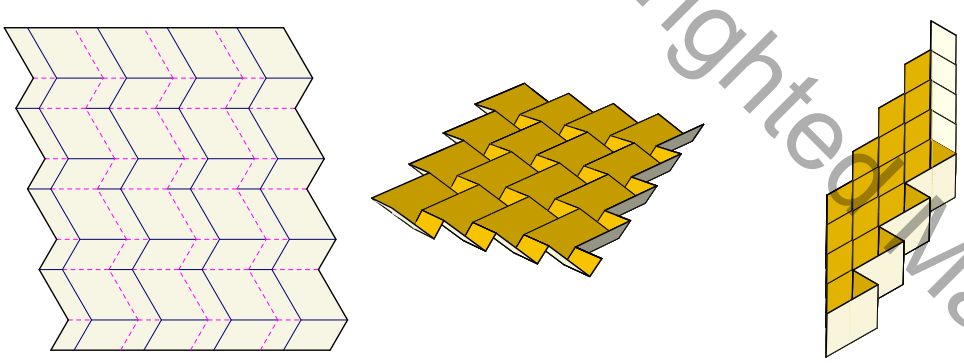

Figure 2.41.
A Miura-ori pattern with four fold lengths around each vertex: ($d_1 = 1, d_2 = 1.5, d_3 = 2, d_4 = 2.5, \alpha = 60°$).
Left: crease pattern.
Middle: partially folded form (turned over).
Right: flat-folded form.

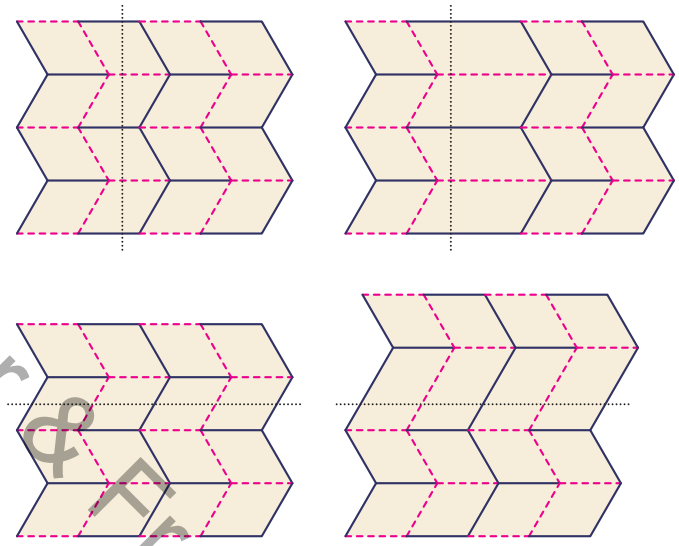

Figure 2.42.
Changing the length of a single row or column of a Miura-ori.
Top: any column can be widened by adding the same amount of length to each horizontal edge in a given column.
Bottom: any row can be widened by adding the same amount of length to each diagonal edge in a given row.

facets are "stair-stepped," with sets of corners, but not full creases, residing in common planes. In the fully folded state, this gives rise to a scale-like overlapping pattern.

It is also clear from this pattern that if we are willing to give up strict periodicity, we can vary this pattern further because we can independently add or subtract length to the folds of any single row or column of quadrilaterals, as illustrated in Figure 2.42. In fact, as this construction makes clear, we should be able to arbitrarily specify the width of each column and height of each row independently. And so we can. But there is yet one more degree of freedom open to us in the design of Miura-ori-like fold patterns, which we will explore first.

⋆ 2.3.5. Barreto's Mars

As already noted, in all of these varieties of the Miura-ori, the vertices have the same geometric configuration: the sector angles are the same around each vertex, in the same order; the crease assignments are mountain-like for half of the vertices and valley-like for the other half; and the fold angles are the same (except

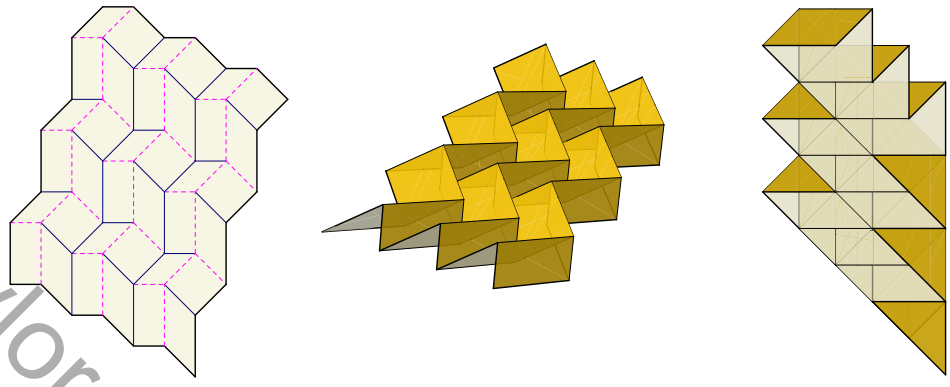

Figure 2.43.
James Minoru Sakoda's "Staircase" pattern (from [105]).
Left: crease pattern.
Middle: partially folded.
Right: flat-folded (different scale).

for sign) for all of the major folds, and the same (except for sign) for all of the minor folds. In all the examples shown thus far, the vertex is a symmetric bird's-foot vertex, and that makes the vertex, and hence, the entire pattern, flat-foldable.

We saw in the previous chapter that a flat-foldable degree-4 vertex does not need to be bird's-foot with two pairs of identical sector angles; in fact, in the general case, the four sector angles can be different, as long as they satisfy the Kawasaki-Justin Condition that opposite angles sum to 180°. That raises the question: is it possible to create a Miura-ori-like pattern, but by using non-symmetric degree-4 vertices?

The answer is yes, and examples of both were presented by James Minoru Sakoda [105] and, especially, Paulo Taborda Barreto [4], at the Second International Meeting of Origami Science and Scientific Origami in 1994. A small patch of Sakoda's "Staircase" pattern is shown in Figure 2.43.

Sakoda's "Staircase" is a specific example of a more general family. Barreto gave several recipes for constructing such patterns, both periodic and non-periodic, which he dubbed the "Mars" family of designs. Both Sakoda's and Barreto's patterns were similar to the Miura-ori in crease assignment—major crease chains that alternated as all-mountain and all-valley, and minor crease chains consisting of alternating mountain and valley—but instead of using a symmetric bird's-foot vertex, they were constructed from a different type of flat-foldable vertex, one illustrated in Figure 2.44.

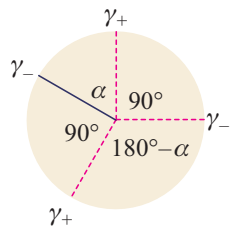

Figure 2.44.
The generating vertex of Sakoda's "Staircase" and Barreto's "Mars" patterns.

The generating vertex for a Mars pattern consists of two opposite 90° angles and two opposite angles that sum to 180°. We can define one of them as α; the other then must be $180° - \alpha$. The vertex is, obviously, flat-foldable. In Sakoda's "Staircase," we have $\alpha = 45°$, but in general, α can take on any value in the range $(0, 90°)$.

As we did with the symmetric bird's-foot vertex of the Miura-ori, we will call the two opposite creases of the same fold type the major creases and the two opposite creases of opposite fold types the minor creases. As with the symmetric bird's-foot vertex, the fold angles of the two major creases are equal, and we will denote its magnitude by γ_+ and its sign by the fold line style. Also as with the symmetric bird's-foot vertex, the fold angles of the two minor creases are equal and opposite, and we will denote their magnitude by γ_-.

To understand the construction of such a pattern, let us try constructing a small patch—a single quadrilateral. We start with a single generating vertex; we then arrange this with copies of itself to create a fully self-consistent crease pattern, and by consistent, I mean one where the crease directions and fold angles leaving one vertex match up with those entering the adjacent vertex. Such an assembly is shown in Figure 2.45.

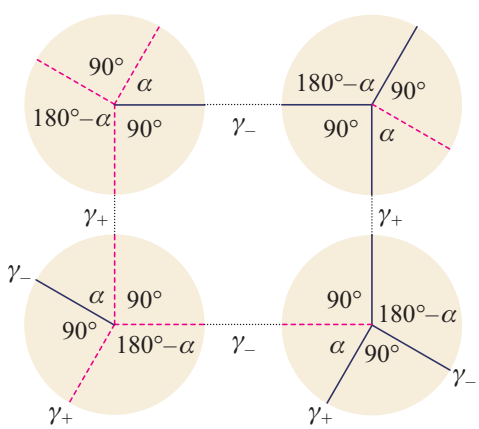

Figure 2.45.
Four copies of the generating vertex (two of each type) can be assembled into a quadrilateral with matching fold directions and angles.

If we are aiming for a flat-folded periodic pattern, then the only thing that matters is the fold direction: mountain or valley. But if we are seeking a structure that will be used in the partially folded state, then we need to match in both fold parity and in the actual value of the fold angle, which is somewhere between 0° and +180° for a valley fold and between 0° and −180° for a mountain fold. We'll learn how to compute the fold angles and their relationship to one another in subsequent chapters, but we can get the matching right from a purely qualitative consideration, ensuring that we only line up major creases with other major creases of the same fold angle and parity, and similarly with minor creases.

We can build up the crease pattern by arranging copies of the vertex—some mountain-like, some valley-like—so that their fold angles line up with each other by (a) being collinear, (b) having the same fold parity, and (c) matching in fold angle. In order to form a closed polygon, we need two copies of each type of vertex: two each of mountain- and valley-like versions of the original vertex.

As we continue to build up the crease pattern, it will consist of rectangles and parallelograms, as you can see in Figure 2.43. Both types of polygon have the property that opposite edge lengths are equal. That means that, as in the Miura-ori, within a single column of quadrilaterals, every crease that cuts across the column has the same length (these were the horizontals in the Miura-ori; in this pattern they are horizontal and tilted, in alternating columns). Similarly, within a single row, every crease that cuts across the row also has the same length.

This property means that we don't have a lot of freedom to choose crease lengths in the pattern; once we've chosen a single length within a row or column, all of the corresponding lengths within that row or column are forced to be the same value, as illustrated in Figure 2.46.

That, in turn, means that we can construct a complete crease pattern by choosing just the edge lengths along the bottom and left side—the two zigzagging green lines in Figure 2.46. Once we have chosen those two lines, which we will call the *generating lines* of the crease pattern, the complete pattern is fully determined.

Better yet, it is very easily constructed. Looking closer at Figure 2.46, we see that all of the chains of major crease lines are identical in shape; each is just a shifted (and crease-reversed) version of its neighbor. The same goes for the chains of minor crease

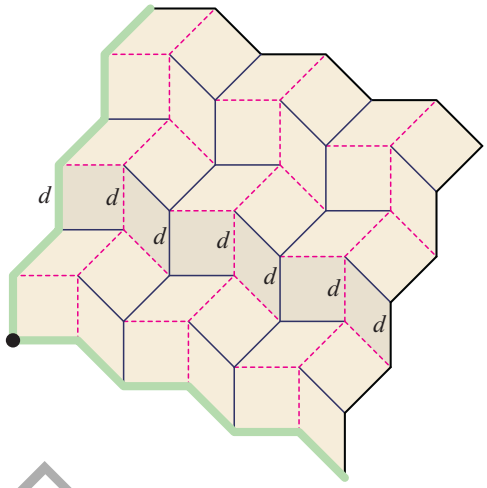

Figure 2.46.
Distance propagation within the "Staircase" pattern. Every vertical crease within the darker row has the same length d.

lines. This property gives rise to a simple geometric construction algorithm that can be carried out with nothing more than pencil, paper, and protractor, as illustrated in Figure 2.47.

In Barreto's algorithm described in [4], the generating lines are drawn on a grid, which automatically sets α to be 45°, and the second generating line is chosen to be a rotated copy of the first. Using this algorithm, Barreto created many beautiful works. A computed reconstruction of one of them, "MarsJoker" (1994), is shown in Figure 2.48.

It is not necessary to make one of the generating lines a rotated copy of the other; distances along both can be chosen arbitrarily. The only requirement for the algorithm in Figure 2.47 is that the angles at the vertices along both generating lines have the same value, which is based on the generating vertex for the pattern.

A similar algorithm works for a generalized version of the Miura-ori. In this case, the construction is simpler, because the minor creases are purely horizontal and the major creases zigzag back and forth. A simple example of a varying-distance Miura-ori is shown in Figure 2.49.

⋆ 2.3.6. Generalized Mars

The next logical step in exploring variations of the Miura-ori would be to consider flat-foldable vertices that are not bird's-foot nor have a 90° sector angle.

The basic concept is the same as for Mars patterns; we create mountain-like and valley-like versions of the generating vertex, then arrange them so that major and minor fold angles match up in

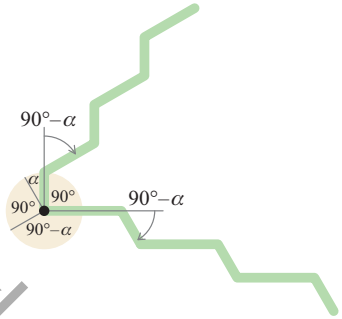

1. Start with the generating vertex at the dot and draw two generating lines, initially at right angles. You can add the bends anywhere you like, but all of the alternating bend angles should be equal.

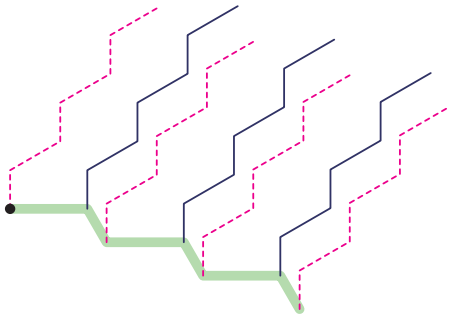

2. Create copies of the left generating line and place one copy at each vertex of the lower generating line, assigning them to be alternately mountain and valley folds.

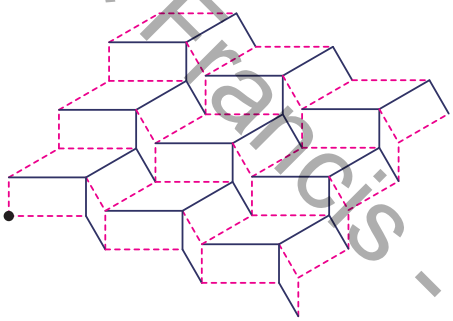

3. Create copies of the bottom generating line and place one copy at each vertex of the left generating line, alternating mountain and valley within each copy and from one copy to the next.

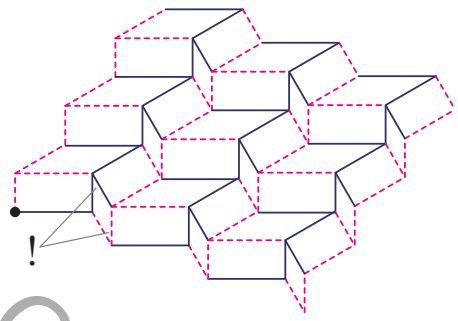

4. If, as in this example, the acute angle at each vertex has the (non-flat-foldable) iso assignment, you can swap the crease assignment of all of the bottom-generating-line copies to fix it.

Figure 2.47.
Construction sequence for a Mars-type origami pattern.

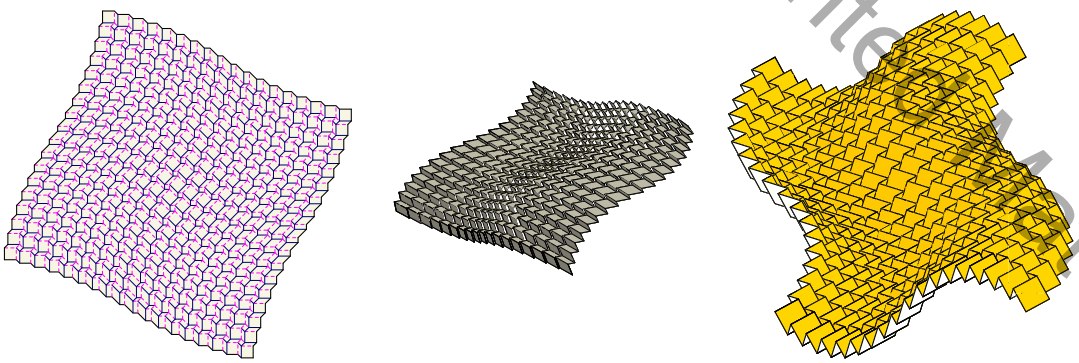

Figure 2.48.
Left: crease pattern for Barreto's "MarsJoker."
Middle: partially folded form.
Right: flat-folded form (turned over).

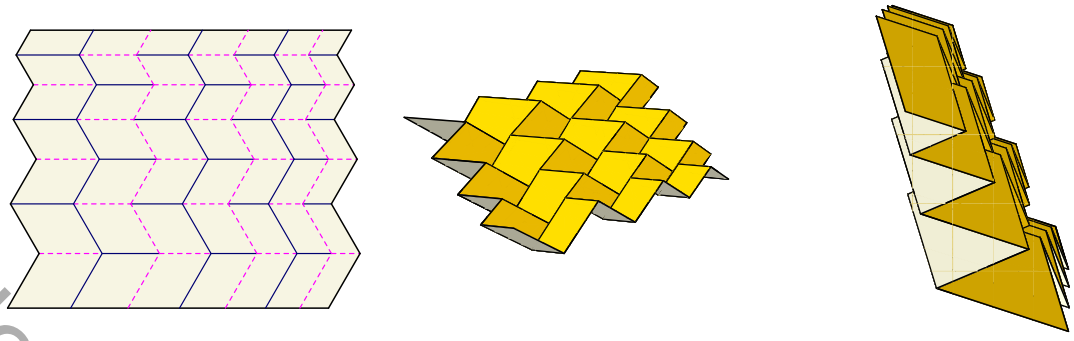

Figure 2.49.
Left: crease pattern for a varying-distance Miura-ori.
Middle: partially folded form (turned over).
Right: flat-folded form.

both angular value and fold direction. Figure 2.50 shows a general flat-foldable vertex and an arrangement of four copies that meets these requirements.

There are two notable differences from the corresponding configuration for the Mars construction. If the generating vertex is valley-like, then the two mountain-like vertices must be the *mirror images* of the valley-like vertices (they are also rotated, of course). You can see the mirror reversal in the figure; in the valley-like vertices, the sector angles α_1–α_4 circulate counterclockwise around their vertex, while in the two mountain-like vertices, they circulate counterclockwise.

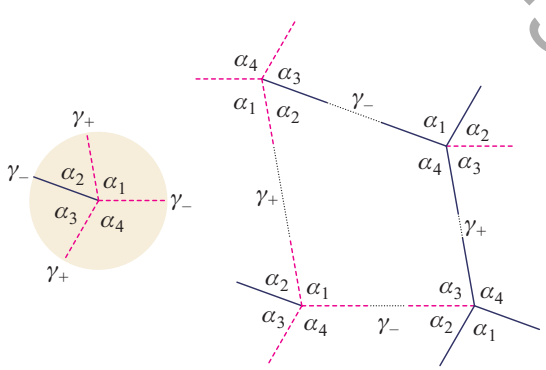

Figure 2.50.
Constructing a generalized Mars pattern from a generating vertex.
Left: the generating vertex.
Right: four versions of the vertex can be arranged to create a closed quadrilateral where the folds match in both direction and fold angle.

This construction is a generalization of the construction in Figure 2.45; in point of fact, the mountain-like vertices in that construction must also be mirror-images of the valley-like generating vertex. However, since a flat-foldable degree-4 vertex with a 90° angle is its own mirror image (plus a rotation), one can simply use rotated copies of the original vertex when constructing a Mars pattern—or for that matter, when constructing a Miura-ori, since the symmetric bird's-foot vertex is also its own mirror image.

For a general vertex, though, the mirror images must be explicit, as in Figure 2.50.

There is another difference, though. In Figure 2.45, the polygons were parallelograms and so every column-crossing crease had the same length within a single column and every row-crossing crease had the same length within a single row. But now, in Figure 2.50, opposite edges of each quadrilateral have different lengths.

This has ramifications for the construction of the crease pattern. Opposite edges of each quadrilateral are no longer necessarily equal, but they are still determined; if we have two edges, then the other two are fully specified, just as we saw in the Huffman grid.

So, to construct such a pattern, we can still start with two generating lines, as before, as illustrated in Figure 2.51. But now the edge lengths are found by projecting the lines from the two adjacent vertices and finding their intersection, as illustrated in the figure for the vertex at the gray dot.

By constructing each vertex from its neighbors, one can iteratively build up the crease pattern, but instead of copying and moving lines, as in Figure 2.47, one must build up the pattern one vertex at a time. Figure 2.52 shows a small patch of such a pattern.

For this pattern, the segments of the generating lines were taken to have unit length, but as the pattern propagates from the lower left toward the upper right, some edges get longer, some shorter, and had we continued this pattern further to the right, two or more chains of minor folds would have eventually crossed, breaking the pattern. So, while it is technically feasible to construct generalized Mars patterns, the deterministic variation in the quadrilateral dimensions limits the flexibility and, in some cases, the sizes of the possible patterns.

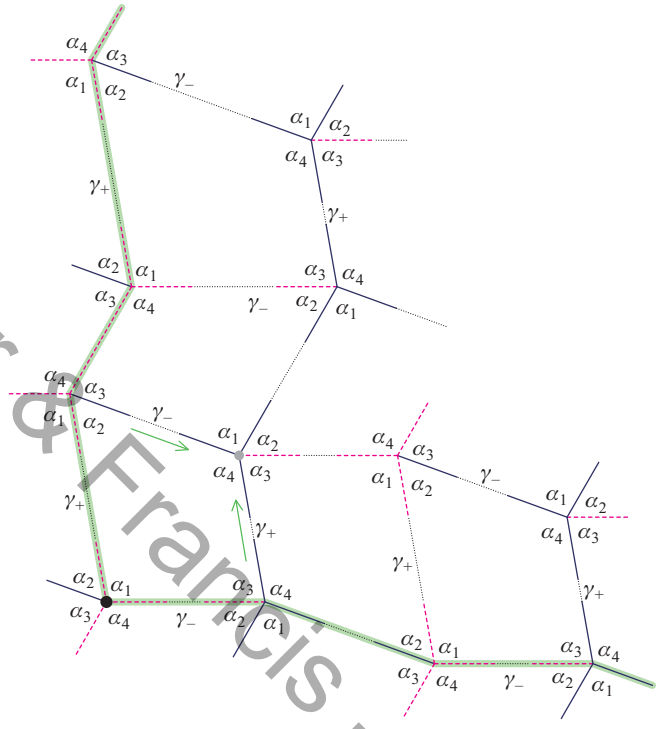

Figure 2.51.
Construction of a generalized Mars pattern from a non-mirror-symmetric generating vertex (black dot) and two generating lines (green). Each vertex is at the intersection of two lines emanating from previously-defined vertices.

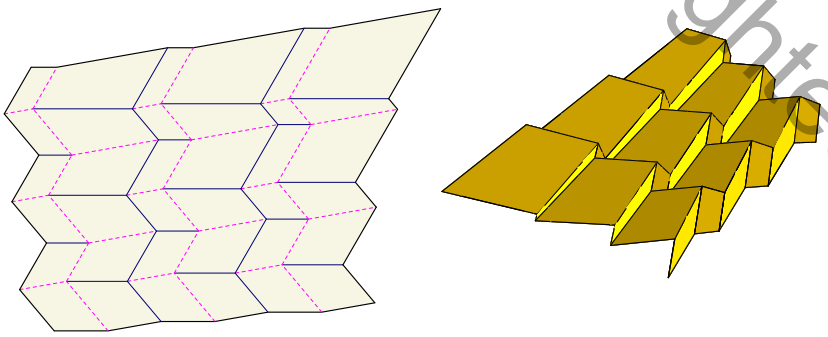

Figure 2.52.
A generalized Mars pattern for a generating vertex with sector angles (130°, 60°, 50°, 120°).
Left: crease pattern.
Right: partially folded form (turned over).

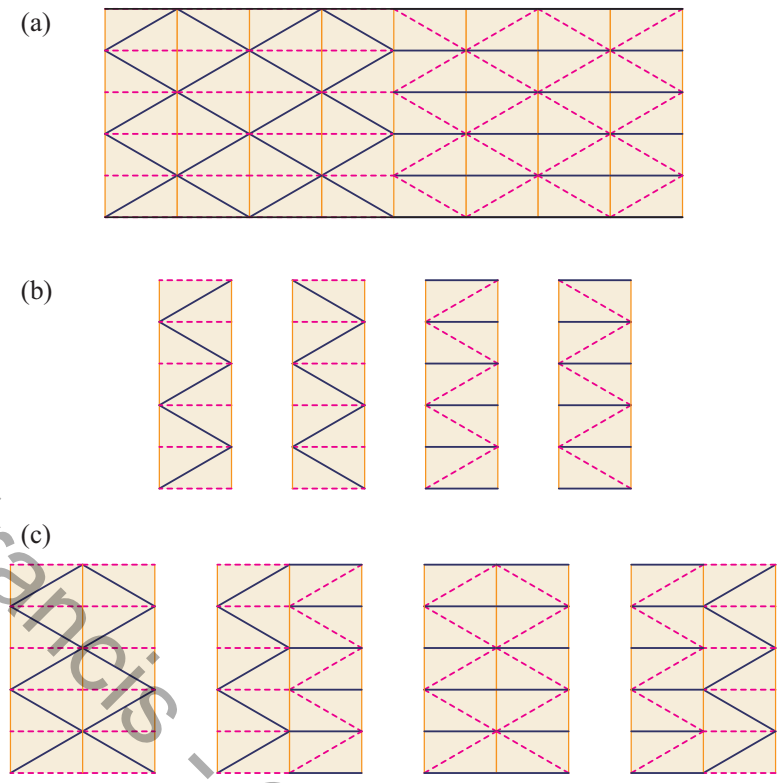

Figure 2.53. Building block tiles for creating hybrid Yoshimura-Miura patterns. (a) Joined Yoshimura patterns, divided into vertical tiles. (b) Four types of tiles. (c) Four ways of joining tile pairs.

2.4. Partial Periodicity

2.4.1. Yoshimura-Miura Hybrids

The Miura-ori building block arises from necessity if we try to glue together two Yoshimura patterns that have opposite curvature. If we divide the joined pattern of Figure 2.29 into vertical stripes, we see that all of the vertical stripes fall into one of four distinct types, as illustrated in Figure 2.53(a) and (b).

There are four types of tile, but each can mate with only two of the others in a way that gives rise to a flat-foldable pattern. Four of the eight possibilities are shown in Figure 2.53(c). One type of mating gives rise to a "Yoshimura-like" section of the pattern; the other type gives rise to a "Miura-like" section of pattern. Yoshimura patterns curl; Miura patterns are straight. By mixing and matching different combinations of tiles, one can create folded patterns that display quite varied large-scale curvature, as shown in Figure 2.54.

Yoshimura-Miura hybrid patterns are a family of designs, defined by several different independently variable quantities:

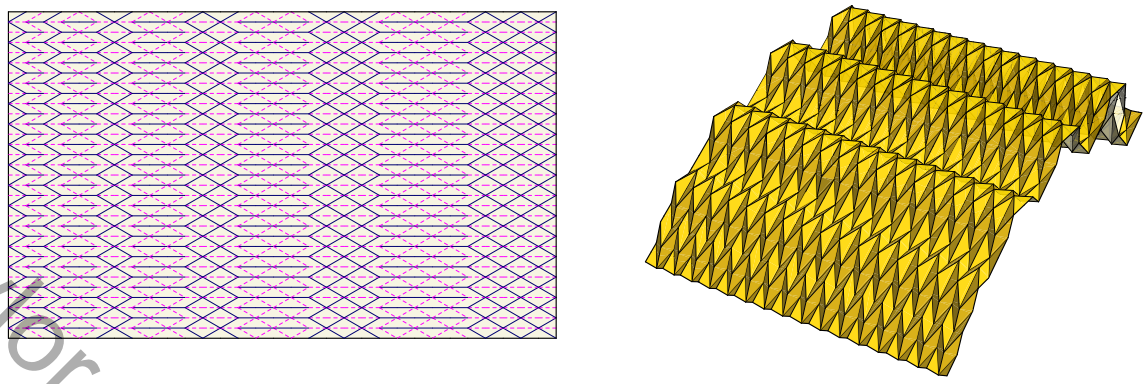

Figure 2.54.
"Gentle Waves" by the author, a hybrid Yoshimura-Miura pattern consisting of varying combinations of Yoshimura and Miura vertical tiles. The tilt angle is $\alpha = 30°$; the minor folds are folded at 70°.
Left: crease pattern.
Right: folded form (turned over).

- the choice of tiles along the horizontal direction in the crease pattern (subject to matching rules);
- the number of repetitions in the vertical direction;
- the tilt angle α, which is common to all of the diagonal folds;
- the degree of foldedness.

The degree of foldedness is something that bears comment. As we already saw, the Yoshimura pattern has two different ways it can be deformed when partially folded: it can be curved tighter or looser, and its ends can be shifted relative to each other (i.e., varying the helicity of the minor folds). For each type of motion, all of the fold angles are affected if we perform a large-scale shift in the pattern. The Miura-ori, by contrast, has only a single degree of freedom; it can open or close with all folds moving together in a prescribed way. If we splice together a Yoshimura pattern and Miura-ori, the result will have the reduced freedom of the Miura-ori, so that the entire pattern has the single degree of freedom of the Miura-ori.

At least, that is the case in purely mathematical terms. However, if you actually fold any of the patterns in this section, you will find that, empirically, they have a lot more freedom than the above paragraph would suggest; they can be twisted, compressed at one

end and expanded at the other, and, in general, deformed in many ways. These additional deformations happen because with most folding materials, individual panels can twist, and folds can shift their position slightly, which permits these additional motions. So, my comments about Miura-oris having only a single degree of freedom must be taken with a grain of salt; the model in which that is true is a mathematical approximation of the real world, and ultimately, it is the real-world folding behavior that matters! Mathematical approximations can be a useful tool for design, but we must always be aware of the limits of such approximations.

Within the approximation where we assume that individual panels do not twist, in any Yoshimura-Miura hybrid pattern, all minor folds (the horizontals in the crease pattern) will have the same magnitude of fold angle (whether mountain or valley), and similarly, all major folds (diagonal creases in the crease pattern) will also have the same magnitude of fold angle (albeit one that differs from that of the minor folds in every non-flat state).

In all four of the tiles in Figure 2.53(b), the diagonal folds have the same tilt angle α, which we can choose to be anything between 0 and 90°. But can we mix tiles that have different tilt angles? It turns out that we can. If you take two tiles with different values of α, they mate in the same way as tiles with the same α. Most importantly, the resulting closed vertices formed at the tile boundaries not only are flat-foldable but they have fold angles that are compatible across the full range of folding from unfolded to flat. (We will learn how to prove this claim in Chapter 7.)

⋆ 2.4.2. Semigeneralized Miura-ori

One of the variables in the design of Miura and Yoshimura patterns is the number of vertical repetitions in the pattern. They certainly look more interesting with a lot of repetitions, but if we choose a single repetition (two rows), the result is suggestive. A row of Figure 2.55 is shown in Figure 2.56.

This single row captures the essence of the pattern, and conceptually, it is a very simple object: a rectangular strip of paper, reverse-folded at varying angles and varying distances. Such a pattern, on its own, both is flat-foldable and can exist partially folded with no bending of the facets with any value of the fold angle running down the middle. But, as we have seen in the generalized Yoshimura-Miura hybrid, we can array such strips to create a surface that follows the path traced out by the single strip.

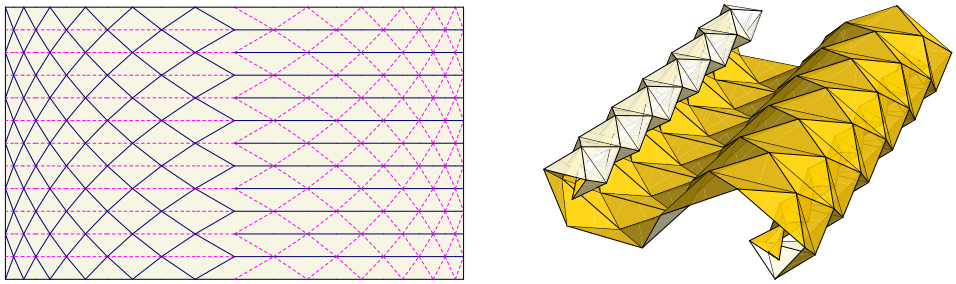

Figure 2.55.
"Double Spiral" by the author, a hybrid Yoshimura-Miura pattern, consisting of two varying-angle Yoshimura patterns joined by a Miura-ori splice.
Left: crease pattern.
Right: folded form (turned over).

This suggests a different way of designing such forms. Rather than starting with a blank crease pattern, picking angles, and then seeing what shape we get, we could instead start with a strip, fold it into a pattern that gives the surface cross section that we want, then unfold it and use it as a template to construct the full crease pattern.

A nice thing about this algorithm is that it can be carried out entirely by folding and/or drawing: no computation needed, with one important reservation, which we'll get to.

We'll start with the path that the minor fold (the center of the strip) follows in the flat-folded form. We will call this path the *generating line* for the surface; it represents the desired cross section in the direction perpendicular to the direction of periodicity. We'll create a strip of the crease pattern that represents a single repetition of the periodic surface, and we will call this the *generating strip* for the pattern. Figure 2.57 shows a sequence for graphically constructing a generating strip from a generating line.

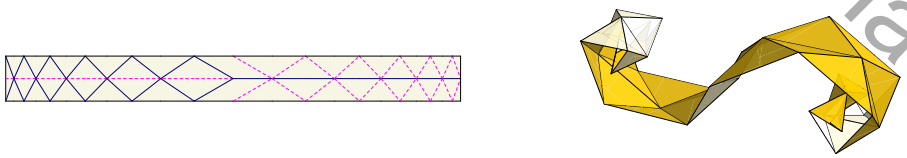

Figure 2.56.
A single row of "Double Spiral."
Left: crease pattern.
Right: folded form (turned over).

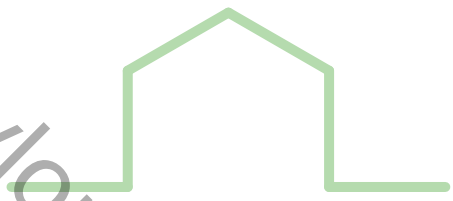

1. Begin by drawing the generating line that the desired strip (and surface) will follow.

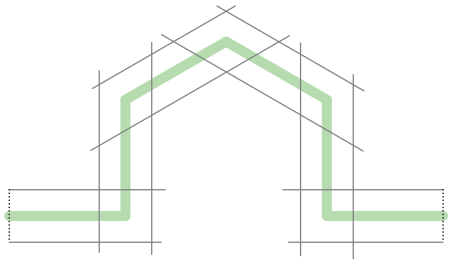

2. Draw pairs of lines parallel to and equally spaced from each of the segments of the generating line. Make sure each line of each pair is long enough to intersect both of the next pair.

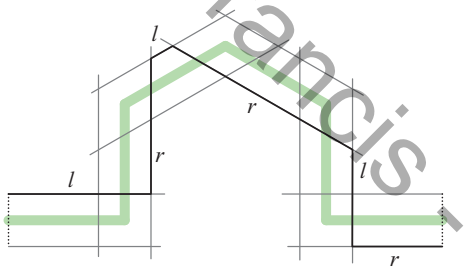

3. Now picture yourself traveling along the generating line (from left to right, in this example). Draw along the line lying on the left side of the generating until you hit the line to the right of the next segment; follow it until you hit the left line of the next segment; and so on, until you get to the end.

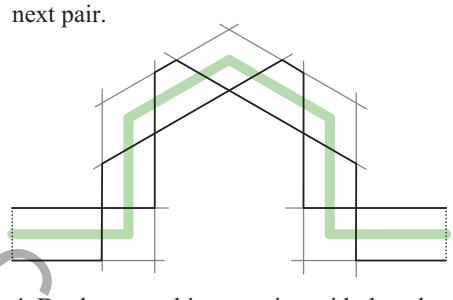

4. Do the same thing, starting with the other line, again alternating between right and left.

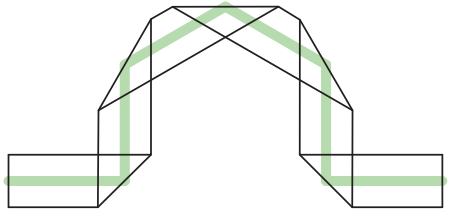

5. Connect corresponding corners of both pairs of lines and erase all of the guidelines.

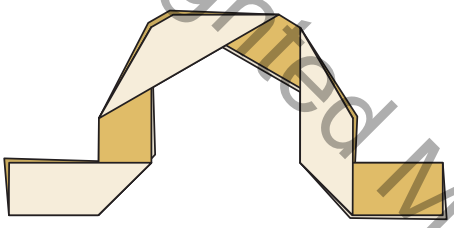

6. The line drawing is the silhouette of the folded strip that follows the desired path.

Figure 2.57.
Graphical construction of a strip that follows a specified path when it is folded flat.

We begin by constructing a drawing of a folded form (or rather, the silhouette of the folded form) that follows the path and is a valid folded form for some flat-sheet crease pattern.

Next, to get the crease pattern for the generating strip from the drawing of its folded form, we take each of the overlapping polygons in the drawing and arrange them into a single rectangular strip, as shown in Figure 2.58. This gives the locations and orientations of all of the creases, which we can then assign using our existing known rules for Miura-oris and their kin: minor folds (horizontals) alternate in sign; major folds (zigzag verticals) have the same sign. Once a single row is constructed, it can be arrayed with copies of itself to make a full surface.

Figure 2.59 shows the resulting complete crease pattern and a folded form for the sample generating line.

It is also possible to carry out the design using a folded strip of paper, as shown in Figure 2.60. Fold the doubled strip to follow the path, then unfold it, and use it as a template to transfer the creases to the paper to create an array.

I call such a surface a *semigeneralized Miura-ori* (SGMO). We can think of such a surface as being created by splicing together individual slices of Miura-ori, in either of two orientations, with varying angles and distances between them. A semigeneralized surface can take on any arbitrary cross section in one direction, but it exhibits strict periodicity in the other (which is the reason for the "semi" part of "semigeneralized").

The concept of the semigeneralized Miura-ori, like so many other origami structures, has deeper roots (though not by that name). Conceptually, the SGMO can be created by making a series of pleats in a sheet of paper in one direction, then repeatedly reverse-folding it at several angles in the other direction to create the 3D shape. This technique can be found in a centuries-old magic trick, called "Troublewit" [63], which we will come back to.

The design recipe above is a very straightforward way to create a semigeneralized Miura-ori with any desired cross section; in fact, you could create a surface whose cross section is your own signature! I've not done that, but in 2012, I was asked to create an origami version of the "Google Doodle" to honor the great 20th-century folding master Akira Yoshizawa. I created each letter as an instance of a semigeneralized Miura-ori. The silhouettes, crease patterns, and resulting "Doodle" (decorated with Yoshizawa's "Butterfly") are shown in Figures 2.61 and 2.62.

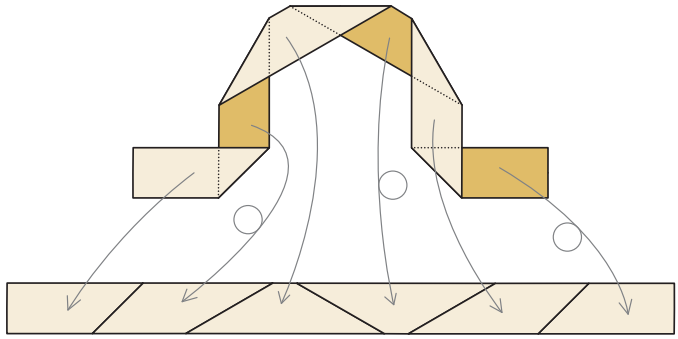

1. Rearrange the polygons to form a strip, turning over the colored ones.

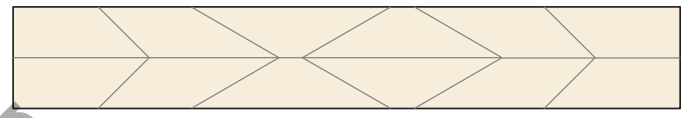

2. Create a mirror image of the pattern of polygons above the original strip, and make creases at the boundaries between the polygons.

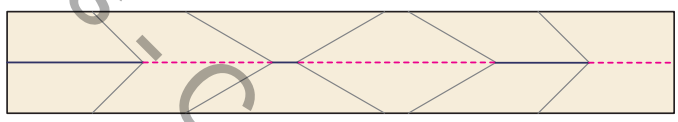

3. Assign the center creases to alternate between mountain and valley (you can choose which one you start with).

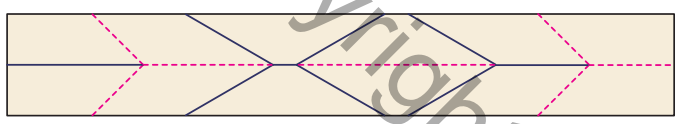

4. Assign the diagonal creases so that each vertex becomes a bird's-foot vertex.

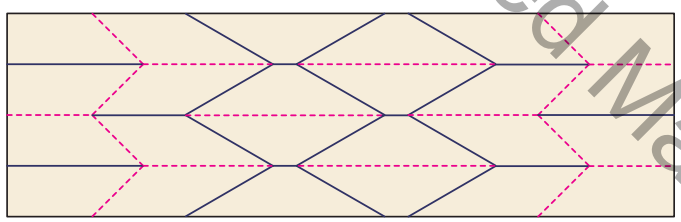

5. Array two (or more) copies vertically, alternating the sign of the horizontal creases in each column.

Figure 2.58.
Graphical construction of the unfolded strip.

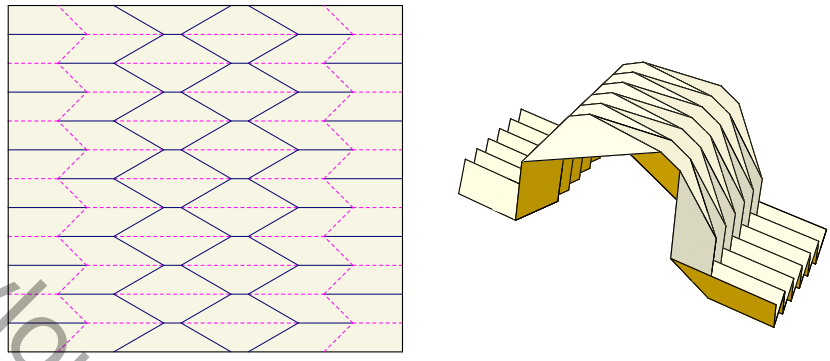

Figure 2.59.
A periodic array of the computed strip.
Left: crease pattern.
Right: partially folded form. The horizontal folds all have a fold angle of ±150°.

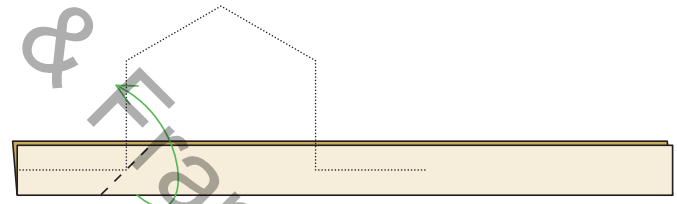

1. Lay a folded strip of paper down on the desired path. Fold it over at each bend so that it follows the path.

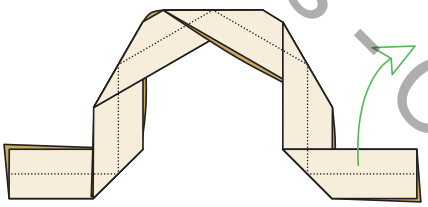

2. Unfold the strip.

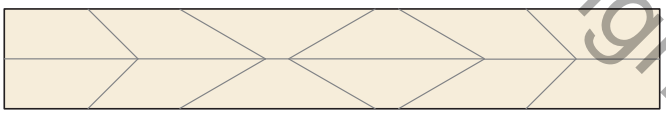

3. Use the unfolded strip as a template to draw the array of creases.

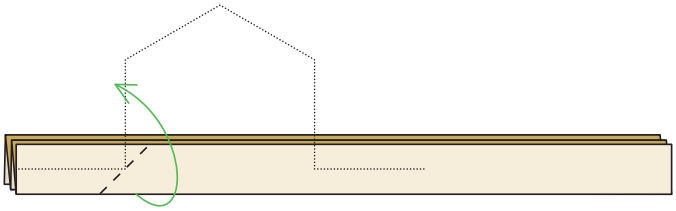

4. For small arrays, you can precrease the entire paper by starting with a pleated strip.

Figure 2.60.
Folding sequence to create the desired creases by manual folding.

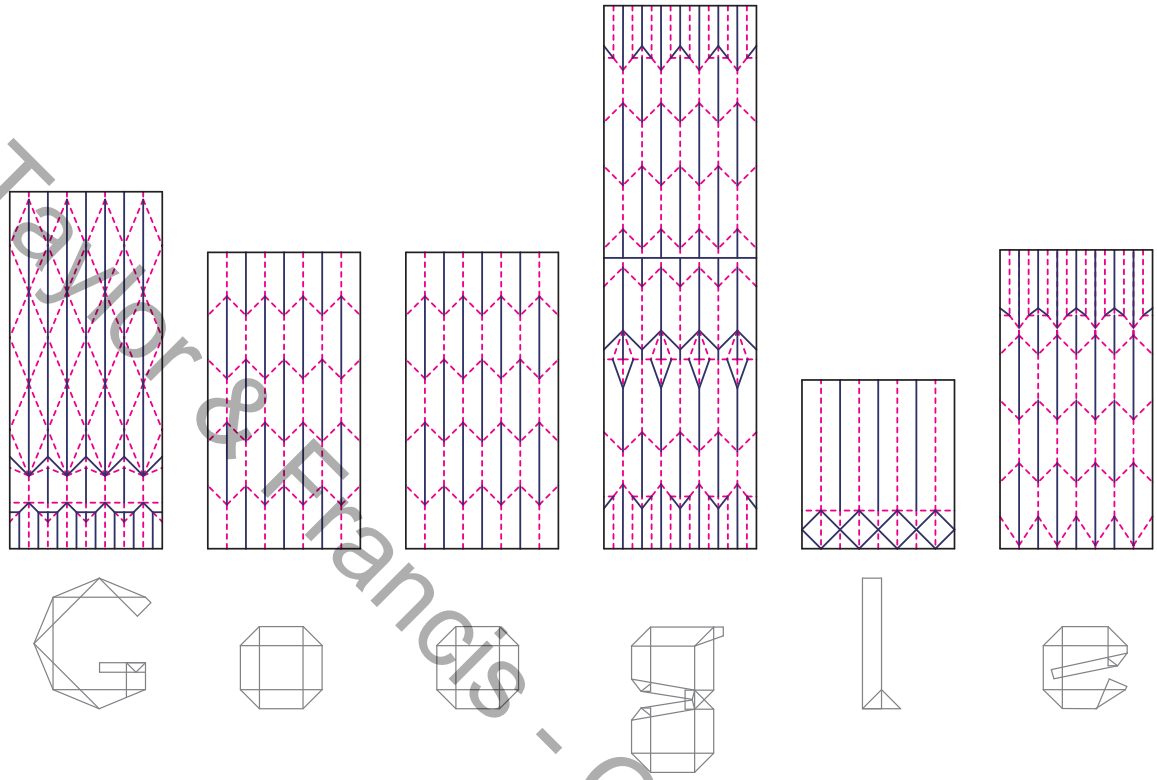

Figure 2.61.
Top row: crease patterns for the letters of the "Google Doodle."
Bottom row: the desired letterforms.

Figure 2.62.
The Google Doodle for March 14, 2012.

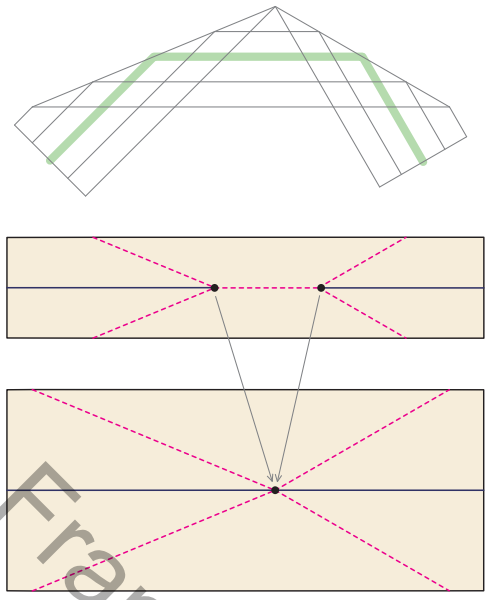

Figure 2.63.
Two bends in the same direction impose a minimum width on the strip because consecutive vertices collide.
Top: the path and guidelines for two different widths.
Middle: a narrow strip.
Bottom: a wide strip. The two bird's-foot vertices have merged into a Yoshimura vertex.

There is great variety possible in semigeneralized Miura-oris; one can choose the path to be followed by the surface to be almost any piecewise continuous sequence of connected straight lines; it can even double back on itself (which you can see in the "Doodle" patterns). Still, there are a few issues that may arise in their design.

The first is that for any given generating line, there may be a minimum strip width whose value depends on the lengths and angles in the generating line. If two consecutive bends in the desired path go the same direction (like the "roof" in Figure 2.57), that gives rise to two back-to-back birds's-foot vertices, which, as the strip grows wider, must move toward each other, as illustrated in Figure 2.63.

As the strip becomes wider, the two consecutive bird's-foot vertices move toward each other and eventually collide, merging into a Yoshimura vertex. If we made the strip wider, the two vertices would cross, as would their connected creases, and we would have to introduce additional vertices and creases into the pattern to create a valid foldable crease pattern.

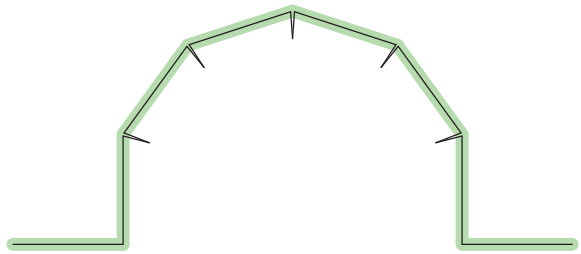

Figure 2.64.
Creating a semigeneralized Miura-ori with shallow bends in the surface. The solid green line is the desired generating line. The thin black line is the actual path we use, which forces all bends to be 90° or sharper.

The point of merging sets a natural limit on the strip width for such a pattern; the permissible width is the minimum width set by any of the segments of the surface. If we choose the width to be exactly one of the minimum values, then at least some of the vertices of the pattern will be Yoshimura vertices. This can be seen in the crease patterns for the Google Doodle letters in Figure 2.61.

You can see from Figure 2.63 that the width limitation will arise sooner for short segments than long ones and, especially, for segments bounded by shallow bend angles. That makes it difficult to approximate smooth surfaces using this technique. Subdividing a surface into many short segments with slight bends—what one would desire for such an approximation—will force an extremely small strip width; one smaller than might be desired from considerations of the aesthetics or functionality of the target surface.

However, there is a nice trick we can use to overcome this problem: wherever there is a shallow bend in the surface, we can replace it by a series of sharper bends, as illustrated in Figure 2.64. Instead of having a shallow bend of angle β where β is small, we replace it by three consecutive bends of values $(-90° + \beta/2, 180°, -90° + \beta/2)$, so that all three angular bends are large.

I call such a feature—a bend and doubling-back in order to realize a shallow bend—a *shallow-angle divot*. The realized implementation of this example is shown in Figure 2.65.

In this example, I've placed the divots to all point down, which makes the top surface relatively smooth, and I've angled them so as to equalize the bend angles to either side. I should point out, though, that we can point the divots at any angle on either the top

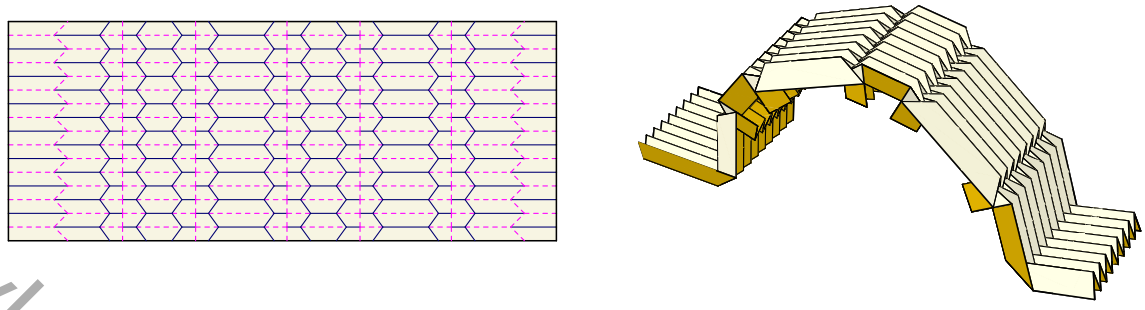

Figure 2.65.
A semigeneralized Miura-ori with shallow-angle divots.
Left: crease pattern.
Right: folded form (minor fold angle of ±150°).

or bottom surface. If we place the divot on the outside of the bend, we can angle it so that one side of each divot is collinear with one of the two sides of the path and, effectively, remove one of the major creases, reducing the number of creases at the bend to two, as in Figure 2.66.

The structure in the bottom row of Figure 2.66 is familiar to most origami artists; it is an example of what would be called a *crimp*, a very common maneuver in representational folding.

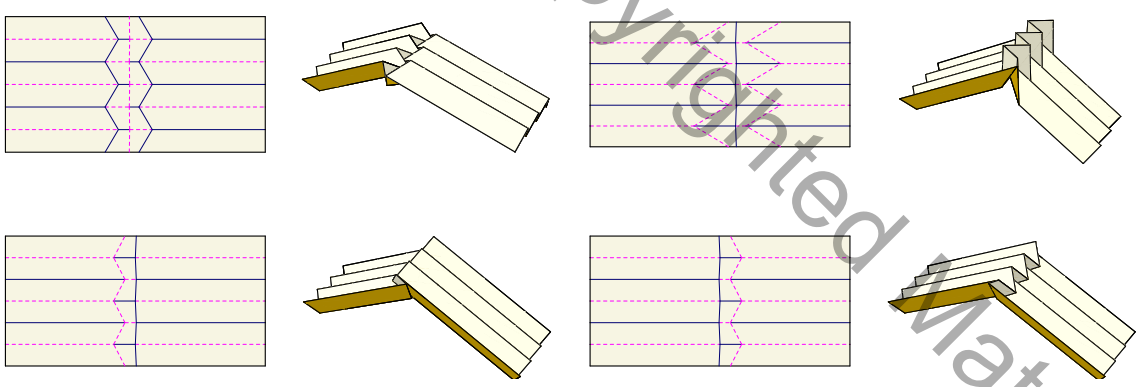

Figure 2.66.
A comparison of divots angled in different directions for the same desired generating path (a single bend of −120°).
Top left: divot on the bottom, evenly divided.
Top right: divot on the top, evenly divided.
Bottom left: divot collinear with the right side.
Bottom right: divot collinear with the left side.

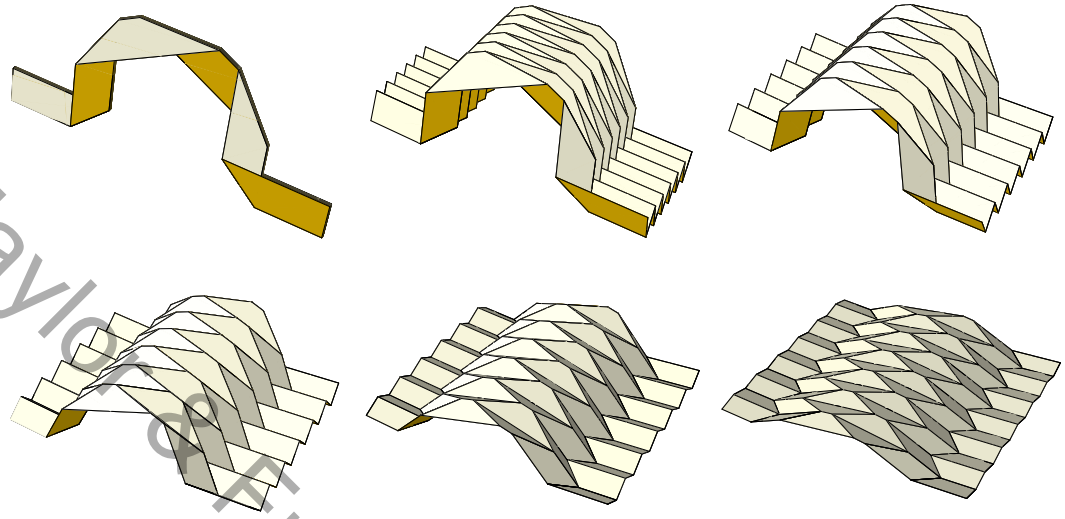

Figure 2.67.
The crease pattern of Figure 2.59 for different values of minor fold angle.
Top row: left to right, −180° (flat-folded), −150°, and −120°.
Bottom row: left to right, −90°, −60°, and −30°.

In the figure, the folded form is shown partially folded, i.e., not pressed flat, and there is an interesting detail: although these were designed for the same generating line, with the same bend angle when folded flat, the bottom edges are bent at slightly different angles from one another—and none of them are bent at precisely −120°, the design angle. In semigeneralized Miura-ori, the angle between consecutive sections of pleats is not fixed but varies with the degree of foldedness. This property has several ramifications, as we will now see.

⋆⋆ 2.4.3. Predistortion

It should not be surprising that the angles between consecutive sections of pleats would vary with the state of foldedness; after all, when the pattern is fully unfolded, all angles are zero. We should expect that the angles would vary from zero at the unfolded state to some fixed value at the flat-folded state. Indeed, we can see this behavior in action in Figure 2.67, where we show our test case of Figure 2.59 for a range of different minor fold angles.

If we are going to design a surface that follows a particular path, we will need to take into account the fold angles at which it will be displayed. To do that, we will need to understand the

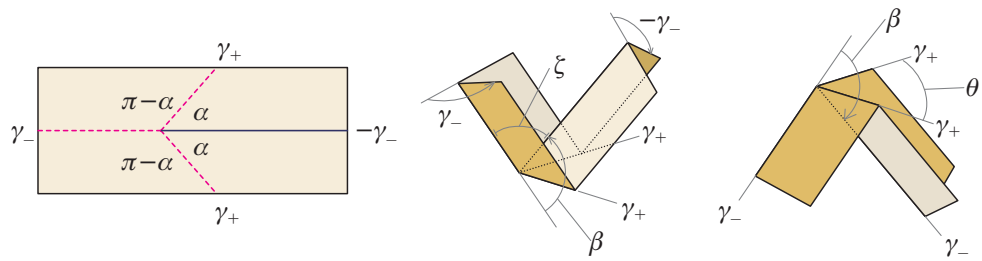

Figure 2.68.
Geometry of a partially folded bird's-foot vertex.
Left: crease pattern. The sector angles are, in order, $(\alpha, \alpha, \pi - \alpha, \pi - \alpha)$. The major and minor fold angles are, respectively, γ_+ and γ_-.
Middle: the partially folded form; ζ is the angle between the two minor creases, and β is the bend angle of the minor folds.
Right: the partially folded form turned over; θ is the angle between the two major creases.

relationship between the desired fold path and the sector and fold angles at any state of partial folding. Every vertex in a generalized Miura-ori is some form of bird's-foot vertex (albeit for possibly varying characteristic angle α), so we should look at all the various angles of such a vertex—the sector angles, the fold angles, and the angles in 3D between the various folds. A general bird's-foot vertex with angles labeled is shown in Figures 2.68.

We have already seen the sector and fold angles. For our purposes, we need one more angle: the angle between the two minor creases of the folded vertex, which we denote by ζ and which (for reasons we will learn) we call the *ruling angle* of the vertex.

In the case of fold angles, we find it is usually more convenient to work with the fold angle (deviation from straightness) rather than the dihedral angle (angle between planes), and the same situation will arise here; it is a bit more convenient to work with the deviation from straightness of the minor fold line. In this case, we will give this quantity its own variable, β, and call it the *bend angle* of the pair of minor folds incident upon the vertex.

We also introduce, for completeness, the angle between the two major folds. We denote this angle by θ, and we call it the *osculating angle* of the vertex.

The fold angles, sector angles, and angles θ, ζ, and β are all related to one another. We will work out their relationships in general in Chapter 8, but for now, we will simply present the special case of a bird's-foot vertex as a given.

First, the major and minor fold angles are related to one another through the sector angle α:

$$\frac{\tan \frac{1}{2}\gamma_+}{\tan \frac{1}{2}\gamma_-} = \sec \alpha, \tag{2.2}$$

which means that, given one of the two angles, we can derive the other:

$$\gamma_+ = 2 \tan^{-1} \left[\sec \alpha \tan \tfrac{1}{2}\gamma_-\right], \tag{2.3}$$

$$\gamma_- = 2 \tan^{-1} \left[\cos \alpha \tan \tfrac{1}{2}\gamma_+\right]. \tag{2.4}$$

The osculating angle θ satisfies[3]

$$\sin \tfrac{1}{2}\theta = \sin \alpha \cos \tfrac{1}{2}\gamma_-. \tag{2.5}$$

The ruling angle ζ satisfies[4]

$$\cos \tfrac{1}{2}\zeta = \sin \alpha \sin \tfrac{1}{2}\gamma_+, \tag{2.6}$$

which exhibits a pleasant symmetry with Equation (2.5). Note that each of the trigonometric functions in Equations (2.5) and (2.6) is strictly nonnegative for all values of the various angles that appear within them. Using the fact that $\zeta = \pi - \beta$, Equation (2.6) is equivalent to

$$\sin \tfrac{1}{2}\beta = \sin \alpha \sin \tfrac{1}{2}\gamma_+. \tag{2.7}$$

We would ultimately like to compute the value of α from the minor fold angle γ_-, not γ_+. Using Equation (2.2), though, we can find that

$$\tan \tfrac{1}{2}\beta = \tan \alpha \sin \tfrac{1}{2}\gamma_-, \tag{2.8}$$

which gives the desired relationship.

Given a desired path for the surface to follow, using Equation (2.8), we can work out the sector angles we need at each vertex of the crease pattern from the bend angles at each corner of the path and the desired minor fold angle γ_-, which we can choose to be any nonzero angle—with certain limits, as we will see.

To make this concrete, let us define the desired path as a series of segments of length $d_i, i = 1, \ldots, N$, with angles $\theta_i, i = 1, \ldots, N-1$, between consecutive segments, as illustrated in Figure 2.69.

[3] This can be derived from Equation (8.37).
[4] This can be derived from Equation (8.23).

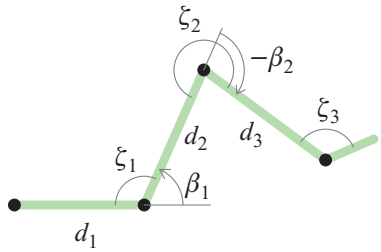

Figure 2.69.
Notation for a specified generating line to be the cross section of a semigeneralized Miura-ori.

Denote the sector angle for the ith vertex by α_i. Then, from Equation (2.8), each of the desired sector angles is given by

$$\alpha_i = \tan^{-1}\left[\frac{\tan\frac{1}{2}\beta_i}{\sin\frac{1}{2}\gamma_-}\right]. \tag{2.9}$$

Note that the right side of this equation can be positive or negative, depending on the signs of β_i and γ_-. Negative solutions should be shifted by the periodicity of $\tan^{-1}$, i.e., by adding π to negative values to bring them into the range $(0, \pi)$.

What about the distances between consecutive vertices? This will depend upon how we position the folded surface relative to the desired generating line. In Figures 2.57 and 2.60, we positioned our strip so that it extended equally above and below the generating line in the fully flat-folded state. If we choose the same approach for a partially folded semigeneralized Miura-ori, then the distances between consecutive vertices will be a bit longer or a bit shorter than the distances d_i.

If we imagine cutting the folded surface by the target surface, then, independently of the minor fold angle γ_-, the target surface cuts through each panel halfway across its width, as illustrated in Figure 2.70.

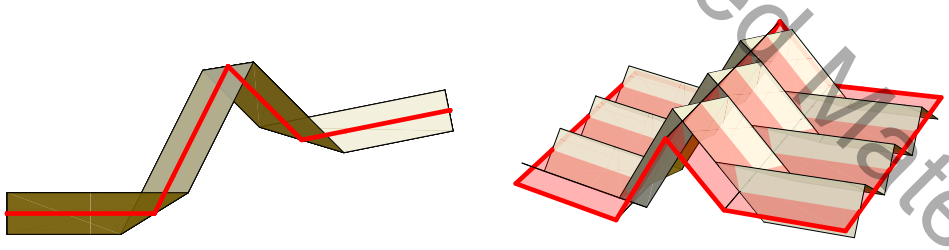

Figure 2.70.
The target surface cuts through the middle of each horizontal panel as portions of the folded surface extend above and below the target.
Left: looking along the direction of periodicity.
Right: 3D view.

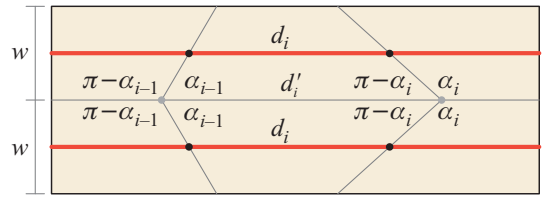

Figure 2.71.
A portion of a single strip of the crease pattern; d_i is the distance between consecutive vertices of the path, and d_i' is the distance between consecutive vertices along the chain of minor folds.

Compare this now to a portion of the crease pattern, as in Figure 2.71; if the target surface cuts each panel along its midline, then we can trace back the line of intersection to the crease pattern and, from that, work out the relationship between the lengths of the segments of the path that defines the target surface and the distances between the vertices of the crease pattern.

If we choose the width of each vertical panel to be w, then the distance between consecutive vertices is given by

$$d_i' = \frac{w}{2}\cot\alpha_{i-1} + d_i + \frac{w}{2}\cot\alpha_i. \tag{2.10}$$

And that completes the design algorithm: we now know all of the distances and angles in the crease pattern. If we choose to have m repetitions of the pattern along the direction of periodicity, then the overall width in that direction in the folded form will be

$$W_{\text{tot}} = 2mw\cos\tfrac{1}{2}\gamma_-. \tag{2.11}$$

A typical method of folding such a pattern would be to precrease all of the creases, press it fully flat, then open it back up to the desired minor fold angle. The fully flat-folded form does not have the same cross section as our desired path, as shown in Figure 2.72. In general, the bend angles will all be sharper than their corresponding angles in the desired path (although to varying degrees). Thus, I call this design technique *predistortion*; we are intentionally distorting the flat-folded form so that when it is partially unfolded, it takes on the desired path in 3D.

Once we've got a toolkit for creating semigeneralized Miura-ori with arbitrary cross section, there are many possibilities for forms both in the artistic realm and with functional applications. As an example of the latter, Figure 2.73 shows an architectural

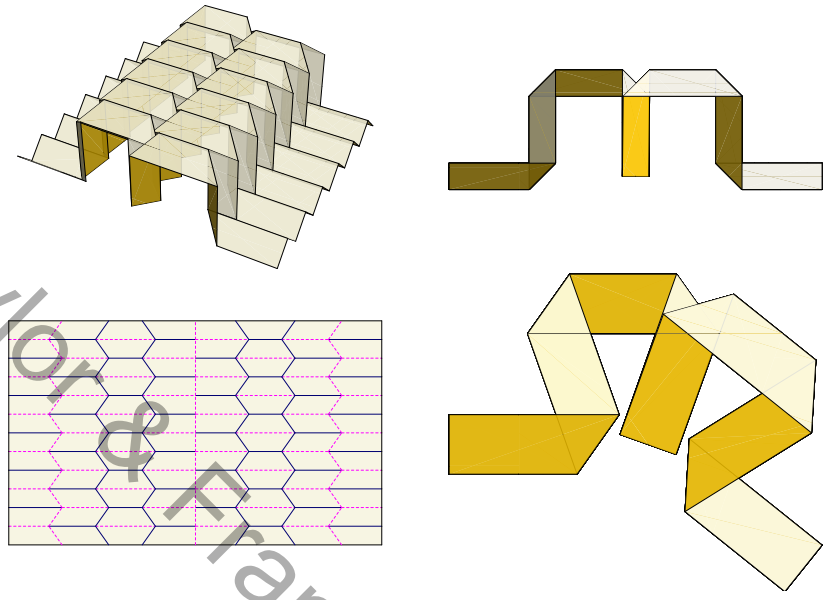

Figure 2.72.
A semigeneralized Miura-ori designed for a right-angled folded form with a minor fold angle of 90°.
Top left: folded form.
Top right: same thing, viewed along the direction of periodicity.
Bottom left: crease pattern.
Bottom right: flattened form, now distorted.

barrel vault designed using this technique. The cross section is a semicircle, and I have introduced divots at each joint to allow for the shallow bends in the overall surface.

There is much more that can be done with semigeneralized Miura-ori concepts, and we will explore them further, but I would like to pause to make a comment on the name: why only "semi"-generalized Miura-ori?

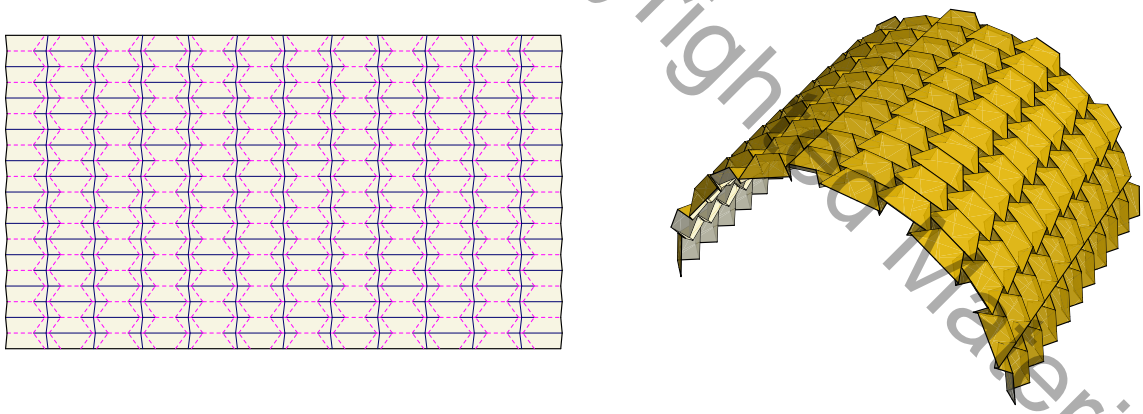

Figure 2.73.
A cylindrical barrel vault, implemented from a semigeneralized Miura-ori with a minor fold angle of 90°.
Left: crease pattern.
Right: folded form.

The semigeneralized Miura-ori has the topological folding pattern of a Miura-ori with the cross section taking on some arbitrary form in one direction while remaining strictly periodic in the other. We can envision the possibility of varying the cross section arbitrarily in *both* directions; *that* would be a fully generalized Miura-ori. Because the fold angles and sector angles are all related, the analysis of such a pattern becomes rather complex; one must choose fold and sector angles so that they are consistent at every vertex. Such a construction has been carried out by University of Tokyo professor Tomohiro Tachi, who has worked out the underlying mathematics [111] and written design software [119] for creating such patterns, which, in general, make use of arbitrary degree-4 vertices, not just the highly symmetric (and much simpler) bird's-foot vertex. We will develop the descriptive mathematics necessary to handle such structures a bit later on, in Chapter 8.

⋆ 2.4.4. Tachi-Miura Mechanisms

As we saw in Equation (2.8), at each bend in the surface of a semigeneralized Miura-ori, the bend angle varies with the minor fold angle in a nonlinear way. If we have a chain of several different bend angles, the angular difference between the inclinations of the first and last segment will also vary with the minor fold angle, as illustrated in Figure 2.74.

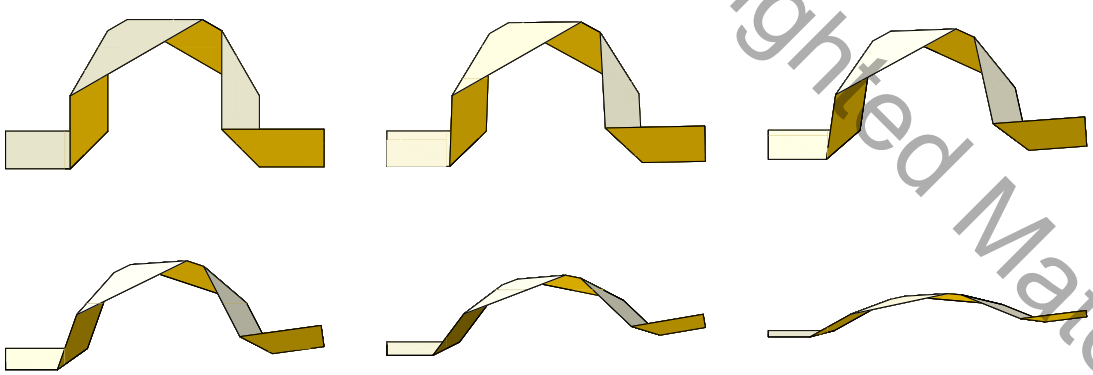

Figure 2.74.
The crease pattern of Figure 2.59 for different values of minor fold angle, viewed along the direction of periodicity.
Top row: left to right, −180° (flat-folded), −150°, and −120°.
Bottom row: left to right, −90°, −60°, and −30°.

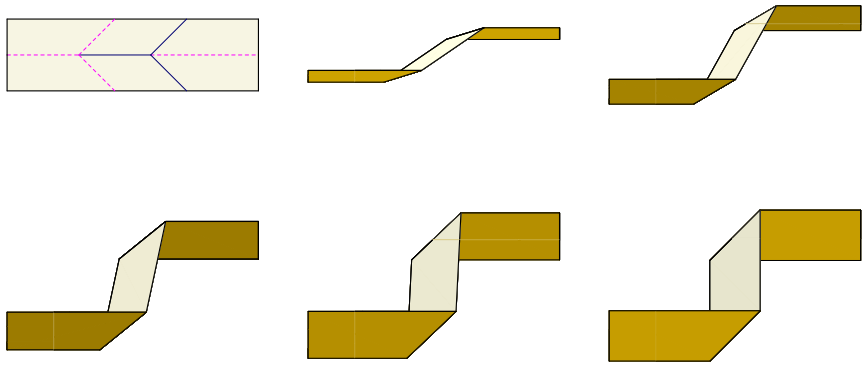

Figure 2.75.
A folded strip with two consecutive vertex sector angles of 45° for different values of minor fold angle, viewed along the direction of periodicity.
Top row: left to right, crease pattern, −36°, and −72°.
Bottom row: left to right, −108°, −144°, and −180° (flat-folded).

While the relationship between bend angle and minor fold angle is not linear, there is a symmetry with respect to the sector angle α; if we replace α with its supplement, $180° - \alpha$, then the bend angle has the same magnitude, but opposite sign, and this is the case over the full range of minor fold angles. And since the minor fold angle changes sign across a vertex, if we have two consecutive vertices with the same sector angles α, then the two segments on either side of the pair will remain parallel across the range of minor fold angles, as illustrated in Figure 2.75.

This behavior can be exploited. If we combine such a strip with its mirror image, then in the resulting mechanism, the bottom edges remain parallel and in the same plane across the full range of minor fold angles, as in Figure 2.76. What's more, if we replace each sector angle α with $180° - \alpha$ and adjust the distances between the vertices, we can obtain a strip that displays the same behavior, but in which the middle buckles downward, as in Figure 2.77.

The vertex-to-vertex distances in Figures 2.76 and 2.77 were chosen so that the generating paths (the red lines in Figure 2.70) were mirror images of one another. This ensures that not only the two folded forms have their leftmost and rightmost panels remaining parallel to each other across the folding range, but the upward- and downward-pointing forms also have the same lengths across their full folding ranges. And this, in turn, means that one could, in principle, glue the two sheets together by their horizontal flanges, and the entire assembly would remain flexible, as shown in Figure 2.78.

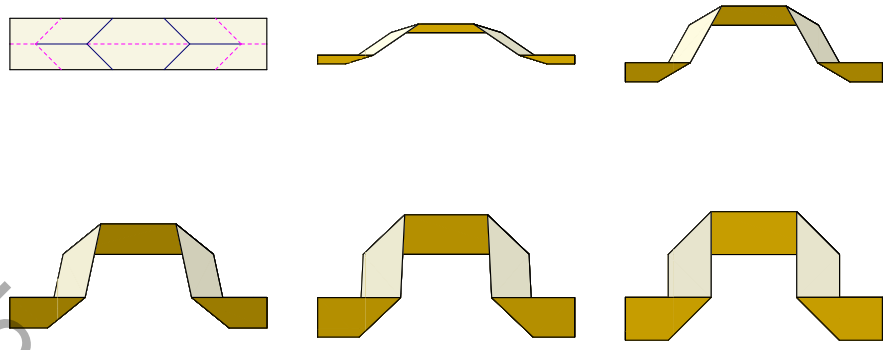

Figure 2.76.
A folded strip with vertex sector angles of $(45°, 45°, 135°, 135°)$ for different values of minor fold angle, viewed along the direction of periodicity.
Top row: left to right, crease pattern, $-36°$, and $-72°$.
Bottom row: left to right, $-108°$, $-144°$, and $-180°$ (flat-folded).

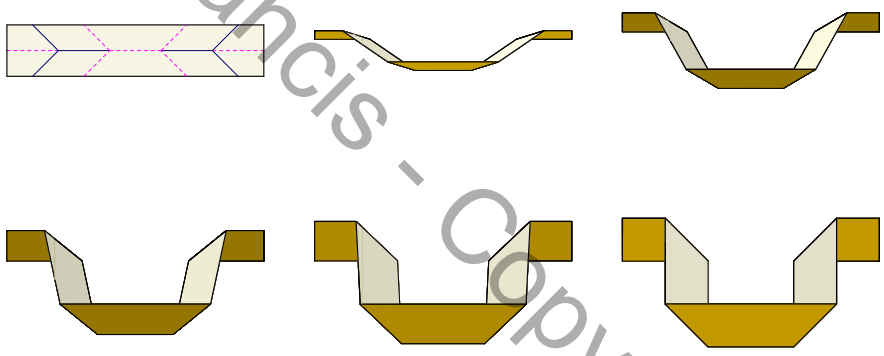

Figure 2.77.
A folded strip with vertex sector angles of $(45°, 45°, 135°, 135°)$ for different values of minor fold angle, viewed along the direction of periodicity.
Top row: left to right, crease pattern, $-36°$, and $-72°$.
Bottom row: left to right, $-108°$, $-144°$, and $-180°$ (flat-folded).

The *Tachi-Miura polyhedron* is a flexible tube that can extend and contract while keeping its facets planar without stretching. It is *rigidly foldable*, to use a term we will explore more deeply in later chapters. This mechanism has applications in the technological world; for example, it could be used as an extensible boom or shroud, as part of a deployable structure.

It might seem that one could achieve the same result with a simple semigeneralized Miura-ori, i.e., a shape obtained by repeatedly reverse-folding pleats to form a loop and then joining the ends. However, as Figure 2.79 shows, the tube obtained by

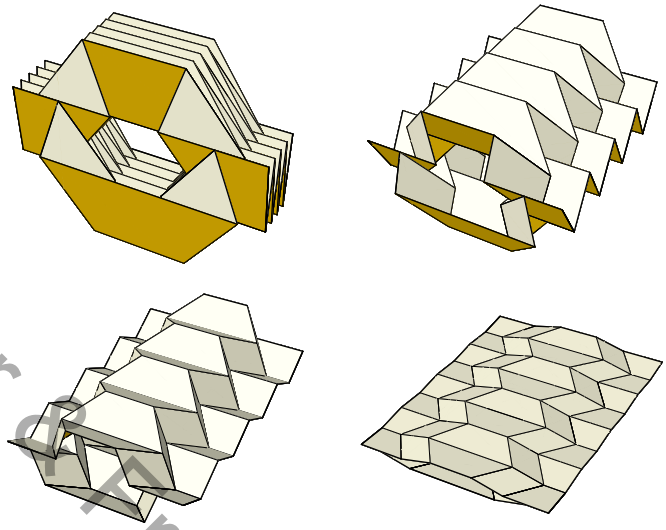

Figure 2.78.
A Tachi-Miura polyhedron based on sector angles of 60° at four different minor fold angles.
Top left: 170°.
Top right: 120°.
Bottom left: 60°.
Bottom right: 10°.

that strategem will not stay closed as the minor fold angles flex; rather, as the minor folds unfold, the entire tube uncurls.

Tomohiro Tachi and Koryo Miura have developed several variations of this concept [88, 120] (hence the name "Tachi-Miura" polyhedron). For example, one can construct the full polyhedron from a single sheet, by joining the two halves along one of their shared edges. Conversely, one could cut away the double-layered regions of paper and re-glue the cut edges, to produce a polyhedron with no doubled edges (albeit at the expense of creating some non-developable vertices, interior vertices whose sector an-

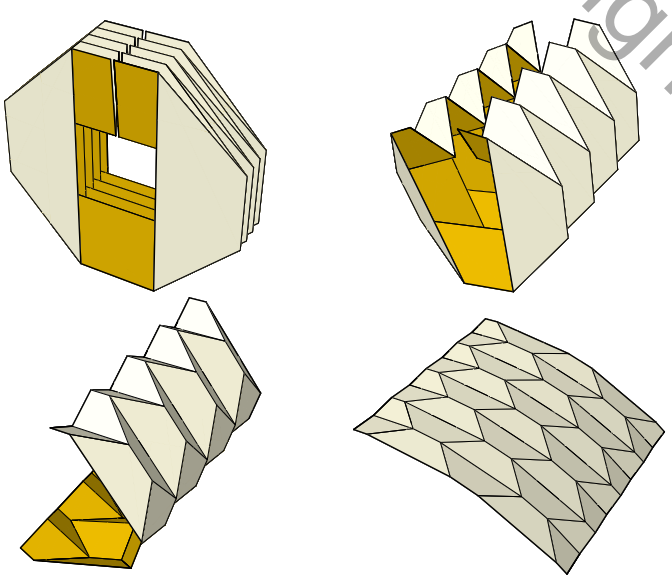

Figure 2.79.
A tubular semigeneralized Miura-ori at four different minor fold angles.
Top left: 170°.
Top right: 120°.
Bottom left: 60°.
Bottom right: 10°.

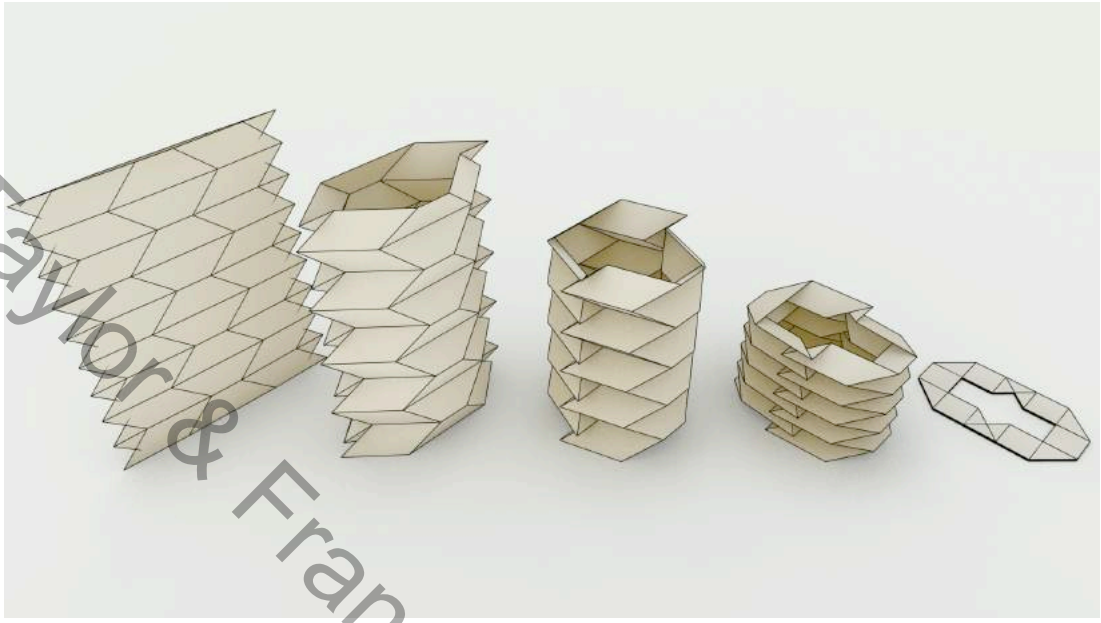

Figure 2.80.
A Tachi-Miura polyhedron with no excess paper (but some non-developable vertices). *Rendering courtesy of Tomohiro Tachi.*

gles sum to less than or greater than 180°). An example, generated by Tachi, is shown in Figure 2.80.

An additional family of structures based on the same concept was also demonstrated by Tachi and Miura: by layering and attaching folded sheets that individually have the same structure that gives rise to the Tachi-Miura polyhedron, one can achieve a cellular mechanism that is rigidly flexible and that has the interesting property that its overall dimensions change in different proportion to one another as the mechanism is flexed. An example of such a material is shown in Figure 2.81.

These objects stray a bit from the single-sheet philosophy of origami, as the various stacked layers should be glued together for best effect. They have the interesting behavior that when you expand them in one direction, they can expand in one of the other directions (or in both). With ordinary materials, if you stretch the material in one direction, it will typically get smaller in the other direction. The ratio between expansion in the one direction and shrinkage in the other is called the *Poisson's ratio* for the material; if a material expands in both directions, it is said to have a *negative Poisson's ratio* (at least, for that pair of directions).

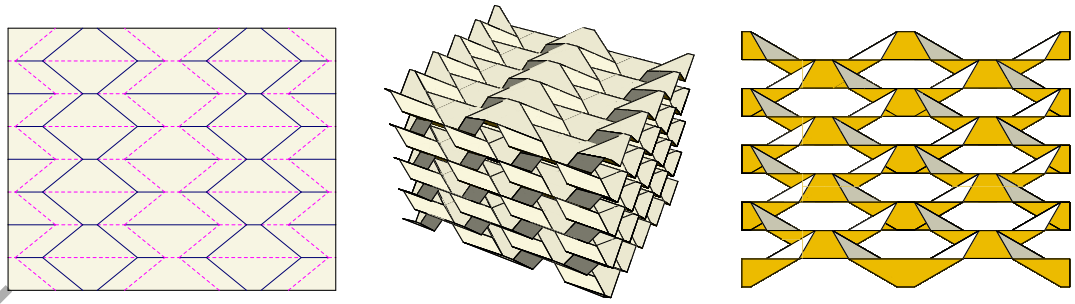

Figure 2.81.
A Tachi-Miura cellular form, composed of a stack of eight layers (four each of two opposite-polarity sheets).
Left: crease pattern of a single sheet.
Middle: folded form at a minor fold angle of 90°, oblique view.
Right: folded form at a minor fold angle of 90°, viewed along one of the directions of periodicity.

Many origami mechanisms can be viewed as a type of bulk material where the fine structure of the folding pattern gives rise to large-scale mechanical properties that are analogous to those of more homogeneous materials. Mechanisms that behave like bulk materials but whose mechanical properties differ from those of the underlying material are called *mechanical metamaterials*; "meta" (Greek for "beyond") because they exhibit properties that go beyond the underlying materials from which they are made. Many origami mechanisms can be considered to be mechanical metamaterials, and several of them display a negative Poisson's ratio—stretch them in one direction, they expand in another.

In fact, the conventional Miura-ori is a mechanical metamaterial; if you stretch it along its length, it also expands across its width. But it also gets slightly shorter in height, so it has a negative Poisson's ratio in one direction, but a positive (ordinary) Poisson's ratio in the other.

A single Miura-ori can easily be scaled in length and width by adding rows and columns, but its height remains limited by the size of a single quadrilateral facet. By stacking Miura-oris or other folding patterns, though, one can build up three-dimensional metamaterials of arbitrary length, width, and height.

The Tachi-Miura cellular structures are a class of mechanical metamaterials that exhibit negative Poisson's ratio in at least one direction, as can be seen in Figure 2.82, which shows the object from Figure 2.81 at four different minor fold angles. These objects

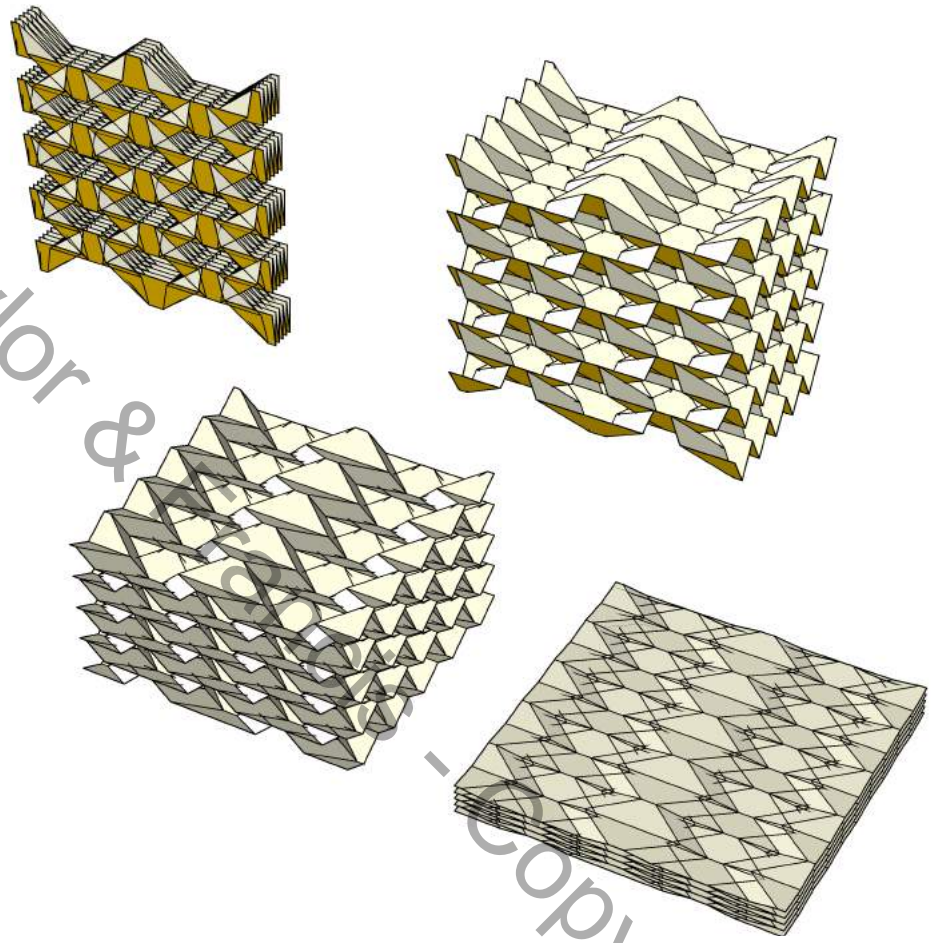

Figure 2.82.
The Tachi-Miura cellular form from Figure 2.81, composed of a stack of eight layers (four each of two opposite-polarity sheets) at four different minor fold angles.
Top left: 170°.
Top right: 120°.
Bottom left: 60°.
Bottom right: 10°.

have the unexpected property that they change state from almost entirely flat in one direction to almost entirely flat in the other.

In general, Tachi-Miura cellular forms will expand (or contract) in two directions while contracting (or expanding) in the other one. By careful choice of bend angle and operating range of minor fold angle, though, it is possible to obtain simultaneous expansion along all three axes. The object shown in Figure 2.83 has been designed to exhibit negative Poisson's ratio in all direc-

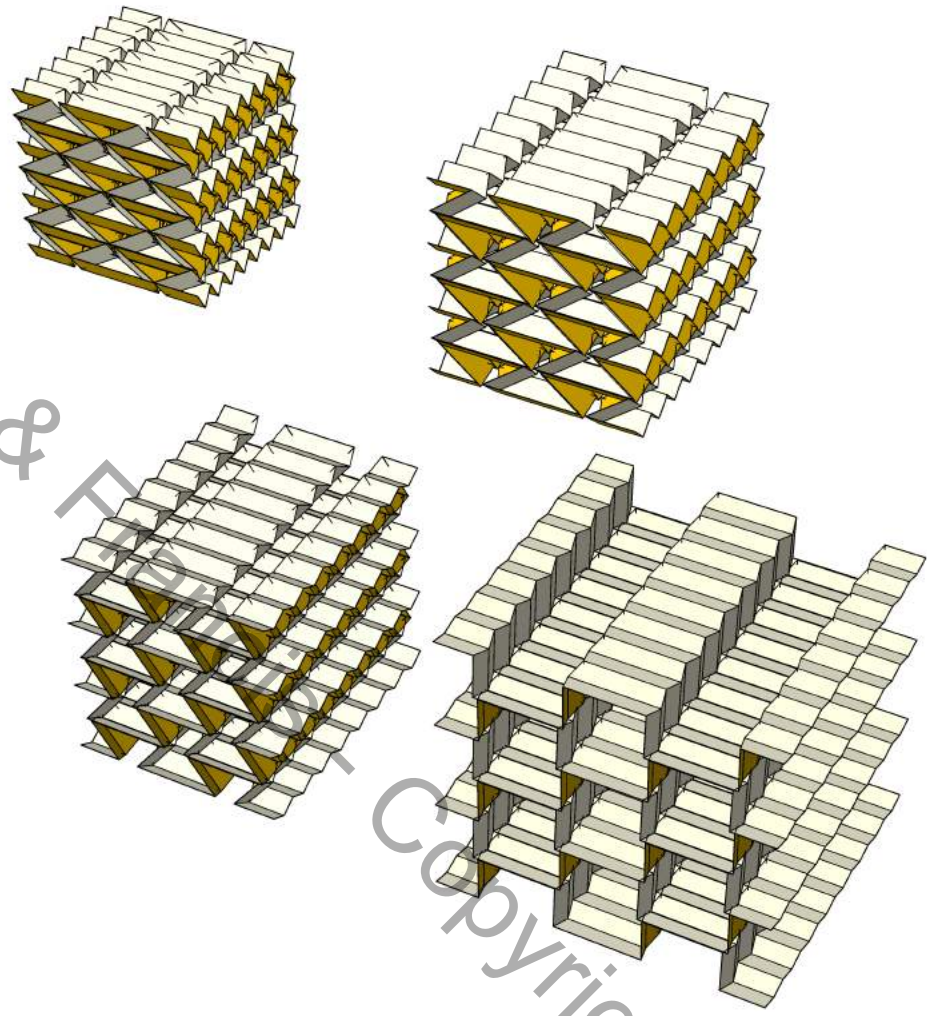

Figure 2.83.
An origami cellular structure that exhibits near-isotropic negative Poisson's ratio at four different stages of flexing.

tions, meaning that all three directions expand or all three contract. From smallest size to largest, it expands by a factor of about 1.9 in all three axes.

These mechanisms (and all such mechanisms based on the Miura-ori) exhibit a single degree of freedom in their motion: as one fold angle is flexed, all of the others flex in lockstep. At least, that's the theory—but that theory only describes materials where the facets are perfectly stiff and non-stretchable and the hinges are perfectly flexible. These conditions rarely hold in practice. There is almost always a little bit of "give." Facets can bend, hinges can

exhibit residual stiffness that can impose flexing on facets, and folds can soften and deform in ways that mimic stretching and/or compression of facets.

Consequently, if you build objects like the ones described in this section, you may find that they don't behave precisely the way the mathematics would predict. Surfaces, objects, and mechanisms can twist and distort in unexpected ways. That doesn't mean that the mathematics is *wrong*; but it may mean that we have attempted to apply it beyond its regime of validity because we have not taken into account all of the non-idealities of paper, or whatever our folding construction medium may be.

In many cases, the non-idealities of paper can be undesirable; our mechanism doesn't behave the way we want or expect it to. In others, though, we can make use of the non-idealities of paper to achieve interesting and useful forms and behavior. We will see a few examples of this phenomenon in the next and coming sections.

⋆ 2.4.5. Triangulated Cylinders

We saw earlier that the Huffman grid naturally curls up to form a cylinder (see Figure 2.16) as well as the Yoshimura pattern (Figure 2.24), which can curl in various cylindrical and/or helical ways. In fact, as Tachi has shown [118], *every* 2D periodic folding pattern displays either in-plane motion (like the classical Miura-ori) or some combination of two different helical motions (like Yoshimura patterns), which includes pure cylindrical motion.

The freedom to flex only happens when the edges are free, however. If we take such a pattern and join its ends, the resulting form becomes quite rigid. This follows intuitively from the observation that as we open and close the vertices of the pattern, the edges move toward and away from each other; the two motions are coupled. By joining the edges, we eliminate both opening/closing of the edges and their ability to slide past one another; if there are only two possible motions, we've eliminated both of them.

While connecting the ends makes a Yoshimura pattern into a rigid tube, we do have some freedom in how we connect the ends, as illustrated in Figure 2.84. If we follow a chain of valley folds (as viewed from the colored side of the paper)—one is shown in red in Figure 2.84—it traces out a polygonal circle or polygonal helix on the surface of the tube. If the chain joins to itself, then it closes into a polygon, as in the left subfigure. But, as shown in the

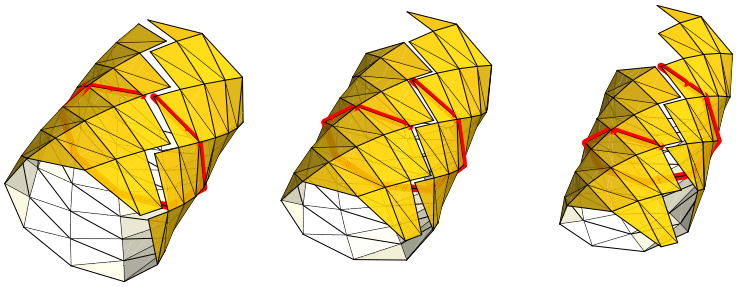

Figure 2.84.
Three different ways of joining the edges of a Yoshimura pattern with different helical offsets of a chain of crease pattern valley folds (marked in red).
Left: no offset.
Middle: offset by one.
Right: offset by two.

middle and right subfigures, it can be offset by varying amounts along the joint as it wraps around the cylindrical axis.

As we saw earlier in Section 2.3.2, there are at most three distinct values of fold angle in a periodic folded Yoshimura pattern, so the creases can be grouped into sets that share the same fold angle. Each set of creases with a common fold angle forms linear chains that wrap around the pattern. In general, each of the chains of valley folds and mountain folds with the same fold angle will form some type of helix; the helicity—offset from one turn to the next—of each chain will vary with the sector angles of the vertices and the mountain fold angles at each vertex (or equivalently, how you join the ends).

If the ends of a chain of valley folds are offset sufficiently far from one another, then instead of a chain of valley folds closing on itself, one of the chains of mountain folds can close on itself, and this occurrence gives rise to a variety of closed tube that has a new and interesting property. Although the closed tube is rigid (as is any closed tube of a Yoshimura pattern), there can be two distinct folded states of the same crease pattern, as shown in the example of Figure 2.85.

The Yoshimura pattern, broadly speaking, is composed of a grid of degree-6 vertices, formed by the intersections of three parallel sets of line segments. As we saw, because of the two degrees of freedom in the crease pattern mechanism, we have different ways of joining the edges to form a tube. If we think

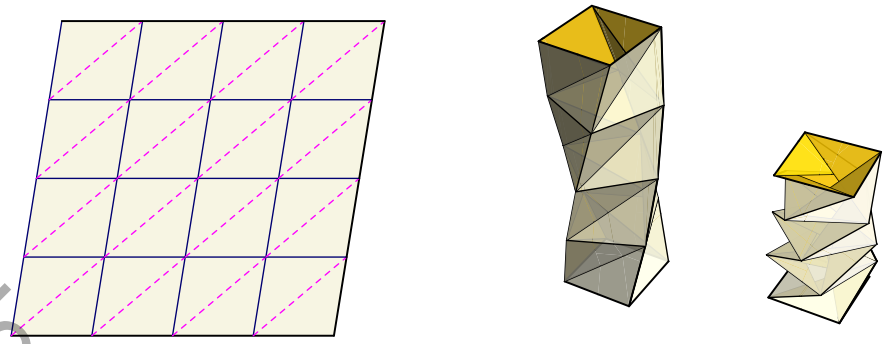

Figure 2.85.
A closed tube formed from a Yoshimura pattern having two folded states with left and right edges joined.
Left: crease pattern.
Middle: one folded state.
Right: the other folded state.

of the pattern as a periodic collection of quadrilaterals (outlined by mountain folds in Figure 2.85) diagonally crossed by folds of the opposite type (valley folds in Figure 2.85), then joining the ends of a row of quadrilaterals creates a tube with a polygonal cross section with faces subdivided into triangles, and we call it a *triangulated cylinder*.

Like so many other periodic folding patterns, this pattern has been discovered and re-discovered repeatedly by various researchers. While it seems likely to be quite old, the earliest mathematical analysis of this pattern was carried out by Simon Guest (now a professor at Cambridge University) during his Ph.D. research [41, 42, 43, 44]. Guest credits the concept to a cardboard model he saw of a bacterial flagellum constructed by one of his professors, C. R. Calladine. Guest coined the name "triangulated cylinder" for this structure, and I have adopted his usage.

It was also popularized by an influential article by Biruta Kresling [65], who noted that it arose naturally as a buckling mode of cylinders under compression. Kresling called the triangulated cylinder pattern "the Kresling pattern," and it has become relatively well known by that name.

Just as the Yoshimura pattern was a buckling mode of a cylinder under pure axial compression, this mode arises naturally by compressing the end of a cylinder while also applying a twisting force. In fact, it takes far less force to create the triangulated

Figure 2.86. Twisting and compressing an aluminum beverage can naturally creates the triangulated cylinder pattern.

cylinder pattern than the Yoshimura pattern; growing up in the 1970s, when beverage cans switched from steel to aluminum, I found amusement in the ease in which a twist-press could create this pattern (see Figure 2.86).

Triangulated cylinders were also extensively explored by Taketoshi Nojima in his master's thesis [95] and a paper [94] that carried out a wide-ranging exploration of Huffman grids, Miura-oris, Yoshimura patterns, and more. More recently, the concept and further structural variations have been explored by Tomoko Fuse [33].

As with the patterns we've seen thus far, there is considerable variation possible in the pattern. In the crease pattern, we can choose

- the number of columns,
- the height of each row (which determines the height of the folded form),
- the lateral shift of each row (which determines the rate of twist in the folded form).

Several more examples are shown in Figure 2.87.

In general for these tubes, there will be two stable states that have two different heights. If we seek to design such a structure, we would likely wish to choose the heights and then work backward to find the crease pattern that gives those particular heights.

There are two limiting cases to contemplate. The tallest that the tube could possibly be is the height of the crease pattern itself, and that could only occur if there is no twisting at all; in this case, the facet outlined by mountain folds would simply be rectangles

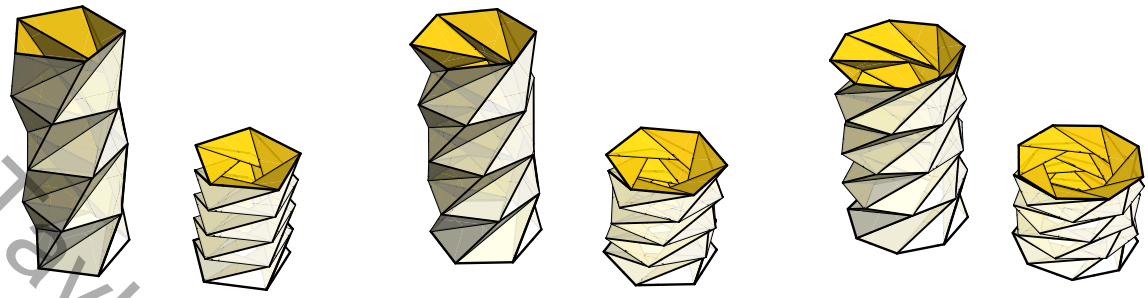

Figure 2.87.
Three examples of triangulated cylinders, each with two stable states, one half the height of the other.
Left: 5-fold rotational symmetry.
Middle: 6-fold symmetry.
Right: 8-fold symmetry.

crossed by an (unfolded) valley fold along the diagonal, as in Figure 2.88.

The other limiting case is when one of the states is completely collapsed flat, as in the right subfigure of Figure 2.88. This is suggestive: the two states are not just distinct; they are very, very different, and that suggests application as a deployable structure, as well as for artistic effect. Although there are only two stable states—with rigid panels and undeformed creases—if these

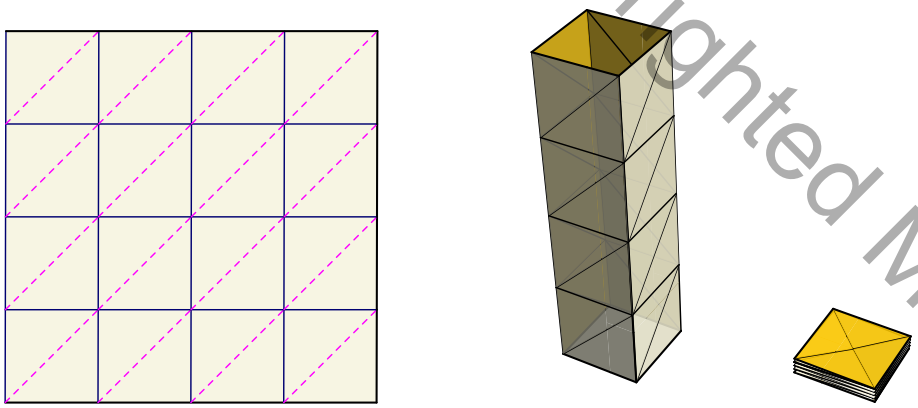

Figure 2.88.
A triangulated cylinder pattern of maximum height.
Left: crease pattern.
Middle: one folded state (maximum height, no twist).
Right: the other stable state (fully flattened).

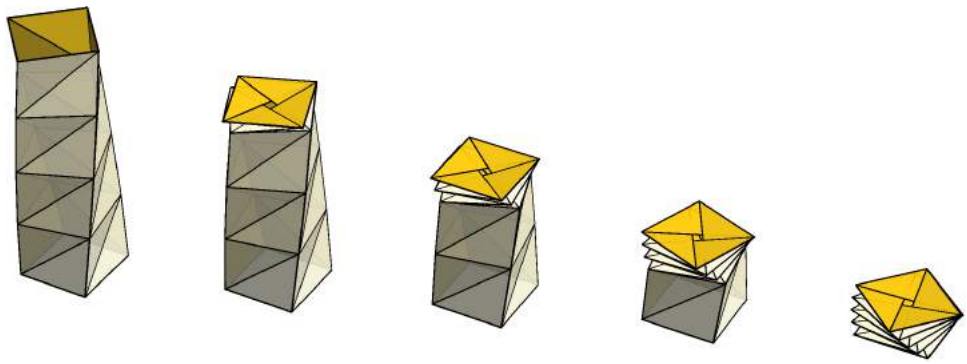

Figure 2.89.
A triangulated cylinder pattern, sequentially collapsed.

structures are fabricated with somewhat pliable materials, such as paper or plastic, then they can be deformed from one state to the other. The deformation happens by introducing strained deformations into the system; the strains create stresses; the stresses push the structure toward one or the other stable state; and the net result is that the tube can "click" from one state to the next. Or, more precisely, the rows will click from one state to the next (usually, in an unpredictable order), as illustrated in Figure 2.89.

Many origami artists have explored this twist-tube concept in their art. As the figures suggest, each row of the crease pattern is somewhat independent of its neighbors; you can give each row a different amount of twist, or even reverse the twist from one row to the next. Artist Tomoko Fuse, who has also extensively explored twists and has an entire book on the subject [33], devised an elegant and clever way to exploit this phenomenon; by alternating twist directions, one achieves a tube that, by twisting one direction and then the other, can expose and conceal alternate layers of the tube. By coloring the clockwise and counterclockwise sections separately, a striking color-change effect can be created, as shown in Figure 2.90. I encourage you to transfer the crease pattern to a large sheet, cut it out, glue the top and bottom edges together (using the tabs), and then try it out.

A similar concept was also discovered independently by Vietnamese-American artist and engineer Uyen Nguyen, whose company has used such twists in the world of high fashion, notably in a series of small handbags, as shown in Figure 2.91.

This pattern has also found application in deployable structures. Professor Stavros Georgakopoulos at Florida International

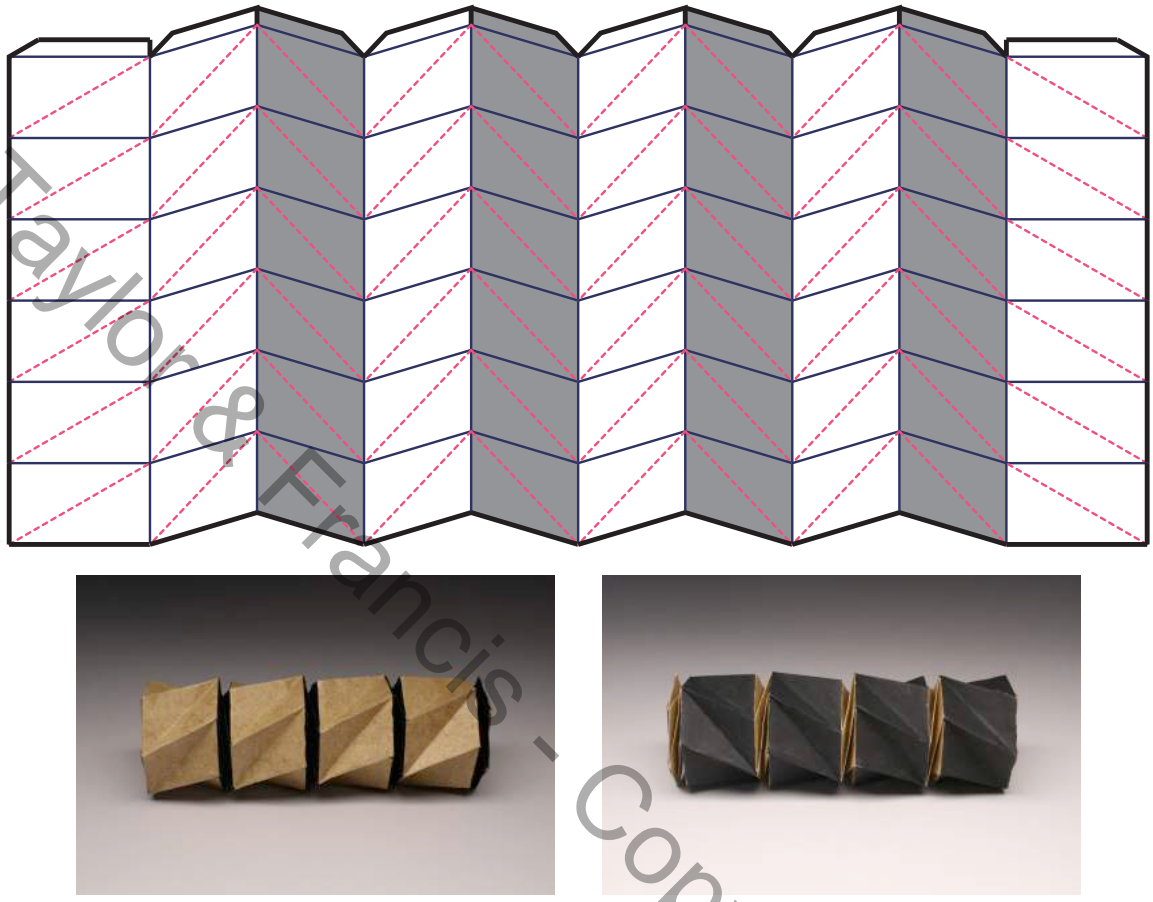

Figure 2.90.
Top: crease pattern for the bidirectional tube.
Bottom: two states.

Figure 2.91.
A twist-tube-based handbag, designed by Uyen Nguyen.
Photo by Bao-Khang Ngoc Nguyen.

Figure 2.92.
An origami quadrifilar helical antenna on Kapton substrate, based on the triangulated cylinder pattern.
Photo courtesy of Stavros Georgakopoulos and Xueli Liu, Department of Electrical and Computer Engineering, Florida International University, Miami, FL.

University and his students have developed deployable microwave antennas using this family of patterns; an example is shown in Figure 2.92.

You can make these tubes by simply picking values for the width-to-height ratio of a single parallelogram panel and the base angle of the parallelogram, then gluing the ends together. You will find that the tube naturally clicks into its stable positions and different tubes resist switching between the two states to varying degrees; some (like the square tube in Figure 2.89) are very resistant to collapse; others switch readily from one state to the other. Empirically, you will find that the closer the heights of the two stable states are to each other, the more readily the tube twists from one state to the other.

In application, though, we would like to specify dimensional parameters such as the folded height: in particular, if we want the tube to collapse flat, we would like to specify one of the two design heights (and perhaps the other, if we want to control the stiffness against collapse). In order to do that, we need to carry out a parameterized analysis of a single level of the twist. This requires a bit more mathematics than we have needed up to this point, and it may be safely skipped if you wish. For a comprehensive mathematical analysis, see Guest [42, 43, 44].

⋆⋆⋆ 2.4.6. Triangulated Cylinder Geometry

We will begin by considering a single level of the triangulated cylinder with the geometry shown in Figure 2.93. We assume m-fold rotational symmetry (i.e., $m = 4$ for a square, $m = 5$ for a pentagon, and so forth).

There should be two stable folded states, which we will distinguish by indices $i = 1, 2$. The heights of the two states are h_i, $i = 1, 2$, and we will denote the height of the crease pattern as h_0. We consider a single panel with corners $\mathbf{p}$, $\mathbf{q}$, $\mathbf{r}_i$, and $\mathbf{s}_i$. The panel consists of two facets, joined by a crease from $\mathbf{p}$ to $\mathbf{s}_i$. We assume that the bottom remains fixed, but the top two vertices $\mathbf{r}_i$ and $\mathbf{s}_i$ are different between the two stable states.

For simplicity, assume the edge from $\mathbf{p}$ to $\mathbf{q}$ is unit length. We also introduce the angle $\phi = \pi/m$ for convenience.

Both the bottom and top polygons are regular m-gons, but the top is going to be twisted relative to the bottom by some angle. We define $\delta\phi_i$ as the angular twist of the top relative to the bottom.

The problem is, then: given the rotational order m and the two desired folded form heights h_1 and h_2, what are the dimensions of the parallelogram for that tube? Specifically, what are the base angle α, side length r, and altitude h_0 of the parallelogram, as illustrated on the right in Figure 2.93?

By setting up a three-dimensional coordinate system and solving for dimensions that give the same crease pattern for the two folded form heights h_1 and h_2, we can find expressions for the parameters that define both crease pattern and folded form. We

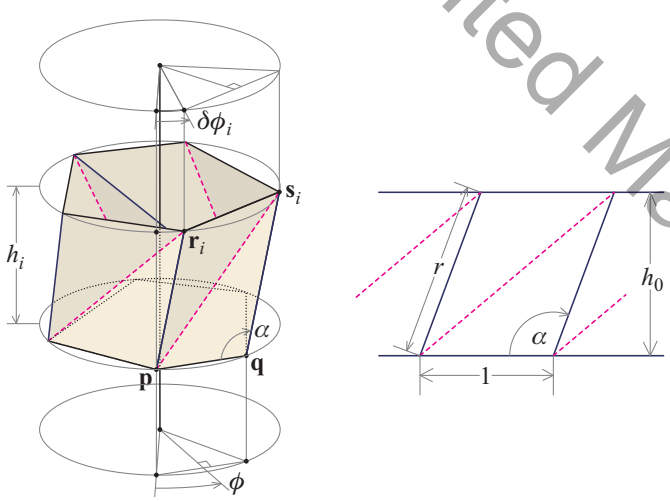

Figure 2.93.
Geometry of the triangulated cylinder for $m = 5$.
Left: folded form.
Right: crease pattern.

find that

$$\alpha = \cos^{-1}\left(\frac{x_2(x_2 - \cot(\phi))}{\sqrt{\left(x_2^2+1\right)\left(h_2^2\left(x_2^2+1\right) + x_2^2\csc^2(\phi)\right)}}\right),$$

$$r = \sqrt{h_2^2 + \frac{x_2^2\csc^2(\phi)}{x_2^2+1}}, \tag{2.12}$$

$$h_0 = \frac{\sqrt{h_2^2\left(x_2^2+1\right)^2 + x_2^3\cot(\phi)(x_2\cot(\phi)+2) + x_2^2}}{x_2^2+1},$$

where the quantities x_1 and x_2 are given by

$$x_1 = 2\sin\phi\frac{\sin\phi\sqrt{\cot^2\phi\csc^2\phi - (h_1^2-h_2^2)^2} - \cos\phi}{(1+(h_1^2-h_2^2)) + (1-(h_1^2-h_2^2))\cos 2\phi},$$

$$x_2 = 2\sin\phi\frac{\sin\phi\sqrt{\cot^2\phi\csc^2\phi - (h_1^2-h_2^2)^2} - \cos\phi}{(1-(h_1^2-h_2^2)) + (1+(h_1^2-h_2^2))\cos 2\phi}. \tag{2.13}$$

The twists of the top polygon relative to the bottom in the two states are given by

$$\delta\phi_1 = 2\tan^{-1}x_1,$$
$$\delta\phi_2 = 2\tan^{-1}x_2. \tag{2.14}$$

Although these expressions are complex, there is some useful information in them.

First, if the two height values h_1 and h_2 are chosen to be equal, then the two polygonal twist angles $\delta\phi_1$ and $\delta\phi_2$ are equal and the pattern becomes *monostable*—there is only a single folded state. Otherwise, it is *bistable*. The two different heights are the heights of the stable states; in between, the folding pattern must deform in some way, via stretching or buckling of the material. (How, precisely, it stretches or buckles depends very much upon the material from which it is made and the properties of the folds that act as hinges.)

If we make the two heights differ, then the tube can switch between the two heights by twisting from one $\delta\phi_i$ value to the other, depending on the pliability of the material from which it is made.

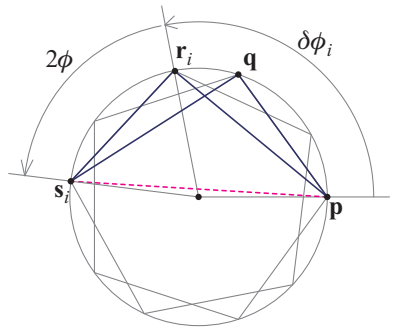

Figure 2.94.
Top view of a twist tube just shy of the critical point where the layers start to collide in the middle.

If you make a set of tubes with varying height differences, you will find that the more different the two heights are, the harder it is to "click" the tube from one height to the other because the greater will be the required material deformation in the intermediate state.

The height difference cannot be too great, though; because of the square root appearing in the definition of x_1 and x_2, there is the potential for an imaginary solution, i.e., no real solution, if the term $(\cot^2\phi\csc^2\phi - (h_1^2 - h_2^2)^2)$ goes sufficiently negative, which it does if the difference between h_1 and h_2 becomes too great.

We can find the boundary of the solution set by setting the argument of the square root to 0, which happens at

$$h_1^2 - h_2^2 = \pm\cot\phi\csc\phi. \tag{2.15}$$

That sets an upper limit on the difference in the two design heights; if $|h_1^2 - h_2^2| > \cot\phi\csc\phi$, then there is no solution for either height.

There is another limitation on the range of possible parameters, set by the amount of twist. If we look straight down the tube from the top, as illustrated in Figure 2.94, we see that as the relative rotation from one layer to the next increases, the valley folds approach the center of the regular polygon. Eventually they touch, and so for rotation angles $\delta\phi_i$ larger than that critical value, the layers will intersect each other somewhere in the middle of the twist.

Clearly from the figure, the valley folds of the parallelograms will collide when the total rotation angle from $\mathbf{p}$ to $\mathbf{s}_i$ is equal to π and the valley fold passes through the center. Thus, we must have (for a right-handed twist with $\delta\phi_i > 0$),

$$\delta\phi_i < \pi - 2\phi. \tag{2.16}$$

Since both values of $\delta\phi_i$ depend on h_1 and h_2, Equation (2.16) is implicitly a limitation on the values of the two design heights.

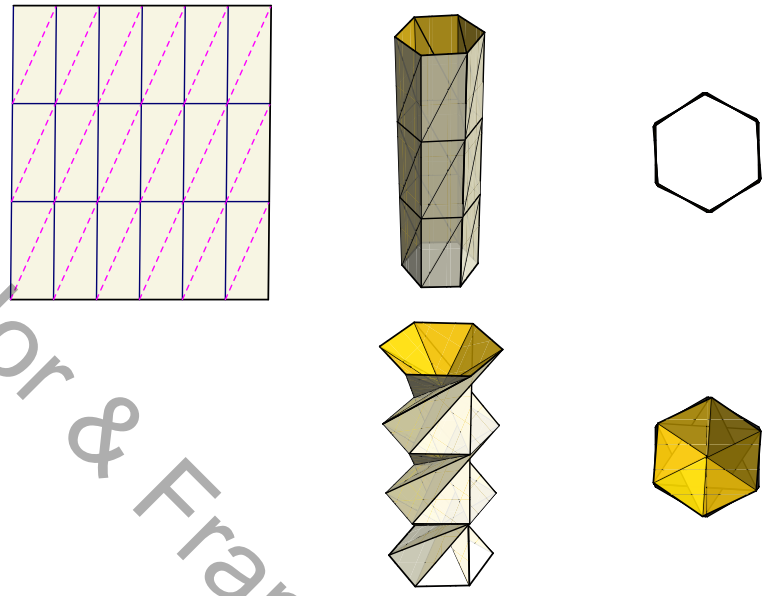

Figure 2.95.
A twist tube that touches at the center.
Top left: crease pattern.
Top middle: first stable state.
Top right: view down the (hollow) center of the tube.
Bottom middle: second stable state.
Bottom right: the edges touch in the middle of the tube.

It defines a critical value of the rotations $\delta\phi_i$,

$$\delta\phi_{i,\text{crit}} = \pi - 2\phi, \tag{2.17}$$

which, in turn, creates a critical value on the parameters x_i,

$$x_{i,\text{crit}} = \tan\left(\tfrac{\pi}{2} - \phi\right), \tag{2.18}$$

which, in turn, places another constraint on the relationship between the two heights. We find that

$$|h_1^2 - h_2^2| \leq \cot^2\phi. \tag{2.19}$$

Comparing Equations (2.15) and (2.19), we see that the latter is always stricter, since the right side contains an extra factor $\cos\phi$. So this condition sets the actual limit on height difference between the two states. If the two heights satisfy Equation (2.19) at equality, we call this a *critical* design.

When we choose heights at the critical value, both the crease pattern and folded form become interesting and distinctive. The example shown in Figure 2.88 was critical, as it turns out. Another example with sixfold rotational symmetry is shown in Figure 2.95. In this case, the critical configuration is not flat, but three-dimensional and quite solid. One could imagine using such a structure for its mechanical stability.

Figures 2.88 and 2.95 share two interesting properties: (a) the parallelograms of the crease patterns are actually rectangles (i.e.,

angle α is $\pi/2$), and (b) the second stable state is a polygonal tube with the valley folds at flat angles. This is more than coincidence: it is, in fact, the case for any combination of rotational symmetry and height parameters at criticality.

Many artists and designers have made use of the triangulated concept already, but considering the number of things you can vary—rotational order, number of segments, parameters of each segment, twist directions, twist heights—there are undoubtedly many possibilities still to be discovered and explored. Artists like Nojima and Fuse have explored conical forms, which give self-similar spirals reminiscent of seashells.

The Yoshimura pattern has two continuous degrees of freedom in its motion, but, as we have mentioned, joining the edges dramatically drops its theoretical flexibility to the two bistable forms. If we don't join the edges, then we're back to two degrees of freedom—at least, considering only the mechanics of the vertices. However, such mechanisms are further constrained by self-intersection avoidance: the paper can't pass through itself. Self-intersection avoidance can be used to constrain a Yoshimura-like mechanism to a lower degree-of-freedom behavior.

One of the most interesting and surprising cylindrical mechanisms is a model called "Spring Into Action," designed by the late British artist Jeff Beynon. It has become iconic in the world of origami, and it is tremendously fun to fold and play with. With Jeff's kind permission, I give folding instructions for it on pages 165–168.

⋆ 2.4.7. Waterbomb Tessellation

The patterns possible with semigeneralized Miura-oris are almost endless, but they do all share two properties: (1) they are strictly periodic in one direction at all folded states, and (2) they have a single degree of freedom in their folding motion (at least, if we don't allow bending of the quadrilateral facets). We saw, though, that the Yoshimura pattern and its variants exhibit two degrees of freedom: they can move in two distinct ways (and mixtures thereof). This extra freedom arises from the degree-6 vertices in the pattern. If we take a semigeneralized Miura-ori and, by eliminating edges in the pattern, allow some of the degree-4 vertices to coalesce into degree-6 vertices, we might expect to pick up some of the additional flexibility of the Yoshimura pattern. And indeed, this is the case.

Spring Into Action by Jeff Beynon

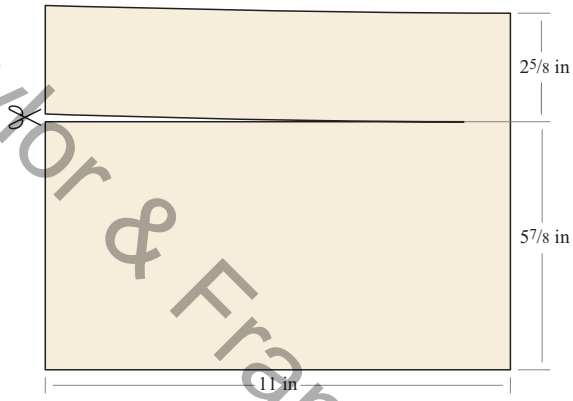

1. Begin with a 15:8 rectangle. You can make this from a sheet of American letter paper ($8\frac{1}{2}$ by 11 in) by cutting a strip $2\frac{5}{8}$ inch wide off of the long side.

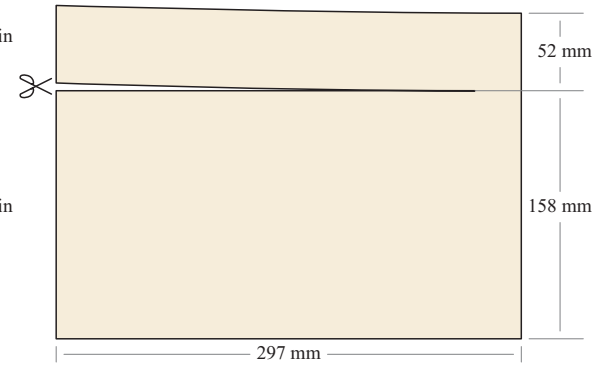

2. Alternatively, you can make this from a sheet of A4 European letter paper (297 by 210 mm) by cutting a strip 52 mm wide off of the long side.

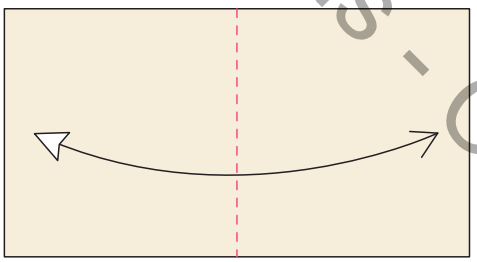

3. Fold the paper in half from side to side and unfold.

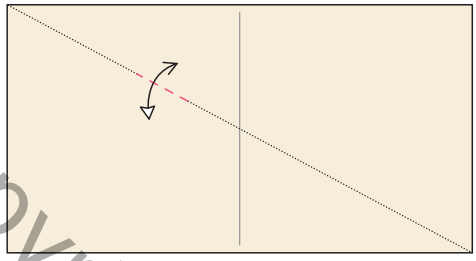

4. Fold the paper along a crease that runs between the upper left corner and the lower right corner, making a pinch about 1/3 of the way along the fold.

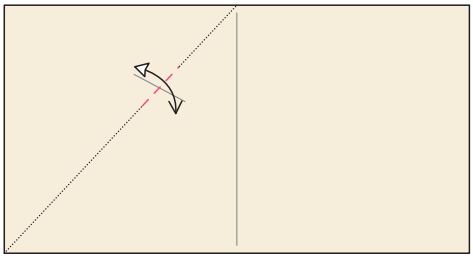

5. Fold the upper left corner down along a crease that runs from the lower left corner to the middle of the upper edge and unfold, pinching at the crossing.

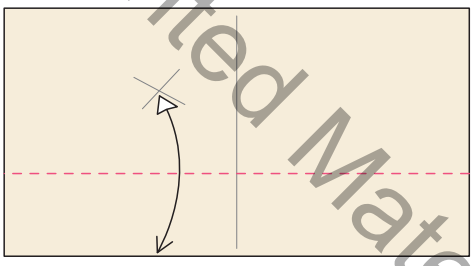

6. The intersection of the two creases is 1/3 of the way down from the top and 1/3 of the way from the left edge to the right. Fold the bottom edge up to touch the crease intersection and unfold.

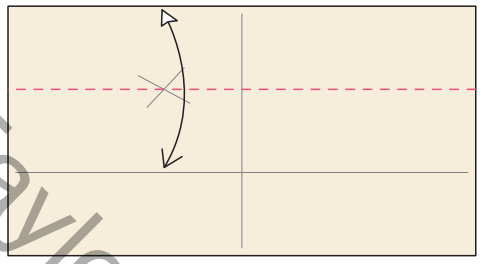

7. Fold the top edge down to touch the crease you just made and unfold.

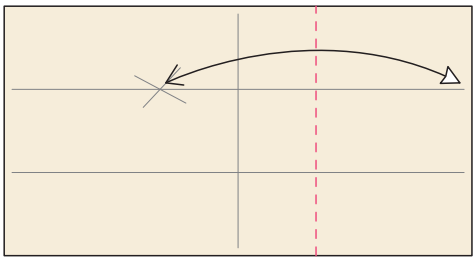

8. Fold the right edge over to the crease intersection and unfold.

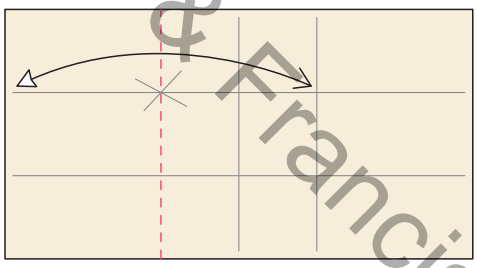

9. Fold the left edge over to the crease you just made and unfold.

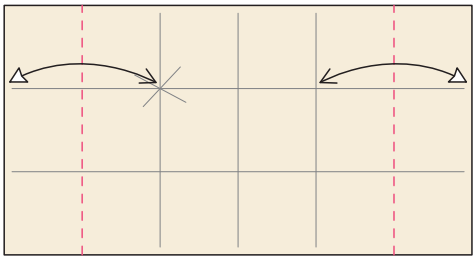

10. Fold the side edges in to touch the existing creases and unfold.

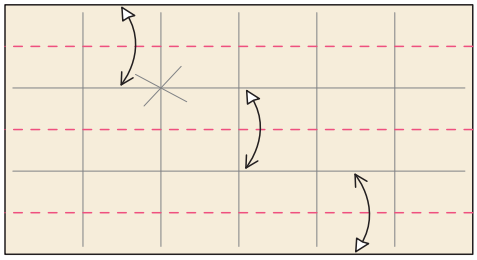

11. Divide each of the horizontal panels in half.

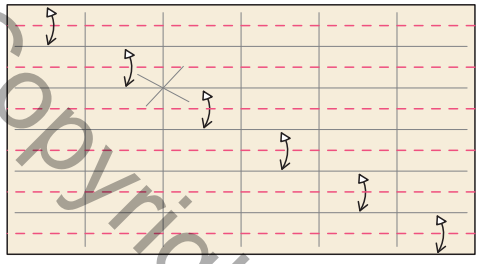

12. Divide each of the horizontal panels in half again.

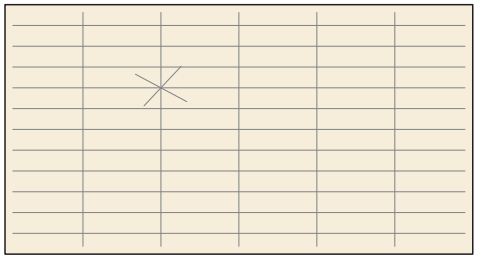

13. Turn the paper over.

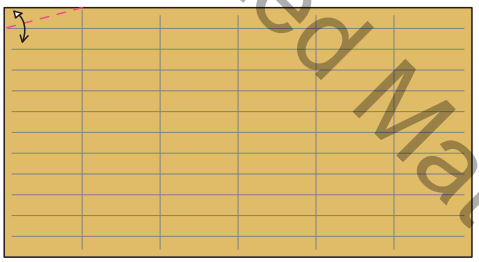

14. Crease the upper left rectangle along the diagonal with the crease running from lower left to upper right.

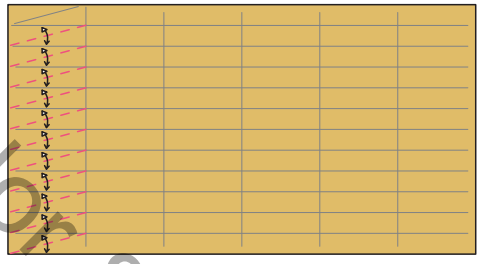

15. Repeat on the remaining eleven panels in the column.

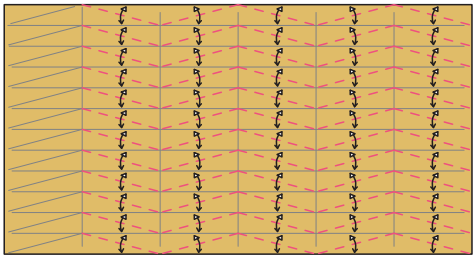

16. Repeat on the remaining 60 panels, reversing the direction of the diagonals in alternating columns.

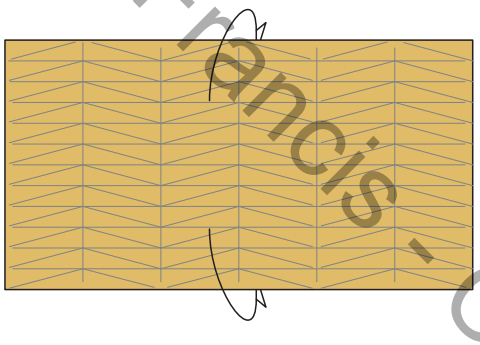

17. Curl the paper into a tube and turn it over.

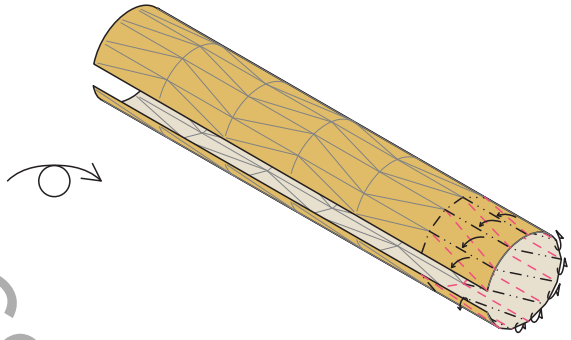

18. Twist the end counterclockwise using the existing creases.

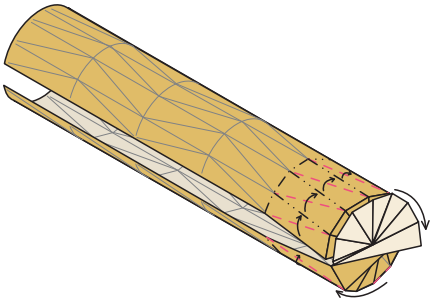

19. Now twist the end clockwise, again using the existing creases. You'll find it very difficult to get all the creases going at once, but when they're all started, it will pop into place.

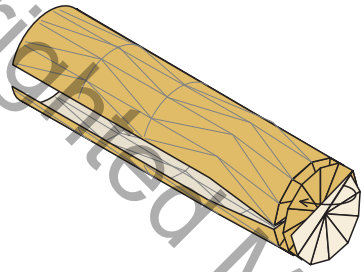

20. Without undoing the twists, bring the white layer out from inside the end.

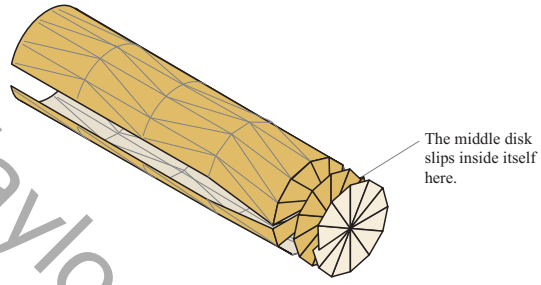

21. The twists should now form two separate disks on the end of the tube.

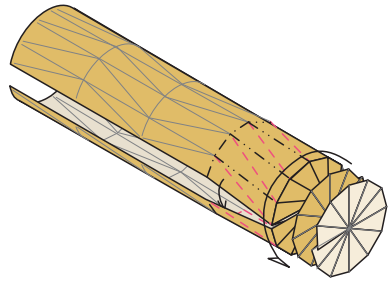

22. Twist the right end one-half turn counterclockwise using the existing creases; make sure you tuck the upper edge inside the pocket as you do.

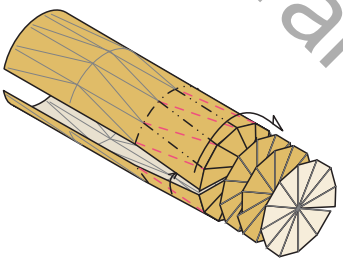

23. Twist the right end clockwise on the existing creases, this time making sure that the lower edge goes inside the upper edge.

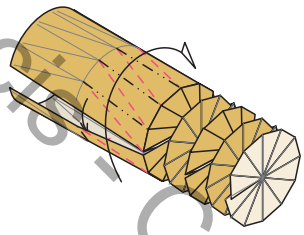

24. Repeat steps 22–23 on the remaining two segments.

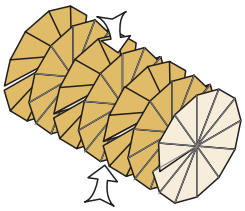

25. Squeeze the middle disk to activate Spring Into Action.

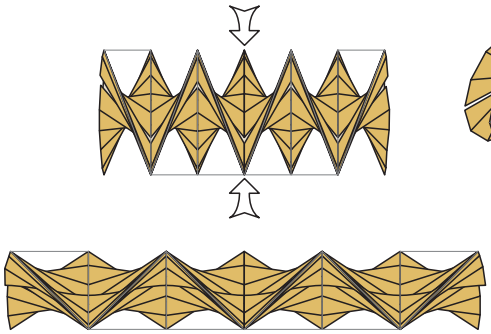

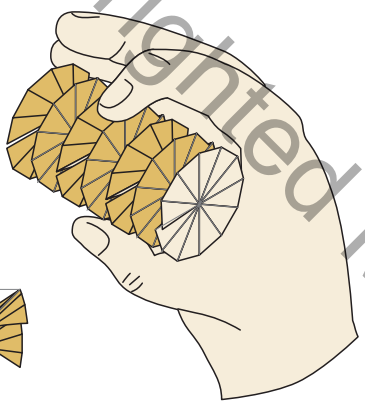

26. Finished Spring into Action. Squeeze the center of the model to make the sides spring out. The model works best if you use somewhat heavy paper and store it compressed (for example, under a heavy book) before springing it.

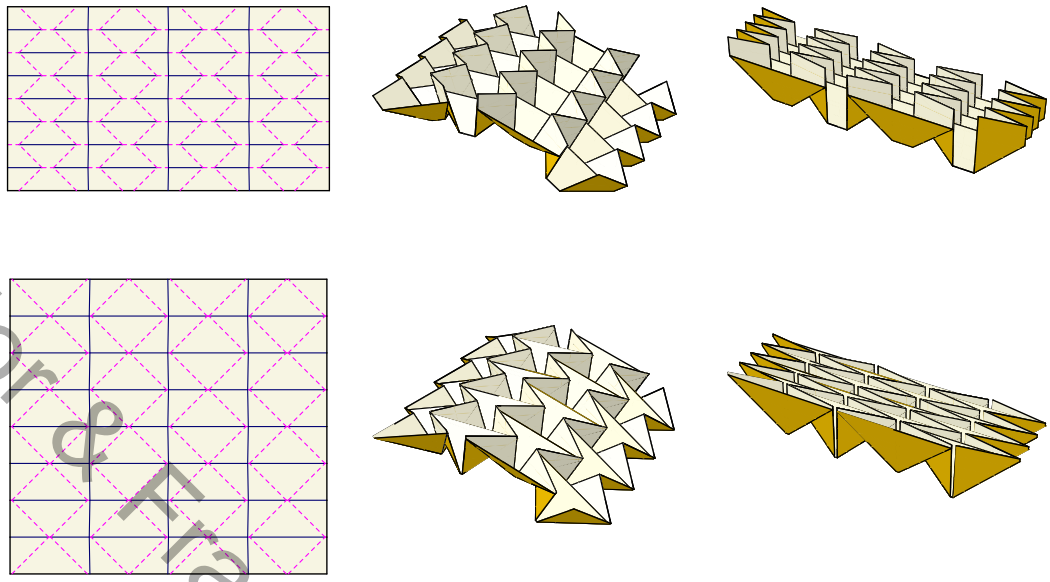

Figure 2.96.
Evolution of the Waterbomb tessellation.
Top row: a semigeneralized Miura-ori, which flexes with a single degree of freedom.
Bottom row: reducing the distance between selected pairs of vertices.
Left: crease pattern.
Middle: partially folded form.
Right: nearly flat-folded form.

One possible way of performing this coalescence is illustrated in Figure 2.96, in which the top row shows a particular semigeneralized Miura-ori and how it changes as we eliminate the shortest segments within the crease pattern.

As long as those segments have nonzero length, the pattern has a single degree of freedom and is linearly periodic in the direction transverse to the minor folds—that is, it expands in a straight line perpendicular to the minor folds (horizontal creases) as it is flexed. Note from the middle image that in the intermediate state, it is curved along the minor fold direction, straightening out only as it approaches flat-folded. However, when we completely eliminate those edges, coalescing pairs of degree-4 vertices into degree-6 vertices, something almost magical happens: the pattern acquires a new type of motion, illustrated in Figure 2.97.

Instead of being curved along the minor-fold direction and linear along the perpendicular direction, this motion is straight along the former and curved along the latter. This pattern can move in both ways—and, as well, in mixtures of the two.

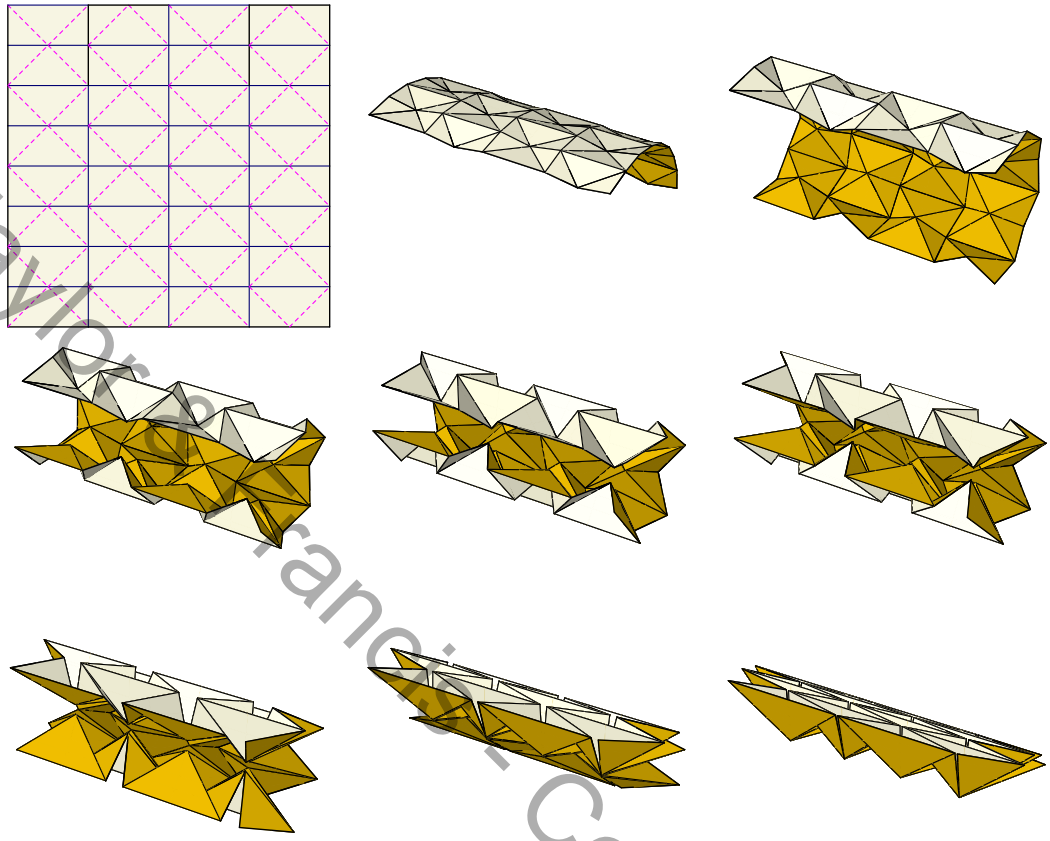

Figure 2.97.
Second periodic symmetry of the Waterbomb tessellation.
Top left: crease pattern.
Remaining figures: evolution of the pattern from unfolded to nearly flat-folded.

This new pattern is, in fact, not that new and is known by several names, depending on the context in which is was discovered (or re-discovered, as the case may be). It was described in an origami context by the great Japanese master of geometric folding Shuzo Fujimoto in his 1976 masterwork *Rittai Origami* [30], but the pattern has, perhaps, achieved its greatest renown in a design by Yuri Shumakov, which we will shortly meet.

One of this pattern's names, and the one I prefer for its descriptive value, is the *Waterbomb tessellation*, because it is composed of arrays of square units, each of which is the traditional Waterbomb base. Alternate columns of Waterbomb bases are offset up or down by one-half unit.

The Waterbomb tessellation exhibits two periodic modes of motion that can be explored as it is flexed. The first, shown in the

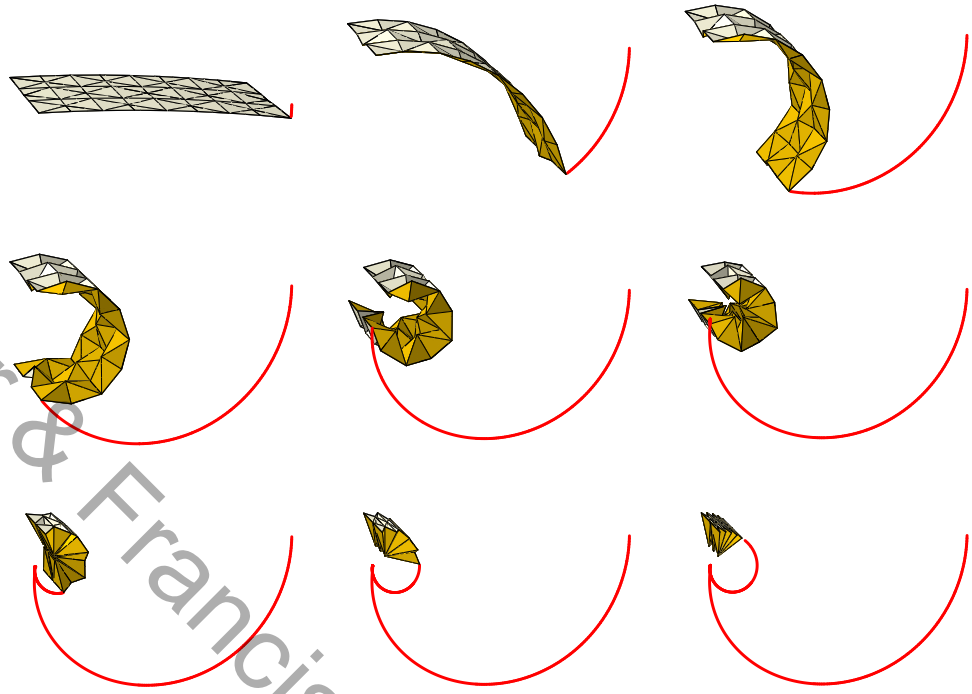

Figure 2.98.
Reversing motion of the Waterbomb tessellation, looking down the cylindrical axis of symmetry, as the pattern folds from near-unfolded (top left) to near-flat-folded (bottom right). The red line traces the rightmost corner of the initial pattern.

bottom row of Figure 2.96, is a linear motion—the pattern expands linearly in the direction transverse to the minor folds of the crease pattern. The second, shown in Figure 2.97, is cylindrical; the pattern is rotationally symmetric about a cylindrical axis that runs in the direction of the minor folds of the crease pattern.

What is even more interesting is that this cylindrical motion is not uniform: it actually reverses direction over the course of the folding motion. This can be seen in the sequence of images in Figure 2.98, showing the motion from unfolded to flat-folded, looking "down the barrel" of the cylindrical axis.

As you can see, with four rows to the pattern, it nearly closes on itself, and in fact, for five or more rows, the pattern does collide with itself during the course of the motion. This does not mean that such patterns are impossible to fold; only that they must be distorted into a non-periodic and/or bent form at some point during their construction and flexing.

Because all the vertices are degree-6, the overall pattern actually has many, many degrees of freedom (we will learn more

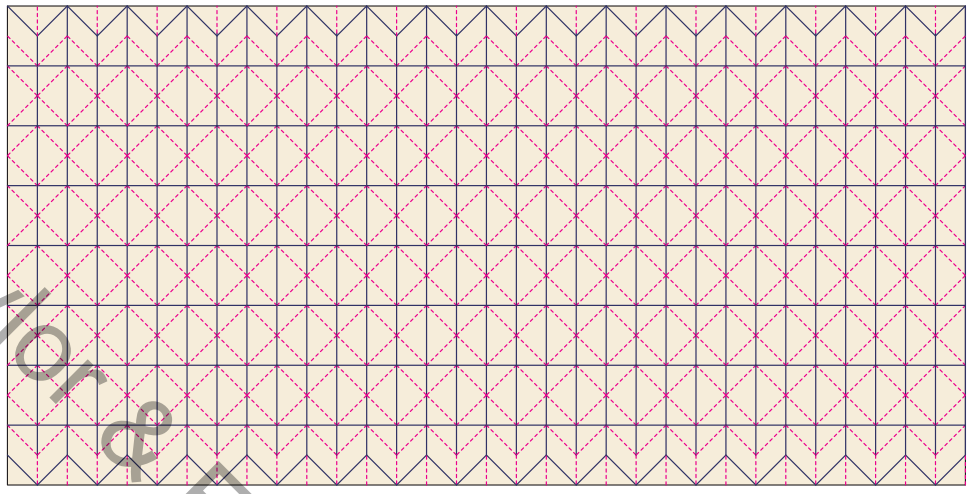

Figure 2.99.
Crease pattern for Yuri Shumakov's "Magic Ball." This is the Waterbomb tessellation (rotated 90° from Figure 2.97), with a touch of Miura-ori at the top and bottom.

about this in Chapter 7). A physically folded model will have a preferred state, however. The actual configuration that any real folded object takes comes from an equilibrium found by balancing the springiness of the folds and constraints upon the motion determined from the folding pattern.

In the Waterbomb tessellation, that motion is what is called *synclastic*: if you bend the pattern into a curve without tightly constraining it, it curves transversely in the same direction as the original bend, forming a shape like the surface of a sphere. The Miura-ori, by contrast, is *anticlastic*; if you bend it in one direction (forcing the quadrilateral facets to bend), it also curves transversely, but in the opposite direction, like a saddle. The Waterbomb tessellation, like the Miura-ori, is another example of a mechanical metamaterial, in which the pattern of folds gives the overall surface, on average, mechanical properties that are very different from those of the unfolded material.

The synclastic behavior of the Waterbomb tessellation gives rise to a lovely origami design, the "Magic Ball" of Yuri Shumakov [108], shown in Figures 2.99 and 2.100. In this design, a Waterbomb tessellation is formed into a tube and two opposite edges joined. The resulting springy surface is both beautiful to look at and oddly beguiling to play with. Yuri and his wife Katrin Shumakov have developed a wide range of variations of this concept, and online video instructions for some of them are readily

Figure 2.100.
Three configurations of Yuri Shumakov's "Magic Ball."

available. I give a crease pattern here, leaving the folding and assembly as an exercise for the reader.

The "Magic Ball" is squishy: compressing it at its end makes it bulge out in the middle. This is an illustration of the synclastic behavior of the Waterbomb tessellation. The Shumakovs have developed an enormous variety of shapes based on this pattern [108], both single-sheet and modular forms and variations shaped like balloons, trees, and more. As just one example of the pattern's versatility, Figure 2.101 shows a set of lampshades designed by them that make use of it.

Figure 2.101.
Lampshades by Yuri and Katrin Shumakov, based on the Waterbomb tessellation.
Image courtesy of Yuri and Katrin Shumakov.

The concept of joining the ends of the Waterbomb tessellation into a tube was conceived even earlier, by Fujimoto [30], who showed that many periodic patterns can be similarly treated, by stretching into a cylindrical form. We will come back to this concept.

Now, if we constrain an unjoined Waterbomb tessellation pattern to be periodic along the cylindrical axis (no localized bulging allowed) and only permit expansion perfectly transverse to the axis of rotation, as illustrated in Figure 2.97, then the resulting motion has only a single degree of freedom, and the angular fraction of a cylinder that the pattern subtends varies continuously with the motion. Hence, if you were to join the ends into a tube—and you would need at least five rows to do that—that joining would freeze the motion and the tube would be rigid, at least, theoretically.

In practice, however, small deviations of the creases from their theoretical positions—which can occur naturally with softly rolled creases—allow a great deal more flexibility than a simple theoretical model would suggest. The "Magic Ball" can expand and contract cylindrically both with and without bulging by making use of such small distortions of the pattern. And this ability of the tube to expand and contract in diameter thereby makes it useful in the real world.

One of the more interesting applications of the Waterbomb tessellation was developed by Oxford University professor Zhong You and his postdoc Kaori Kuribayashi-Shigetomi [131]. They developed an aortic stent based on this tessellation, shown in Figure 2.102. The stent is fabricated from shape-memory alloy that is compressed to a smaller size on the fold pattern, which allows it to be guided into place in the circulatory system. Once in the desired location, it is warmed via a catheter, and it expands out, holding the blood vessel open.

⋆ 2.4.8. Troublewit and Pleats

Different periodic patterns exhibit different flexural motions. The Huffman grid has a single degree of freedom, and its flexing motion is always cylindrical. The Waterbomb tessellation has two degrees of freedom and both of its flexing motions are purely cylindrical. The Miura-ori and its periodic generalizations, though, always exhibit straight-line motion transversely to the minor folds of the pattern—at least, if we force all of the facets to remain straight.

Figure 2.102.
You and Kuribayashi-Shigetomi's aortic stent, based on the Waterbomb tessellation along helical lines.
Image courtesy of Zhong You.

If we allow the quadrilateral facets of a semigeneralized Miura-ori to flex along their diagonals—which is quite common if we're working with paper, even fairly stiff paper—then such patterns can often be bent cylindrically in the direction transverse to the minor folds, adding a new level of diversity to the structures and mechanisms that can be formed with such patterns.

This versatility has not gone unnoticed. During the Victorian period in England, a popular magic routine involved the manipulation of a pleated sheet of paper into a wide range of (usually) cylindrical forms. The routine is called "Troublewit." It begins with a large sheet of paper, pleated first one way, then the other, as shown in Figure 2.103.

This folded form is an example of a semigeneralized Miura-ori. By shifting the angles of the various pleated segments and then stretching the pattern into a cylindrical form, it can be manipulated into a wide variety of surprisingly different shapes, a few of which are shown in Figure 2.104. With a bit of practice, the transformations can be made smoothly and quickly, and when worked into a story, provide an entertaining interlude as part of a magic routine. "Troublewit" is a classic routine [63] and is well known among magicians. Versions of the routine has been traced back as far as 1676 [85]. As we have seen, people were pleating

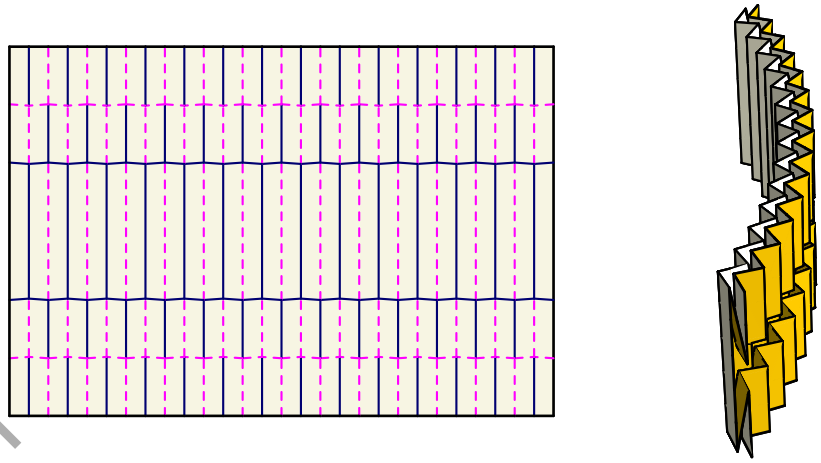

Figure 2.103.
The Troublewit.
Left: crease pattern.
Right: initial folded form.

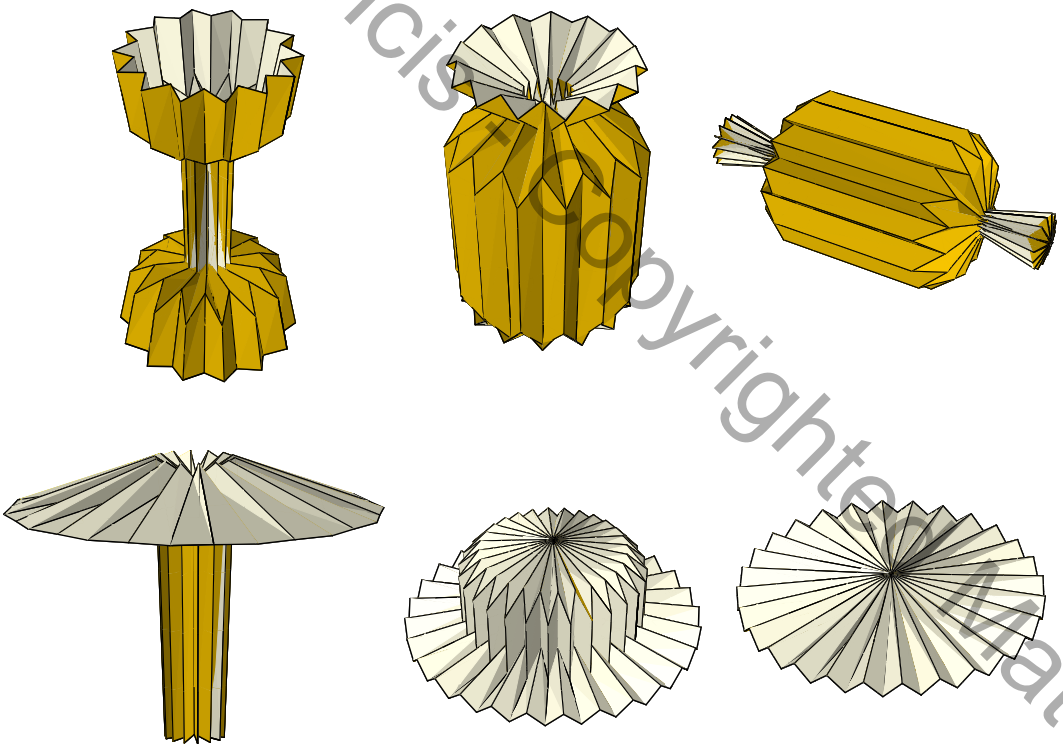

Figure 2.104.
Some of the Troublewit shapes.
Top row: left to right, "Dumbbell," "Vase," and "Christmas Popper."
Bottom row: left to right, "Parasol," "Hat," and "Rosette."

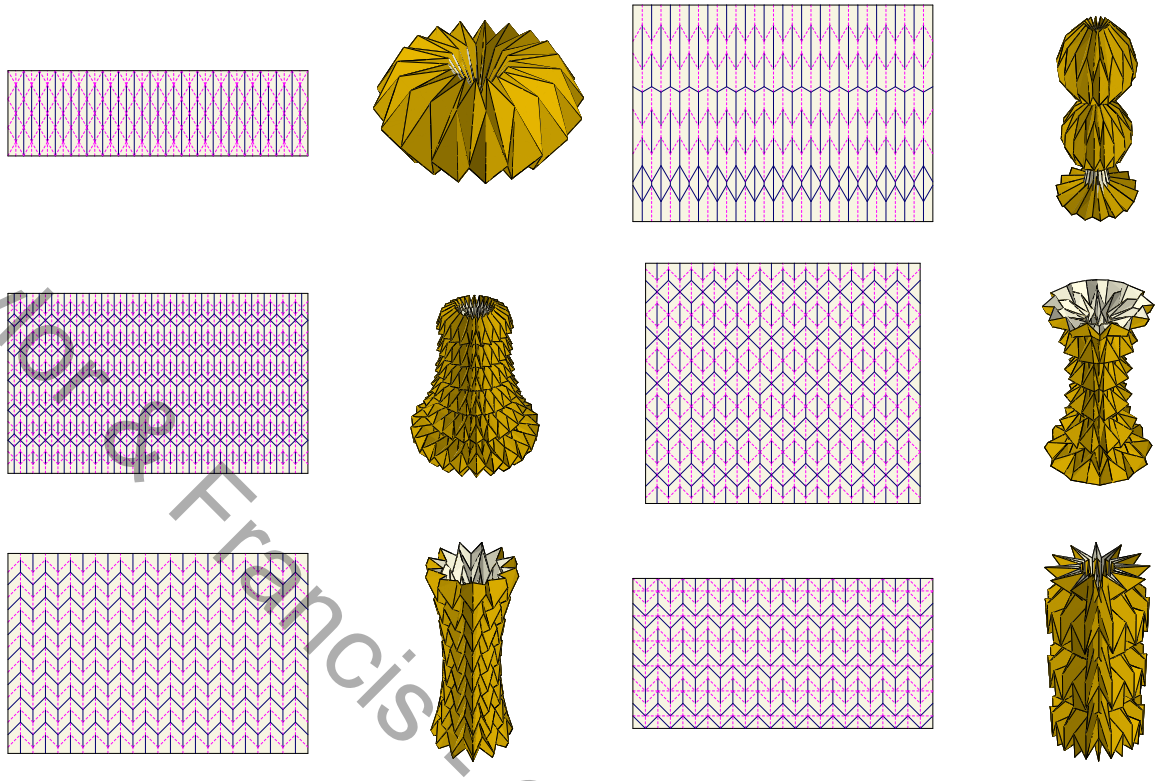

Figure 2.105.
Several of Shuzo Fujimoto's rotationally symmetric pillars, from *Rittai Origami*.

napkins and paper back in the 1600s, so it is not surprising that manipulations of multiply pleated forms also have a long heritage.

Also unsurprising is that the concept of stretching pleats into rotationally symmetric forms has been repeatedly rediscovered by many people in the course of folding paper. The students of Josef Albers (who we have already met) developed stretched pleated forms in their 1920s Bauhaus development, and stretched pleats have a long history in Japanese origami: not just in the simple paper fan, but also in representational folding.

The technique was explored in purely geometric (non-representational) forms within the Japanese folding tradition by the great geometric folding artist Shuzo Fujimoto in his book *Rittai Origami* [30], in which he showed many examples of geometric shapes created via this technique. A few reconstructed examples are shown in Figure 2.105.

Fujimoto describes more than 50 different designs in his book that show a wide variety of shapes and textures.

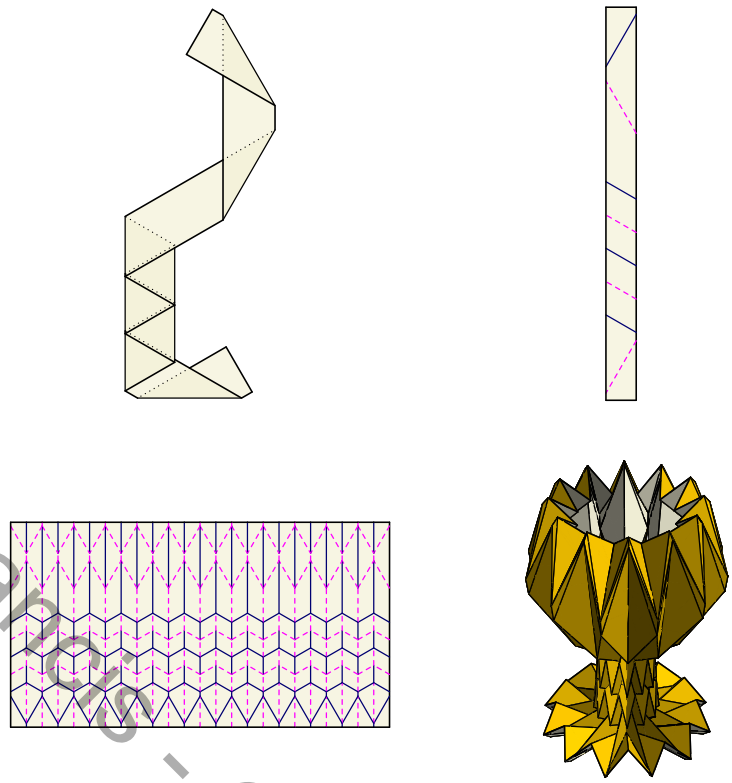

Figure 2.106.
Design of a rotationally-stretched goblet.
Top left: a strip of paper folded into the cross section of the desired shape.
Top right: the unfolded strip.
Bottom left: the crease pattern of the strip, mirrored and then repeated.
Bottom right: the resulting shape after bending it cylindrically and joining the ends.

Remarkably, one can construct patterns for this family of shapes using a very simple procedure that involves almost no mathematics at all. The symmetries in the crease patterns themselves suggest a method of construction.

In Figure 2.105, each crease pattern consists of a vertical strip paired with its mirror image; these pairs are then replicated horizontally to make up the full crease pattern. If we were to cut and flat-fold a single one of these strips, we would find that the shape of the strip is approximately the cross section of one side of the cylindrical form, as shown in Figure 2.106.

To design such a form, you take a strip of paper and flat-fold it into the cross section of the desired shape, then unfold it. The creases left in the paper provide the positions and angles of the

creases needed for the folded form. You can use the unfolded strip as a template to replicate the pattern on a larger rectangle to create the desired folding pattern.

This method also works to design a semigeneralized Miura-ori without doing any angle/distance calculations. In fact, each of these rotationally stretched pleated forms *is* just a semigeneralized Miura-ori; any SGMO may be (in principle) stretched into a cylindrical form, at the cost of having some bent quadrilateral facets and some distortion of the form.

Note that the shape taken by the flat-folded strip is an approximation of the cross section of the rotational form, but it is not exactly the same. This mirrors the situation with SGMOs that we saw earlier. When we stretch out a flat-folded form, the minor fold bend angles open up, as in Figure 2.72, which changes the shape. With SGMOs, it was possible to precisely calculate the amount of distortion needed in the flat-folded form to give a desired 3D cross section. With rotationally stretched pleats, the situation is more complicated, because the amount that any given fold is stretched varies with its radial distance from the axis of rotation and the number of repetitions in the pattern—and the bending of quadrilateral faces adds further complication. Nevertheless, as Figure 2.106 shows, the flat-folded shape is usually a pretty good approximation of the finished cross section, good enough to be used as the basis for design.

You might have noted that the crease assignment in the folded strip is not the same as in the periodic pattern in Figure 2.106. There is obviously an ambiguity in assignment when forming the cross section, because for a given set of crease positions, every non-self-intersecting assignment will give the same cross section. But not every assignment will allow a non-self-intersecting 3D form, and, in fact, it is possible to create flat-folded strips that cannot be transformed into a non-self-intersecting SGMO or rotationally stretched pleated form.

There is, though, a simple method to determine the proper assignment (if it exists) for the folds that cross the strips (i.e., the non-vertical creases in the crease patterns of Figure 2.106). If we label the two long edges of the strip A and B, as in Figure 2.107, the desired crease assignment for the cross-creases is the one for which on one side of the strip, edge A is never covered by the interior of a facet, and if you turn the strip over, edge B is never covered by the interior of a facet.

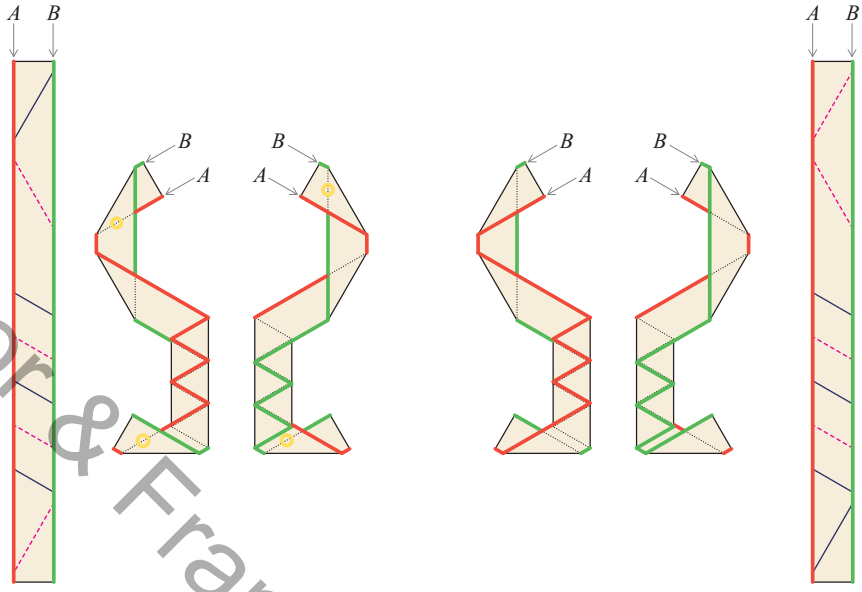

Figure 2.107.
Determining the crease pattern for a semigeneralized Miura-ori or rotationally-stretched pleat.
Left: alternating mountain and valley folds won't work because there are regions (indicated by the amber circles) where edges A and B are covered by the interior of facets.
Right: changing a few of the folds gives a valid crease assignment for the strip, which can then be used to build a repeated pattern. Note that the A path (on the left) and B path (on the right) are both uncovered along their full length.

Why the distinction about "covered by the *interior*"? That's because it *is* allowed for an A edge to be covered by the B edge or vice versa, if the two edges are collinear. As for why the edge is allowed to cover but the interior isn't: this follows directly from the Justin Non-Crossing Conditions.

For the vertical creases, what about their assignment once we've arrayed the strips into a rectangular crease pattern? There is a similarly simple rule for determining their assignment, but I will leave the discovery of that rule as an exercise for the reader. I'll give a hint, though: if you use two-colored paper, as in Figure 2.108 to fold the strip, the crease assignment is related to the exposed colors of the folded strip.

The path of the folded strip does not need to strictly follow the outline of the desired shape; by incorporating short "detours" perpendicular to the path, one can create additional folded edges that add texture and beauty to the folded shape, as in the two examples in Figure 2.109 by Israeli artist Ilan Garibi.

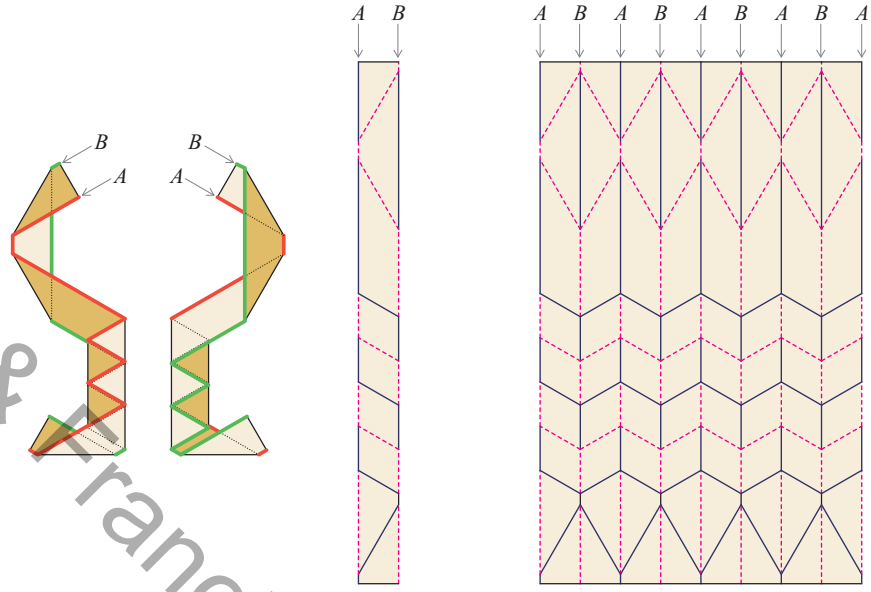

Figure 2.108.
Arraying the folded strip.
Left: folding the strip from two-colored paper gives a simple rule for the assignment of the vertical folds.
Right: the arrayed crease pattern, composed of alternations of the strip and its mirror image.

Figure 2.109.
Rotationally stretched forms by Ilan Garibi.
Left: "Faberge Egg" (2011), flat egg configuration.
Right: "Faberge Egg," vase configuration.

Figure 2.110.
"Tavolini" (2013), by Ilan Garibi.

Garibi has applied folding techniques to many materials: not just paper, as shown here, but also wood, metal, and other materials. Figure 2.110 shows a rotationally-stretched form folded from laser-scored wood veneer laminate. Note that the vertices of this pattern includes both degree-8 and degree-5 vertices; the latter are clearly not flat-foldable, but many non-flat-foldable patterns can be used to create 3D surfaces.

An even simpler construction method for rotationally stretched pleated forms was developed by British artist Paul Jackson and used in numerous works whose style is now inextricably associated with his name. Instead of flat-folding a strip and using it as a template, Jackson cross-pleats a rectangle with folds at 90°, then stretches the pleats individually to form the curved cross section. He has used this technique (along with dry pastels to accentuate the folds) to create a wide variety of beautiful forms, two of which are shown in Figure 2.111.

Figure 2.111.
Left: a cross-pleated pattern stretched into a curve.
Photo originally published in [53]. Used by kind permission.
Middle: "Brown Bowl," by Paul Jackson (from the Organic Abstract series. Folded paper and dry pastel).
Right: "Pod," by Paul Jackson (from the Organic Abstract series. Folded paper and dry pastel).
All photos courtesy of Paul Jackson.

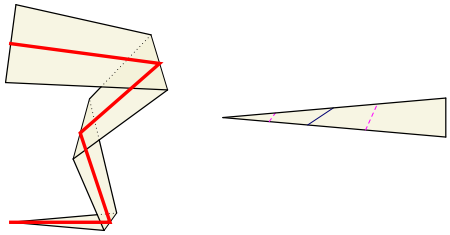

Figure 2.112.
You can fold a triangle into a strip that defines the cross section created by a circular crease pattern.

Now, the technique of using a strip as a template works for other shapes of strips, not just rectangular ones. If you use a triangle instead of a rectangle, then when you join copies of the strip into an array, the resulting crease pattern will curve around onto itself as you add units. If you start with a triangle whose tip angle is an integral fraction of a half-circle, then you can build up a complete circular crease pattern that, when folded, will automatically stretch into a rotationally symmetric form, as illustrated in Figures 2.112 and 2.113.

When joining rectangles, it is relatively easy to create the 3D form by flat-folding the entire pattern, then stretching it into shape. With a circle, though, it is not possible to flat-fold the pattern, at least not with the proper crease assignment. However, you can fold the pattern in half, flat-fold the double-layered half-circle, then unfold and reverse the fold direction of half of the creases to get the proper form.

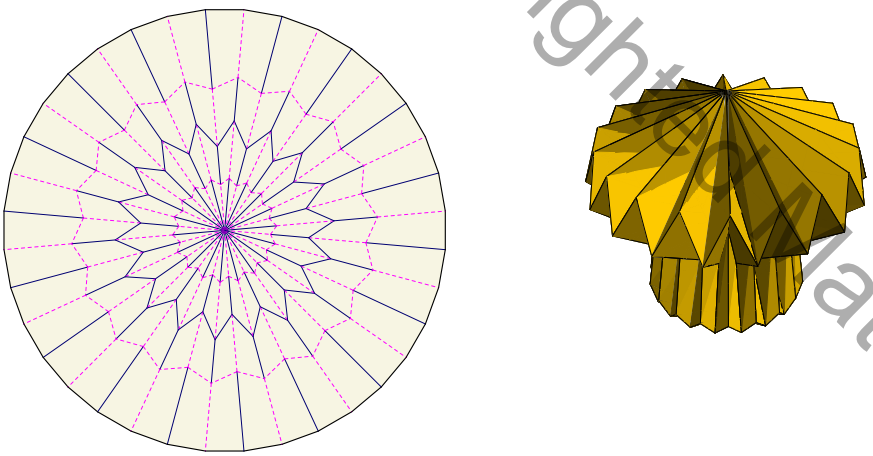

Figure 2.113.
Arraying the triangular strip as alternations of the strip and its mirror image gives a complete circular crease pattern and folded form.

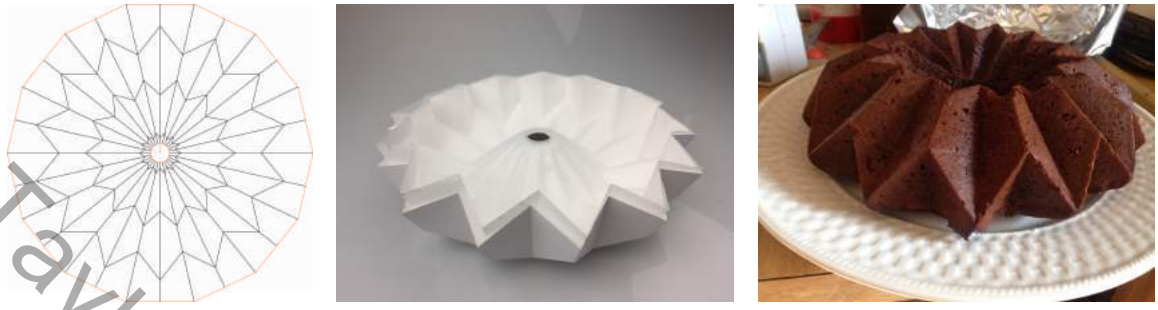

Figure 2.114.
A circular rotationally pleated origami Bundt™ cake mold.
Left: crease pattern.
Middle: paper mold (with parchment liner).
Right: baked cake.

David Morgan in the Industrial Design Department of Brigham Young University and his students have developed a particularly tasty application of this folding procedure: an origami version of a Bundt™ cake mold, shown in Figure 2.114.

⋆ 2.4.9. Corrugations and More

Tubes, triangulated cylinders, Troublewits, rotationally-stretched pleats, semigeneralized Miura-oris, and more: these are all examples of a genre of origami known as *corrugations*. While there is some discussion about just what, precisely, constitutes a corrugation, most of the folds called corrugations are geometric forms in which the majority of the creases are only partially folded, as opposed to flat-folded. The scope of corrugations is vast; the ones shown in this section are only a small sampling of the possibilities. Corrugations are often highly symmetric, exhibiting combinations of rotational symmetry and/or one- and two-dimensional periodicity, but they need not be symmetric. In fact, some of the most visually striking corrugations arise when an obvious periodicity is broken on a different length scale from the periodicity. This effect can be seen in the works of Japanese paper artist Yuko Nishimura, whose works, commonly from 100×100 cm squares, take the regularity of pleats but interrupt them by superimposing larger-scale, swooping boundaries between regions of different periodicity and/or orientation, as in Figure 2.115.

The technique exemplified by "Troublewit" and rotationally stretched pleats, of flat-folding a shape repeatedly then stretching it into three-dimensionality, can be applied to much more complex

Figure 2.115.
Artwork by Yuko Nishimura.
Top left: "Organic," 2006.
Top right: "Organic," 2006.
Bottom left: "Stir," 2006.
Bottom right: "Thick," 2006.

paths and pleats than shown above. One of the modern masters of this technique is Ray Schamp, who has created many lovely corrugations based on both linear and rotational stretching. A few are shown in Figure 2.116.

Rotational stretching poses two additional challenges: first, the pattern often cannot be fully flat-folded (though it can sometimes be flat-folded in sections to set the creases a few at a time). One way around this challenge, which has the side benefit of creating a more interesting 3D state, is to add slits to the paper. Schamp's design "S-curve" in Figure 2.116 takes this approach.

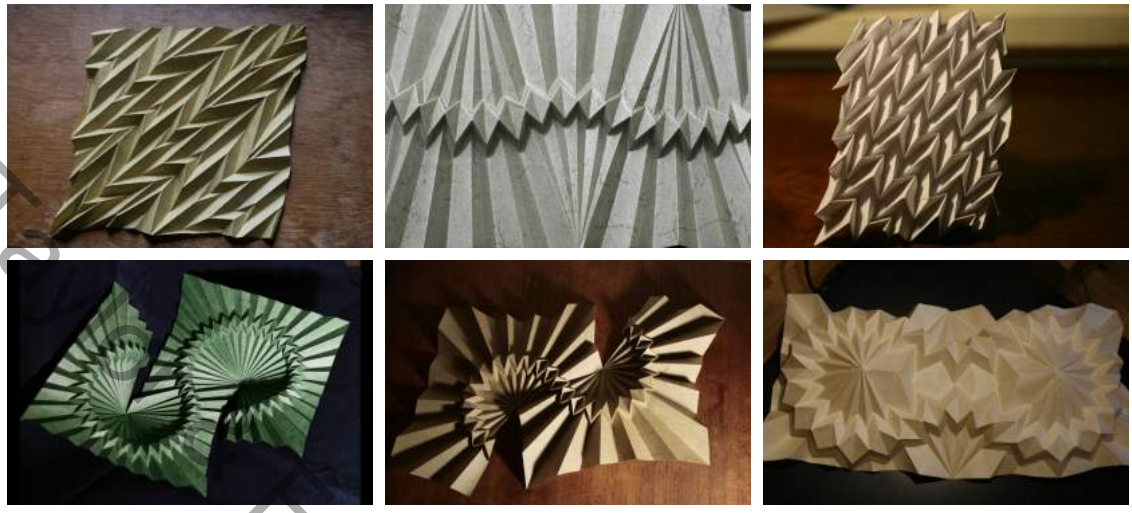

Figure 2.116.
Artwork by Ray Schamp.
Top left: "3rd Degree Corrguation," 2012.
Top middle: "Marble Wave," 2007.
Top right: "Equidistant Weave," 2010.
Bottom left: "Around and Between," 2007.
Bottom middle: "S-Curve," 2007.
Bottom right: "Figure 8," 2007.

A second challenge is that, even if a rotationally stretched form is flat-foldable in sections, the full pattern may not be mathematically self-consistent in any state other than fully flat and unfolded. However, once the paper has been given "memory" of the folds by forming a crease, the balance between the strains of folded creases and small distortions throughout the fold can allow the form to still take on a three-dimensional form reminiscent of a bas-relief sculpture, as in Figure 2.117.

The partially folded creases in corrugations make the resulting surfaces visually interesting, usually much more so than when they are collapsed into the flat-folded state. At least, that's the theory. In the real world, though, real paper has thickness and springiness, which can bring life and form to ostensibly flat-folded patterns. The three-dimensionality of "flat-folded" patterns was displayed by Paul Jackson in a work he titled "Bulge," formed by alternating flat-folded pleats; the residual springiness of the paper popped it into an elegant curved organic form. This concept was taken up by Croatian-American artist Goran Konjevod, who developed the genre into a wide variety of three-dimensional shapes, several of which are shown in Figure 2.118.

Figure 2.117.
"Nine Centers" (2007)
by Ray Schamp.

Figure 2.118.
Cross-pleated forms by Goran Konjevod.
Top left: "Bowl:32, fancy" (2007).
Top right: "Wave:32" (2008).
Bottom left: "Bowl:32 locked" (2006).
Bottom right: "64-grid pureland improvisation" (2006).

In these works, the theoretical model says it should be "flat and uninteresting," but the non-idealities of paper—finite thickness and springiness—actually give rise to beautiful and unexpected structures. This is a reminder that we must always be aware of the limitations of our theoretical models!

The Miura-ori pattern is flat-foldable, but a simple modification of it gives a non-flat-foldable variation that has several desirable mechanical properties, notably, a "hard stop" that prevents it from collapsing to flatness. Such patterns have been investigated by Yves Klett and his colleagues at the Institut für Flugzeugbau (Institute of Aircraft Design) at the University of Stuttgart as structural elements within sandwich panels, except instead of using standard honeycomb cores, he and his colleagues are using Miura-oris and their kin. In order to fold these materials in high volume from high-performance materials—paper, resin-impregnated textiles, carbon fiber, and more—they have developed automated machines for folding these patterns: a modern update on the machine described in Henry Hochfeld's patent (Figure 2.37). These patterns can be incredibly strong: Figure 2.119 shows one such modified Miura-ori pattern supporting the weight of a car.

The notion of stretching pleated patterns into curved forms is not restricted to abstract geometric shapes; several artists have incorporated such patterns into representational designs. Two particularly beautiful such examples are Jun Maekawa's "Peacock," introduced in Kunihiko Kasahara's landmark 1983 book on Maekawa, *Viva Origami* [58], and a more recent example, a lovely "Butterfly" by the young Russian artist Andrey Ermakov, both shown in Figure 2.120.

Because they are three-dimensional, corrugations are challenging to design and analyze mathematically, requiring mathematical techniques that we will explore in later chapters. Flat-foldable origami designs are often considerably easier to develop mathematically (though they, too, can call for sophisticated mathematics). It might seem that restricting consideration to flat-foldable origami patterns would limit designs to relatively simple folded patterns, but this is not the case; flat-folded geometric patterns offer remarkable complexity and beauty. In the next few chapters, we will explore another vast genre, this time of flat-folded forms: that of twist-fold-based tessellations.

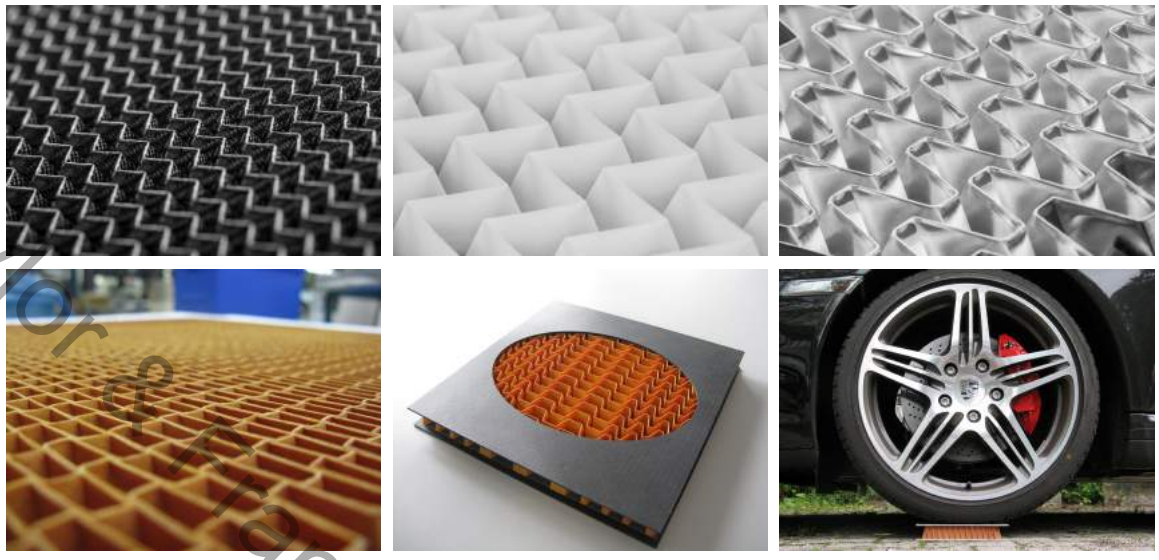

Figure 2.119.
Top left: a Miura-ori folded from carbon fiber textile.
Top midde: a Miura-ori folded from vellum.
Top right: a modified Miura-ori folded from aluminum.
Bottom left: a machine-folded modified Miura-ori folded from resin-impregnated aramid fiber.
Bottom middle: use of the modified Miura-ori as the core of a structural panel.
Bottom right: the modified Miura-ori can support the weight of a car.

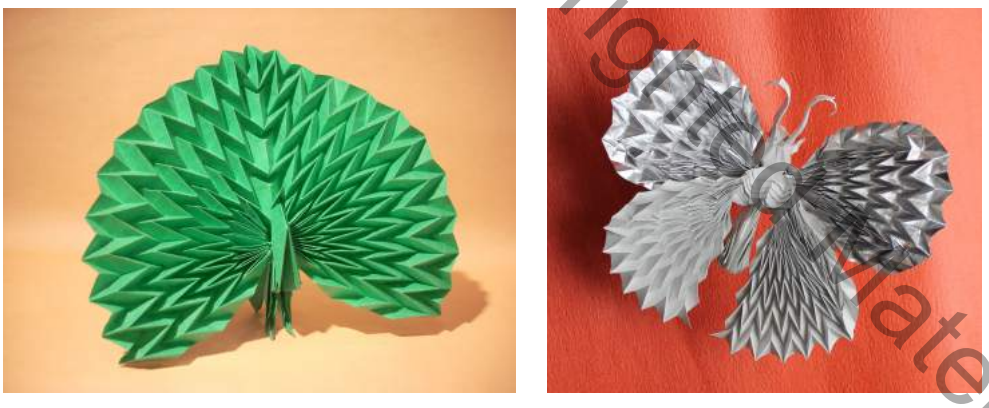

Figure 2.120.
Left: "Peacock" (2010) by Jun Maekawa, incorporating Miura-ori for the tail. Based on a 2000 revision of the original ca. 1980–1983 design.
Right: "Butterfly" (ca. 2009) by Andrey Ermakov, incorporating Miura-ori to pattern the wings.

⋆ 2.5. Terms

Anticlastic A pattern that when bent in a curve along one direction curves in the opposite direction, forming a saddle shape.

Aperiodic A pattern that is not periodic.

Basis vectors Two vectors that describe both translation distances and directions for a doubly periodic pattern.

Bend angle The 3D angular change between the two minors folds in a folded Miura-ori.

Bistable A folded pattern that has two unstrained folded states but that cannot switch between them without undergoing some form of strain and/or distortion.

Chicken wire pattern A version of the Huffman grid constructed from a mirror-symmetric bird's-foot vertex.

Corrugation An origami pattern, usually geometric, in which the majority of the creases are partially (not flat-) folded.

Crimp A pair of opposite-parity creases roughly perpendicular to a fold; a combination of two pleats.

Crossing embedding A choice of vertex positions for a crease pattern (or any plane graph) that allows edges to cross each other at points other than the defined vertices.

Doubly periodic A pattern that is translationally periodic in two different directions.

Generating line A line used to define a periodic pattern, such as the Mars-type crease pattern or semi-generalized Miura-ori.

Generating vertex A vertex that can be replicated into a periodic pattern, such as the Huffman grid or Yoshimura pattern.

Huffman grid A 2D periodic grid composed of a single type of degree-4 vertex.

Kresling pattern A periodic pattern of identical triangles and degree-6 vertices around a closed cylinder. See also *triangulated cylinder*.

Major fold (Miura-ori) In a Miura-ori, the two folds at each vertex that are opposite one another and have the same crease assignment.

Mechanical metamaterials Fine-grained mechanisms that give a bulk mechanical behavior that is different from that of the constituent materials, such as a negative Poisson's ratio.

Minor fold (Miura-ori) In a Miura-ori, the two folds at each vertex that are opposite one another and have the opposite crease assignment.

Miura-ori A fold pattern described by Koryo Miura consisting of a doubly periodic array of parallograms and their mirror images.

Monostable A folded pattern that has only a single unstrained folded state.

Osculating angle The angle between the two major folds at a vertex of a folded Miura-ori.

Period The distance that a periodic pattern can be translated that leaves it unchanged.

Periodic A pattern that can be translated some distance that leaves it unchanged.

Pleat A mountain and valley fold next to each other, roughly (or exactly) parallel.

Poisson's ratio The amount by which a material or mechanism shrinks in one direction when it is stretched in a perpendicular direction.

Predistortion Designing the flat-folded path of a semigeneralized Miura-ori with sharper angles than the desired trajectory so that when it is partially folded, it takes on a desired trajectory.

Rigid foldability A property of a crease pattern that can fold with all flexing happening along creases; the facets remain flat and vertices and creases do not move within the paper.

Rigidly foldable An origami crease pattern is rigidly foldable if it can be continuously transformed between two different

states (e.g., unfolded to flat-folded) without bending or buckling of the facets or movement of the vertices and creases within the paper.

Rotational symmetry A property of an object that is unchanged after rotating it through some nonzero angle.

Ruling angle The angle between the two minor folds at a vertex of a folded Miura-ori.

Semigeneralized Miura-ori A crease pattern similar to the Miura-ori that is periodic in one direction but not necessarily periodic in the other.

Shallow-angle divot A pattern within a semigeneralized Miura-ori that allows small-angle bends.

Symmetry A property of an object that it is unchanged after applying some non-trivial transformation.

Synclastic A pattern that when bent in a curve along one direction curves in the same direction along the opposite direction, forming a spherical shape.

Tile A patch of crease pattern that can be joined with other tiles to create a complete and valid crease pattern.

Tile line A border of a tile along which it can be joined with other tiles.

Translational symmetry A property of an object that is unchanged after translating it some nonzero distance.

Triangulated cylinder A periodic pattern of identical triangles and degree-6 vertices around a closed cylinder. See also *Kresling pattern*.

Vector A combination of a length and direction that can describe a direction of periodicity of a pattern.

Waterbomb tessellation A crease pattern consisting of an array of Waterbomb base patterns with alternate rows offset from each other.

Yoshimura pattern A periodic pattern of identical triangles and degree-6 vertices.